Soft Walls and Heavy Sleptons in a Warped Extra Dimension

A DISSERTATION
SUBMITTED TO THE FACULTY OF THE GRADUATE SCHOOL
OF THE UNIVERSITY OF MINNESOTA
BY

Daniel Gregory Sword

IN PARTIAL FULFILLMENT OF THE REQUIREMENTS
FOR THE DEGREE OF
Doctor of Philosophy

January, 2011

Acknowledgements

I offer my greatest gratitude to Tony Gherghetta for advising on these projects, Brian Batell for his work as both an instructor and collaborator, Arkady Vainshtein and Mikhail Voloshin for being so generous with their time when I had questions, and Tom Kelley and Tonnis ter Veldhuis for many useful discussions.

Dedication

To my mother who suffered for me, my wife who was patient with me, and the rest of my family who always encouraged me.

Abstract

Extensions of the warped extra dimension framework originally proposed by Randall and Sundrum are discussed, including soft-wall models and aspects of supersymmetry breaking. In particular, the standard model in a soft-wall background is covered in detail, including electroweak physics and an extensive treatment of fermions in arbitrary warped backgrounds. Additionally, aspects of lepton flavor violation in models of supersymmetry breaking with hierarchical soft-terms and Dirac gauginos are discussed, as these can occur naturally when supersymmetry is broken near the infrared boundary.

Contents

List of Tables

List of Figures

Chapter 1

Introduction

1.1 The Hierarchy Problem

The standard model (SM) represents the pinnacle achievement of 20th century particle physics. It accurately describes nearly all known particle data–not just that for which it was designed, but also a long list of phenomena predicted as a direct consequence of its minimal structure. Paradoxically, the same structure that has proven so unshakingly successful also gives theorists strong reason to suspect that new physics is just around the corner.

Unless as-yet-unobserved physics appears at the TeV scale, the internal consistency of the standard model breaks down. In order for the chiral matter and heavy gauge bosons to acquire mass while preserving unitarity, the $SU(2) \times U(1)$ gauge symmetry of the standard model must be spontaneously broken at low energies. The actual method nature has chosen to accomplish this symmetry breaking is not known, and this fact provides the basis for a central question facing particle physicists today. In the standard model extroweak symmetry is broken via the Higgs mechanism. A scalar field transforming as a doublet of $SU(2)$ obtains a vacuum expectation value that shifts the ground state of the theory away from its symmetric minimum. After expanding fluctuations about the shifted minimum, one finds that this simple and elegant mechanism not only endows the matter and gauge fields with mass, but also enforces a number of non-trivial relationships between physical observables that have been experimentally

verified to a stunning degree of accuracy.[1]

However, the introduction of a fundamental scalar field introduces a new problem, known as the hierarchy problem. For the W and Z bosons to have their observed masses, the physical Higgs mass should be of comparable size–namely, of order 100 GeV. However, unlike the fermions and gauge bosons, whose masses are protected by chiral and gauge symmetries, there is no symmetry that protects the mass of a fundamental scalar from receiving large quantum corrections. For example, the Yukawa coupling between the Higgs and the top quark results in a one-loop radiative correction to the Higgs mass-squared $m^2_{\text{h,phys}} = m_h^2 + \delta m_h^2$ that is quadratically divergent at leading order,

$$\delta m_h^2 \sim -\frac{3g^2}{16\pi^2}\frac{m_t^2}{M_W^2}\Lambda^2 + \cdots , \tag{1.1.1}$$

where Λ is the momentum cutoff in the loop integral, corresponding to the scale at which new physics enters. If we assume the standard model is valid up to energies where quantum gravity becomes important, the cutoff Λ would correspond to the Planck scale of order 10^{18} GeV. Then for the physical Higgs mass-squared to be of order 100 GeV, there must be a dramatic cancellation between the "bare" mass m_h^2 and the correction δm_h^2 to within about 1 part in 10^{32}!

The "unnatural" amount of required fine-tuning in the standard model is the essence of the hierarchy problem, and it has been a central focus of theorists in predicting the shape of new physics. The reasoning behind this is the following: the problem with equation (1.1.1) arises only if one assumes the standard model is valid up to the highest energies. Instead, the hierarchy problem might be a hint that the standard model is merely an effective low-energy theory. New physics should appear at energies of order a few TeV, cutting off the loop integral.

1.2 Supersymmetry

Supersymmetry (SUSY) is a widely favored candidate solution to the hierarchy problem. In supersymmetric theories, a new symmetry relates fermions and bosons, so that every fermion (boson) of the standard model has a bosonic (fermionic) superpartner with the same mass and couplings. If the symmetry were unbroken, the quadratic divergences

[1] For a review, see Ref. [1].

from loops with respective superpartners would cancel exactly. However, this is clearly not the case, or we would have long since discovered the superpartners. Instead, if supersymmetry in fact provides the resolution to the hierarchy problem, it must be "softly" broken (i.e. broken only by terms with positive mass dimension). Then the quadratic divergences are instead proportional to the difference in superpartner square-masses. This implies that the superpartners should not be too heavy, or else the fine-tuning problem is reintroduced.

Explaining why the scale of SUSY breaking is so low has been a major focus of supersymmetric model builders. A variety of options for breaking supersymmetry dynamically have been explored, with the most promising sharing a common feature of a hidden sector–a collection of fields separate from the SM–in which SUSY is dynamically broken.[2] In gravity mediation [3, 4, 5, 6], supersymmetry breaking is communicated to the visible sector through gravitional-strength interactions, while gauge mediated models [7, 8, 9, 10, 11, 12, 13] couple the hidden sector to the visible sector through ordinary SM gauge interactions, so that the Planck-suppressed effects are relatively unimportant. If SUSY is broken by dynamics in an extra dimension, a variety of mechanisms are available. For example, SUSY can be broken by boundary conditions in a compact space, by the background geometry itself, or it can arise from Boltzmann-suppressed communication between visible and hidden worldsheets separated by some distance along the extra space [14, 15, 16, 17, 18, 19, 20, 21, 22].

A generic pattern of soft supersymmetry-breaking masses can lead to disastrously large flavor violation [23, 24, 25, 26]. Experimental searches for evidence of supersymmetry have included examinations of flavor-violating processes, for example $\bar{K}^0 - K^0$ mixing, $b \to s\gamma$ and $\mu \to e\gamma$. The extremely low bounds on the rates of such processes would seem to indicate that supersymmetry breaking must occur via a flavor-universal mechanism (for example, gauge mediation [27]). However, there is another possibility that does not spoil naturalness: the first-two generations of superpartners may be very heavy, while the third generation superpartners are light [28, 29]. Such a pattern of sfermion masses can arise naturally when SUSY is broken from a warped extra dimension (which we will discuss shortly). Moreover, such models exhibit a continuous R-symmetry that provides an even stronger suppression of flavor violating effects,

[2] See Ref. [2] for a review.

primarily due to the fact that gaugino masses must be of the Dirac type [30]. The implications of hierarchical soft supersymmetry-breaking masses have been studied in the quark sector [31, 32], however relatively little has been done in regards to the lepton sector despite the extreme sensitivity of planned future experimental searches [33]. Reference [34] examines supersymmetry breaking with heavy sleptons and Dirac gauginos.

1.3 Randall and Sundrum

There is another interpretation of (1.1.1), which again focuses on the assumption that the Planck scale should be the cutoff of the standard model, but in a subtly different way. The reason for choosing the Planck scale is that this is the scale at which quantum gravity should become important–thus, we expect that a new theory must enter at this energy scale, unifying the standard model and general relativity. This scale is monstrously large only because gravity is incredibly weak compared to the other three forces, which are all significant at energies around a TeV. Therefore, an alternate approach is to explain why gravity is so weak.

This interpretation led to the consideration of extra dimensions as a possible solution of the hierarchy problem. The key idea is that standard model forces could be confined to a four-dimensional world-sheet–known as a 3-brane–in a compact higher dimensional space. In such a case, gravity necessarily would propagate throughout the bulk of spacetime, as it is the "stuff" of spacetime itself. At distances much smaller than the size of the extra dimension, one would expect to see deviations from Newton's inverse-square law for the force of gravity, as lines of gravitational flux would have more volume to fill. This was the inspiration for proposing extra dimensions as a solution to the hierarchy problem in the context of large, flat extra dimensions [35].

The Randall-Sundrum model (RS) [36, 37] modified this idea by proposing that 4D distance scales change with location along the extra space due to a gravitational metric that is non-factorizable. Randall and Sundrum were able to show that such a metric was a solution to Einstein's equations in 5D under certain assumptions. The solution they discovered corresponded to a slice of anti-de Sitter (AdS) space between two branes, denoted as the "ultraviolet" (UV) or "Planck" brane and the "infrared" (IR) or "TeV" brane. In this picture, the hierarchy problem is solved because apparent energy scales

are a function of position along the extra dimension. While the fundamental scale on the UV brane is of order the Planck mass, the effective scale on the IR brane where the standard model lives is exponentially smaller due to the "warp factor" of the metric. Meanwhile, the weakness of gravity is easily interpreted in terms of quantum mechanical language, because the massless graviton "wavefunction" has a profile that is peaked near the UV brane away from the standard model fields. As a result, the standard model coupling to gravity is exponentially suppressed.

A truly remarkable feature of RS is that it admits a wholly 4D description that avoids any mention of the existence of a fifth dimension. This is due to the AdS/CFT correspondence [38, 39, 40, 41, 42, 43], which relates strongly coupled conformal field theories in 4 dimensions to weakly coupled gravitational theories in AdS_5. Strictly speaking, the original AdS/CFT conjecture linked only type IIB string theory on $AdS_5 \times S_5$ with $\mathcal{N} = 4$ Super Yang-Mills theory in 4D. However, numerous extensions of the original correspondence have passed many non-trivial tests. The AdS/CFT "dictionary" [44] allows one to translate between fields living in the bulk of the AdS spacetime and operators of the dual CFT in 4 dimensions. In particular, fields localized toward the UV brane are interpreted as elementary states of the dual CFT, while those living near the IR brane are interpreted as composite states. A critical point is that the relation can only be trusted when the 5D gravitational theory is weakly coupled, which implies strong 't Hooft coupling on the CFT side. As a result, theories based on RS offer a potential window into the understanding of strong dynamics.

Indeed, the original Randall-Sundrum model has a dual interpretation of electroweak symmetry breaking due to strong dynamics. In the Randall-Sundrum model, the presence of the IR brane corresponds to an abrupt breaking of conformal symmetry at low energies. The Higgs–being localized on the IR brane–corresponds to a composite state of the dual CFT, which is weakly coupled to gravity.

This description is reminiscent of technicolor models [45, 46, 47] where electroweak symmetry is broken by a "techniquark" condensate, similar to the way chiral symmetry is broken by the quark condensate in quantum chromodynamics (QCD). The standard model is augmented with a new gauge group that is asymptotically free but confining at the weak scale. The appearance of the techniquark condensate breaks the chiral symmetry of the massless quarks, leading to Nambu-Goldstone bosons that are then eaten

to provide the longitudinal degrees of freedom for the W and Z bosons. The simplest technicolor models tend to produce excessive contributions to the Peskin-Takeuchi S and T parameters [48, 49]. This has led to the formulation of composite Higgs models [50, 51, 52, 53], walking technicolor and top-color (see Refs. [54, 55] for reviews), and conformal technicolor [56, 57] models. That these models may be given dual, calculable descriptions in terms of a perturbative 5D gravity theory has led to a surge of research into RS models.

1.4 Soft-Walls

The notion that strong dynamics can be described by weakly coupled gravity duals has sparked an ambitious program known as AdS/QCD, which seeks to formulate a gravity dual to quantum chromodynamics (QCD) from the bottom up. At low energies, QCD becomes strongly coupled, leading to confinement of quarks into hadrons. A robust quantitative description of QCD in this regime has remained elusive because it evades perturbative description. Rather than searching directly for a holographic derivation of QCD, the AdS/QCD program seeks to build a dual theory that matches the known features of QCD.

The AdS/QCD program has encouraged model bulders to move beyond the original simplified AdS/QCD models [58, 59] of a warped extra dimension sandwiched between two "hard- wall" branes. The hard-wall framework posits that conformal symmetry is broken in the IR in the simplest possible way by an abrupt low-energy cutoff of space-time. By contrast, the soft-wall proposal admits a much richer potential phenomenology because it considers conformal symmetry breaking in general terms. This has allowed for improvements in the modeling of meson trajectories, for example, but at the cost of added computational complexity.

Though the original soft-wall proposal was in fact made in the context of AdS/QCD models [60], it was used soon after to study electroweak symmetry breaking in soft-wall backgrounds [61]. While originally an ad-hoc implementation of a soft-wall via a "dilaton" prefactor in the action was used, the dynamical soft-wall model put forward in Ref. [62] allowed for the first discussions of stability and naturalness of the soft-wall. The standard model on a soft-wall was first described in Ref. [63], which also noted

that the calculation of physical observables involving fermions was particularly difficult. In fact, fermions evaded quantitative description in all but the simplest cases. What followed were several attempts to document all known special-case solutions and their general behaviors, as well as alternative methods for modeling fermions [64, 65]. In Ref. [66], the first phenomenologically acceptable exact solutions were found and a full numerical approach to modeling fermions was presented in detail.

1.5 Outline and Notation

This dissertation documents research originally published in Refs. [63, 66, 34], which was completed by the author of this thesis with significant contributions from collaborators Brian Batell [63] and Tony Gherghetta [63, 66]. These works focus on soft-wall models and aspects of flavor violation in certain classes of models of supersymmetry breaking. The layout of this document is as follows:

- Chapter 2 discusses the original Randall-Sundrum model in detail as well as the important formulas relevant when the standard model fields are allowed to propagate in the bulk. This material provides the necessary foundation for discussing issues that arise when discussing soft-wall models and supersymmetry breaking. Our approach may be new to many familiar with Randall-Sundrum models, in that it is dressed in the language and notation of "supersymmetric quantum mechanics" [67].

- Chapter 3 discusses the soft-wall framework, provides details on how such a gravitational background can arise dynamically, and places the standard model in the bulk. The difficulty that arises in addressing fermions is presented. Electroweak physics is modeled and aspects of fine-tuning are discussed.

- Chapter 4 addresses the problem of fermion physics in the soft-wall setup in detail. Analytic solutions and approximation methods are presented for the single-generation case. A numerical routine is developed and applied to study the full three-generation problem. It is shown that many of the attractive features of hard-wall models are retained in a soft-wall setup, however there are some intriguing differences.

- Chapter 5 studies lepton flavor violation in models of supersymmetry breaking with heavy first-two generation sleptons and Dirac gauginos. Concrete examples of how such a spectrum can arise in models of SUSY breaking from extra dimensions are discussed. It is shown that highly non-degenerate slepton masses are allowed under certain conditions.

We adopt the following set of rules for the treatment of spacetime indices:

- Latin letters run over all indices (0,1,...,5) while Greek letters run only over the 4D indices (0,1,2,3).
- Letters from the beginning of the alphabet (A, B,...,α, β,...) label Lorentz indices and are raised and lowered using the Minkowski metric and its inverse, $\eta_{AB} = \eta^{AB} = \text{diag}(-++++)$.
- Letters from the middle of the alphabet (M,N,...,μ,ν,...) label spacetime indices and are raised and lowered using the metric and its inverse, g_{MN} and g^{MN}.
- The usual four-dimensional coordinates are labeled as x or x^μ while the coordinate of the extra space is denoted by y or z.

Our treatment of fermions in Chapters 2 and 4 employs additional conventions, which can be found in Section 2.3C.

Chapter 2

The Hard-Wall Warped Dimension

The solution to the hierarchy problem offered by Randall and Sundrum [36, 37] has inspired a large amount of study over the past decade for several reasons. The model provides an elegant solution to the hierarchy problem, predicts the potential existence of Kaluza-Klein matter at energy scales that can be reached by the LHC, offers new ways to study aspects of supersymmetry and supersymmetry breaking, and due to the AdS/CFT correspondence [38, 39, 40, 41, 42, 43] offers a potential path toward understanding strongly coupled gauge theories in four dimensions.

In this section, we review the details of the original model by Randall and Sundrum, as this will provide a solid foundation for our discussion of flavor physics and supersymmetry. Our discussion is structured wherever possible in a general way, so that the later treatment of soft-wall models will suffer from a minimal amount of redundancy and the smallest possible degree of repetitiveness. We start with a general overview of the model, introducing our notation and conventions that we will carry through into later chapters. Additionally, we review the concepts of bulk fields and flavor physics in the Randall-Sundrum background.

2.1 The Randall-Sundrum Model

The original Randall-Sundrum model [36] posits the existence of a single compact extra dimension bounded on either end by two 3-branes. Because four-dimensional distance scales depend exponentially on location in the extra space, the characteristic energy scales of physics localized in separate regions can differ exponentially. This mechanism in fact underlies the solution to the hierarchy problem proposed by Randall and Sundrum. Our discussion here of the details of the model will provide an important reference point for the later chapters.

2.1A The Setup

Overview of the RS1 Set-Up

In the original Randall-Sundrum model (RS1) [36], the extra dimension is compactified on a circle of radius R that is then orbifolded to arrive at the space $S^1/\mathbb{Z}_2$. (In the model we will refer to as RS2 [37], the space is also compactified in such a way before taking the limit $R \to \infty$.) The orbifold compactification enforces two symmetry requirements on the theory under transformations of the coordinate, y, that parameterizes the extra dimension: periodicity under the shift $y \to y + 2\pi R$ and $\mathbb{Z}_2$ parity under the reflection $y \to -y$. Geometrically, the space may be viewed as the result of identifying each point on a circle of radius R with its reflection about the diameter connecting $y = 0$ and $y = \pi R$. Two three branes are located at the orbifold fixed points of $y = 0$ and $y = \pi R$ and are referred to as the UV or Planck brane and the IR or TeV brane, respectively.

It is important to keep in mind that the symmetry requirements only apply to the fields up to global or local symmetries of the Lagrangian. Explicitly, the requirements are symmetry of the Lagrangian under reflection $y \to -y$ and periodicity of the Lagrangian under a shift of $y \to y + 2\pi R$. Generically, for any field Φ, the requirements are:

$$\Phi(-y) = \pm\Phi(y), \tag{2.1.1}$$

$$\Phi(y) = \pm\Phi(y + 2\pi R). \tag{2.1.2}$$

Together, these imply $\Phi(\pi R + y) = \pm\Phi(\pi R - y)$. Thus, the combination can be interpreted as two distinct $\mathbb{Z}_2$ symmetries: a $\mathbb{Z}_2$ symmetry under reflection about $y = 0$ and

a $\mathbb{Z}_2'$ under reflection about $y = \pi R$. One is free to specify the sign under which a field transforms separately under the $\mathbb{Z}_2$ and under the $\mathbb{Z}_2'$.

The spacetime in the bulk is that of anti-de Sitter space (AdS_5),

$$ds^2 = g_{MN}dx^M dx^N = e^{-2A(y)}\eta_{\mu\nu}dx^\mu dx^\nu + dy^2. \tag{2.1.3}$$

where $A(y) = k|y|$ and k is the AdS curvature, while the induced metric on each brane is flat. We denote an induced metric by attaching a superscript (subscript) label to $g_{\mu\nu}$ ($g^{\mu\nu}$):

$$g_{\mu\nu}^{(\mathrm{UV})} = g_{\mu\nu}(x, y = 0), \quad g_{\mu\nu}^{(\mathrm{IR})} = g_{\mu\nu}(x, y = \pi R). \tag{2.1.4}$$

The factor $e^{-2A(y)}$ is often referred to as the "warp-factor." The reason for this is apparent in the form of the metric (2.1.3): movement along the direction of the extra space results in the "warping" of 4D distance scales.

It is easy and often useful to transform the metric (2.1.3) to the conformal coordinate, z, by making use of the coordinate transformation:

$$\frac{\mathrm{d}y}{\mathrm{d}z} = e^{-A}. \tag{2.1.5}$$

Indeed, we make extensive use of these coordinates throughout this work. In these coordinates, the bulk spacetime metric takes the form:

$$ds^2 \;\; = \;\; e^{-2A(z)}\eta_{MN}dx^M dx^N, \tag{2.1.6}$$

where $A(z) = \log k|z|$ for pure AdS_5. Then the locations of the UV and IR branes are $z = z_0 = 1/k$ and $z = z_1 = e^{\pi kR}/k$, respectively. Care must be taken to properly account for the orbifold symmetry when integrating in these coordinates. Integrals over the entire extra space are to be evaluated on the interval $y \in (-\pi R, \pi R)$ or equivalently $z \in \left((k^2 z_1)^{-1}, z_1\right)$. Spacetimes other than pure AdS_5 can be considered by choosing different forms for the function A.

AdS_5 from Einstein's Equations

The set-up above is consistent with Einstein's equations for gravity in 5D under certain conditions. To derive these conditions, we elaborate on the presentations of Refs. [36, 68]. We can model the set-up by considering the classical action in three regions: on the UV brane, in the bulk, and on the IR brane.

We first focus only on the bulk action. The bulk action consists of two gravitational contributions arising from the bulk curvature, $\mathcal{R}$, and bulk cosmological constant, Λ. Note that we use a script typeface $\mathcal{R}$ to distinguish the Ricci scalar (and tensor) from the radius of the extra space denoted by R, while we use the capital G_{MN} to distinguish Einstein's tensor from the metric, g_{MN}. When RS1 is modified by placing gauge or matter fields in the bulk, there will be additional contributions to the bulk action. Assuming the backreaction is small, these contributions can be neglected for the gravitational analysis. However, they can play an important role when discussing stability of models and will become important when we consider "soft-wall" models in Chapter 3. With these caveats aside, the bulk action takes the form:

$$S_{\text{bulk}} = \int \mathrm{d}^5x\sqrt{-g}\left(M^3\mathcal{R} - \Lambda\right). \tag{2.1.7}$$

To find the solution to Einstein's equations in the bulk, we note that the most general form of a 5D metric satisfying 4D Poincaré invariance is given by (2.1.3) or equivalently (2.1.6). We therefore insert as an ansatz the conformal metric (2.1.6). The advantage to using this form is that the Einstein tensor is easily calculated for a conformally flat metric. The result is [68]:

$$G_{55} = 6A'^2, \quad G_{\mu\nu} = 3\eta_{\mu\nu}\left(A'' - A'^2\right). \tag{2.1.8}$$

With our conventions, Einstein's equations then read:

$$G_{MN} = \frac{1}{M^3}T_{MN} = -\frac{1}{2M^3}\Lambda g_{MN}. \tag{2.1.9}$$

The "55" equation following from (2.1.8) and (2.1.9) is:

$$A'^2 = \frac{-\Lambda}{12M^3}e^{-2A} \tag{2.1.10}$$

which clearly implies $\Lambda < 0$. The simplest way to solve this equation is to first take a square root and then rewrite in terms of the coordinate y using (2.1.5) together with the chain rule. This yields the second simplest of all differential equations:

$$\frac{\mathrm{d}A}{\mathrm{d}y} = \sqrt{\frac{-\Lambda}{12M^3}}. \tag{2.1.11}$$

Bearing in mind the reflection symmetry, the solution is that for AdS, as advertised:

$$A(y) = \sqrt{\frac{-\Lambda}{12M^3}}|y| \equiv k|y|, \quad A(z) = \operatorname{sgn}(z - z_0)\ln kz. \tag{2.1.12}$$

We have discarded the irrelevant integration constant.

Inserting this solution into (2.1.9), we see that it is consistent except at the boundaries where A'' will introduce delta functions. To deal with this, one must consider the action on the branes. At this point, it does not matter if we work with the y or z coordinates. However, it is simplest to work with y. Ignoring any matter contribution, the action is given by:

$$\begin{aligned} S_{\rm UV} &= -\int \mathrm{d}^4x\sqrt{-g^{(\rm UV)}}V_{\rm UV} = -\int \mathrm{d}^5x\frac{\sqrt{-g}}{\sqrt{g_{55}}}V_{\rm UV}\delta(y), \\ S_{\rm IR} &= -\int \mathrm{d}^4x\sqrt{-g^{(\rm IR)}}V_{\rm IR} = -\int \mathrm{d}^5x\frac{\sqrt{-g}}{\sqrt{g_{55}}}V_{\rm IR}\delta(y-\pi R). \end{aligned} \tag{2.1.13}$$

The contribution to the energy momentum tensor is straightforward to derive:

$$T^{(\rm UV)}_{\mu\nu} + T^{(\rm IR)}_{\mu\nu} = \frac{1}{2}\eta_{\mu\nu}\left(V_{\rm UV}\delta(y) + V_{\rm IR}\delta(y-\pi R)\right). \tag{2.1.14}$$

The delta function contribution to (2.1.9) from (2.1.12) requires some care in dealing with derivatives at the boundary. Upon crossing $y = 0$, the derivative of $k|y|$ goes from $-k$ to k due to the reflection symmetry, while upon crossing $y = \pi R$, it goes from k to $-k$. Therefore,

$$A'' = 2k\left(\delta(y) - \delta(y-\pi R)\right). \tag{2.1.15}$$

Comparing (2.1.14) and (2.1.15), we see that the solution is consistent provided:

$$V_{\rm UV} = -V_{\rm IR} = 12M^3k = \sqrt{-12M^3\Lambda}. \tag{2.1.16}$$

2.2 The Hierarchy Problem

Up to now, we have said nothing about the physical implications of the model. Since the motivation behind RS is to solve the hierarchy problem, our discussion will begin there. Obtaining a realistic low energy theory requires knowing the relationship between 4D observables and the fundamental 5D parameters that define the theory. Of particular interest are two relationships. First, we are interested in the relationship between the 4D Planck mass, M_P, the 5D Planck mass M appearing in the action (2.1.7), and the radius of the extra dimensions R. Secondly, we would like to know how the electroweak scale is related to these fundamental mass scales. The purpose of this section is to review these issues.

2.2A Gravity in a Warped Extra Dimension

Metric Fluctuations

The most general fluctuations of the metric in a five-dimensional theory include tensor, vector, and scalar modes at the massless level. However, the vector mode is inconsistent with the $\mathbb{Z}_2$ symmetry of the theory, leaving only the tensor and scalar fluctuations. These fluctuations can be parametrized as:[1]

$$ds^2 = e^{-2A(z)} \left[(\eta_{\mu\nu} + h_{\mu\nu}(x,z))\, dx^\mu dx^\nu + dz^2 \right], \tag{2.2.1}$$

where $A(z)$ is now to be treated as a dynamical field. Considering a slice of AdS in particular, we can write an equivalent metric in a more suggestive form,

$$ds^2 = e^{-2k|y|\frac{R(x)}{R_0}} \left(\eta_{\mu\nu} + h_{\mu\nu}(x,z)\right) dx^\mu dx^\nu + \left(\frac{R(x)}{R_0}\right)^2 dy^2, \tag{2.2.2}$$

which makes clear the physical interpretation of the graviscalar as the radion corresponding to fluctuations of the compactification radius of the extra space. Stability of the theory depends critically upon $R(x)$ obtaining a vacuum expectation value of R_0. The Goldberger-Wise mechanism [71] offers one way to achieve this stability. For our purposes, we will accept the existence of some such stabilization mechanism and limit our attention to the tensor modes by setting $R(x) = R_0$.

The Planck Scale and Graviton Modes

The relationship between the 4D and 5D Planck scales can be found by considering the Ricci tensor, $\mathcal{R}_{\mu\nu}$. The effective 4D gravitational action is found by integrating:

$$S = M^3 \int d^5x \sqrt{-g}\mathcal{R} \to M^3 \int d^5x \sqrt{-g} g^{\mu\nu}\mathcal{R}_{\mu\nu} + \ldots \tag{2.2.3}$$

Since the conformal factor $e^{-A(z)}$ is independent of x, the components $\mathcal{R}_{\mu\nu}$ are the same whether one uses the 5D or 4D metrics to calculate them (c.f. [68, 72, 73]). Thus, the 4D action becomes:

$$S^{(4)} \equiv M_P^2 \int d^4x \sqrt{-g^{(4)}}\mathcal{R}^{(4)} = 2M^3 \int d^4x \sqrt{-g^{(4)}}\mathcal{R}^{(4)} \int_{z_0}^{z_1} dz e^{-3A(z)}. \tag{2.2.4}$$

[1] For alternative ways to analyze graviton fluctuations, see refs [68, 69, 70].

The factor of 2 is to take into account the orbifold symmetry. Equivalently, one can integrate over the coordinate $y \in (-\pi R, \pi R)$. Applying specifically to RS, we have:

$$M_P^2 = \frac{M^3}{k}\left(1 - e^{-2\pi kR}\right). \tag{2.2.5}$$

The 4D Planck scale depends very weakly on the radius of the extra dimensions assuming it is moderately larger than about $1/(2\pi k)$.

Graviton modes can be considered by inserting the perturbed metric (2.2.1) into the Einstein-Hilbert action and going to the transverse-traceless gauge (also known as the RS gauge), $\partial_\mu h^{\mu\nu} = h^\mu_\mu = 0$. This results in the following action for the field $h_{\mu\nu}$ [63]:

$$\delta S = M^3 \int d^5x\, e^{-3A}\left(-\frac{1}{4}\partial_\rho h_{\mu\nu}\partial^\rho h^{\mu\nu} - \frac{1}{4}\partial_5 h_{\mu\nu}\partial_5 h^{\mu\nu}\right). \tag{2.2.6}$$

The equation of motion for $h_{\mu\nu}$ is found in the usual way by demanding that the variation (2.2.6) vanish. Integrating by parts once results in the equation of motion:

$$e^{-3A}\partial_\rho\partial^\rho h_{\mu\nu}(x,z) + \partial_5\left(e^{-3A}\partial_5 h_{\mu\nu}(x,z)\right) = 0. \tag{2.2.7}$$

To solve this equation, we expand the bulk graviton in a KK-decomposition. That is, we seek solutions that satisfy separation of variables by inserting the ansatz,

$$h_{\mu\nu}(x,z) = \sum_{n=0}^{\infty} h^{(n)}_{\mu\nu}(x) f_h^{(n)}(z), \tag{2.2.8}$$

where $\partial_\rho\partial^\rho h^{(n)}_{\mu\nu}(x) = m_n^2 h^{(n)}_{\mu\nu}(x)$. The equation of motion (2.2.7) for $f_h^{(n)}$ then becomes,

$$\partial_5(e^{-3A}\partial_5 f_h^{(n)}(z)) + m_n^2 e^{-3A} f_h^{(n)}(z) = 0. \tag{2.2.9}$$

while the states obey the orthonormality condition,

$$2M^3 \int_{z_0}^{z_1} dz\, e^{-3A(z)} f_h^{(m)}(z) f_h^{(n)}(z) = \delta^{mn}, \tag{2.2.10}$$

which leads to a canonical action for the graviton fluctuations.

The action is only minimized if the boundary term arising from the integration by parts vanishes, implying either Neumann or Dirichlet conditions on the wavefunctions at the UV and IR boundaries. Applying Neumann conditions $(\partial_5 f_h^{(n)})|_{z_0,z_1} = 0$ gives rise to a massless 4D graviton with constant wavefunction, $f_h^{(0)} = 1/M_P$, where M_P is

defined implicitly in (2.2.4) or explicitly for RS in (2.2.5). Instead if Dirichlet conditions are applied then the zero mode is projected out.

It is useful to define the rescaled field

$$\widetilde{f}_h^{(n)}(z) \sim e^{-\frac{3A(z)}{2}} f_h^{(n)}(z), \tag{2.2.11}$$

which brings the equation of motion (2.2.7) into the form of a one-dimensional Schrödinger equation:

$$\left(-\partial_5^2 + V(z)\right) \widetilde{f}_h^{(n)}(z) = m_n^2 \widetilde{f}_h^{(n)}(z), \tag{2.2.12}$$

with the potential given by

$$V(z) = \left(\frac{3}{2}A'\right)^2 - \frac{3}{2}A'' = \frac{15}{4z^2}, \tag{2.2.13}$$

where the last equality is for a slice of AdS.

The solutions to this equation can be written in terms of Bessel functions:

$$\widetilde{f}_h^{(n)}(z) = N_h^{(n)} z^{\frac{1}{2}} \left(J_2(m_n z) + b_h^{(n)} Y_2(m_n z)\right) \tag{2.2.14}$$

The factor $b_h^{(n)}$ and m_n are determined by imposing the boundary conditions at the UV and IR branes,

$$\left(\partial_5 + \frac{3A'}{2}\right) \widetilde{f}_h^{(n)}\Big|_{z_0,z_1} = 0 \tag{2.2.15}$$

while the normalization is set by inserting the solution into (2.2.10). Of primary interest is the mass spectrum, which is approximately given by:

$$m_n \simeq \left(n + \frac{1}{4}\right) \pi k e^{-\pi k R}. \tag{2.2.16}$$

Finally, we note that the potential (2.2.13) is of the form $W^2(z) - W'(z)$ where $W(z) = 3A'/2$ is known as the "superpotential." Thus, we can factorize the Schrödinger equation (2.2.12) as [67]:

$$\left(-\partial_5 + W\right) \left(\partial_5 + W\right) \widetilde{f}_h^n(z) = m_n^2 \widetilde{f}_h^n(z). \tag{2.2.17}$$

In this way, the zero-mode wavefunction mentioned above can be easily found through direct integration.

2.2B The Higgs

To solve the hierarchy problem, Randall and Sundrum proposed placing the standard model fields on the IR brane. Let us examine the Higgs boson by considering a scalar field, H, localized on the brane at $y = \pi R$. Then the 4D action for the field depends on the induced metric on the brane (2.1.4):

$$S_H = \int d^4x \sqrt{-g^{(\mathrm{IR})}} \left[g^{\mu\nu}_{(\mathrm{IR})} (D_\mu H^\dagger)(D_\nu H) - \lambda \left(|H|^2 - v_0^2 \right)^2 \right]. \tag{2.2.18}$$

The dimensionful symmetry breaking parameter v_0 is assumed to have a natural value of order k. However, inserting the induced metric, we find that the action is not canonically normalized. Redefining the field $\widetilde{H} = e^{\pi kR} H$ yields a properly normalized action:

$$S_{H,\mathrm{eff}} = \int d^4x \left[(D^\mu \widetilde{H}^\dagger)(D_\mu \widetilde{H}) - \lambda \left(|\widetilde{H}|^2 - e^{-2\pi kR} v_0^2 \right)^2 \right]. \tag{2.2.19}$$

The Higgs VEV has been rescaled by an exponential factor:

$$v_0 \to v_0 e^{-\pi kR}, \tag{2.2.20}$$

and thus the Higgs mass itself is rescaled in exactly the same way. For fundamental parameters $M \sim k \sim v_0 \sim R^{-1}$ of order the 4D Planck scale, it is possible to achieve an effective scale on the IR brane of order 1 TeV with very modest hierarchies in the fundamental parameters. All that is required is that $e^{\pi kR}$ be $\mathcal{O}(10^{16})$, implying the product kR is $\mathcal{O}(10)$. Moreover, the result is general and applies to all dimensionful parameters localized on the IR brane.

Referring back to equation (2.2.16), we can see a striking physical prediction of the Randall-Sundrum model. If this solution to the hierarchy problem is correct, then Kaluza-Klein graviton modes should appear at the TeV scale! In fact, this remarkable prediction applies not just to gravitons, but to the excited modes of all types of particles that reside in the bulk of the spacetime. This is the subject to which we now turn our attention.

2.3 Bulk Fields

In their original model, Randall and Sundrum assumed all standard model field content was localized on the IR, or TeV brane. This assumption was made because the hierarchy

problem could only be solved if the Higgs was on the IR brane, where the effective energy scale was "warped down." However, there is no requirement that the gauge or fermion fields of the standard model live on the brane, as their masses are protected by gauge and chiral symmetries.

This fact led a number of authors to consider placing standard model fields in the bulk, starting with scalars [71] followed by gauge bosons [74, 75, 76, 77, 78] and fermions [79, 80, 78], eventually leading to the placement of the entire (supersymmetric) standard model in the bulk [77, 78]. Here, we review the treatment of bulk scalars, gauge fields, and fermions each in turn. We will specialize our treatment to AdS only when necessary to discuss particulars of hard-wall models. Otherwise, we keep our treatment as general as possible so that we can employ it again later.

2.3A Scalar Fields

We begin by discussing scalar fields. This discussion will serve as a useful reference point later when we discuss supersymmetry in the bulk and soft-wall models in which the Higgs boson necessarily resides in the bulk.

The action describing a complex scalar, Φ, is given by:

$$S_\Phi = -\int d^5x\sqrt{-g}\Big\{g^{MN}(D_M\Phi)(D_N\Phi) + M_\Phi^2|\Phi|^2\Big\}, \tag{2.3.1}$$

where D_M is the gauge covariant derivative. For now we study the free theory and set $D_M = \partial_M$. The mass parameter M_Φ^2 can consist of bulk and boundary terms. The bulk term must be even under reflection about y and is naturally of order k^2. It can therefore be parameterized as ak^2, where a is a dimensionless number of $\mathcal{O}(1)$. The boundary mass term must also be even and can be parameterized as $2bk\left[\delta(y) - \delta(y - \pi R)\right] = 2bke^{A(z)}\left[\delta(z - z_0) - \delta(z - z_1)\right]$ (see (2.1.5)). Note that we have assumed the boundary mass term is the same on the two boundaries. This in fact is a requirement in supersymmetric theories [78], which we discuss in Chapter 5. We will effectively drop this assumption when we treat "soft-wall" models in Chapter 3, which require modifying the IR boundary condition.

The bulk equations of motion are found by inserting the metric factors and varying the action. In terms of the conformal coordinate z, we have:

$$\eta^{\mu\nu}\partial_\mu\partial_\nu\Phi + e^{3A(z)}\partial_5\left(e^{-3A(z)}\partial_5\Phi\right) - ak^2e^{-2A(z)}\Phi = 0. \tag{2.3.2}$$

Inserting the ansatz:

$$\Phi(x,z) = \sum_{n=0}^{\infty} \Phi^{(n)}(x) f_{\Phi}^{(n)}(z), \tag{2.3.3}$$

where $\eta^{\mu\nu}\partial_\mu\partial_\nu\Phi^{(n)}(x) = m_n^2\Phi^{(n)}(x)$ yields a Sturm-Liouville equation for $f_\Phi^{(n)}$:

$$e^{3A(z)}\partial_5\left(e^{-3A(z)}\partial_5 f_\Phi^{(n)}(z)\right) + m_n^2 f_\Phi^{(n)}(z) - ak^2 e^{-2A(z)} f_\Phi^{(n)}(z) = 0. \tag{2.3.4}$$

Just as with the graviton field above, we can recast the equation into a Schrödinger equation for the transformed field $f_\Phi^{(n)} = e^{3A/2}\widetilde{f}_\Phi^{(n)}$. The equation then reads:

$$\left(-\partial_5^2 + V(z)\right)\widetilde{f}_\Phi^{(n)}(z) = m_n^2\widetilde{f}_\Phi^{(n)}(z), \tag{2.3.5}$$

but the potential has an extra term compared to (2.2.13):

$$V(z) = \left(\frac{3}{2}A'(z)\right)^2 - \frac{3}{2}A''(z) + M_\Phi^2 e^{-2A(z)}. \tag{2.3.6}$$

The canonical normalization condition is:

$$\int dz\, \widetilde{f}_\Phi^{(m)}(z)\widetilde{f}_\Phi^{(n)}(z) = \int dz\, e^{-3A(z)} f_\Phi^{(m)}(z) f_\Phi^{(n)}(z) = \delta^{mn}. \tag{2.3.7}$$

Specializing to a slice of AdS, $A(z) = \log kz$, it is useful to reparameterize the bulk mass. Without loss of generality, it can be written as

$$M_\Phi^2 = \left((\alpha + \frac{1}{2})(\alpha - \frac{1}{2}) - 15/4\right)k^2, \tag{2.3.8}$$

where $\alpha = \sqrt{4+a}$. Inserting this into the potential (2.3.6),the potential is now of the form $W^2(z) - W'(z)$ where

$$W(z) = \frac{\pm 2\alpha - 1}{2z}, \tag{2.3.9}$$

$$W^2(z) - W'(z) = V(z) = \frac{(2\alpha-1)(2\alpha+1)}{4z^2}. \tag{2.3.10}$$

It is clear that either sign choice yields the same equations of motion in the bulk. The solutions to (2.3.5) are given in terms of Bessel functions:

$$\widetilde{f}_\Phi^{(n)}(z) = N_\Phi^{(n)} z^{\frac{1}{2}}\left(J_\alpha(m_n z) + b_\Phi^{(n)} Y_\alpha(m_n z)\right), \tag{2.3.11}$$

subject to appropriate boundary conditions. The boundary conditions are due to the integration by parts leading to (2.3.2) as well as the brane mass terms in (2.3.1). The

action is extremized for a Dirichlet condition $f_\Phi^{(n)}(z_0) = f_\Phi^{(n)}(z_1) = 0$ or a modified Neumann condition,[2]

$$\left(f_\Phi^{(n)\prime} - e^{-A(z)} bk f_\Phi^{(n)}\right)\Big|_{z_0,z_1} = 0. \tag{2.3.12}$$

A zero-mode exists only when the bulk and boundary masses are appropriately tuned. The tuning condition is most simply revealed by considering the superpotential (2.3.9). Because the Schrödinger equation (2.3.5) can be factorized as

$$\left(-\partial_5 + W(z)\right)\left(\partial_5 + W(z)\right) \widetilde{f}_\Phi^{(n)} = m_n^2 \widetilde{f}_\Phi^{(n)}, \tag{2.3.13}$$

it is easy to see that there is a zero-mode solution given by:

$$\widetilde{f}_\Phi^{(0)}(z) = N_\Phi^{(0)} e^{-\int^z W(z')\mathrm{d}z'} = z^{\frac{1}{2}\mp\alpha}, \tag{2.3.14}$$

$$f_\Phi^{(0)}(z) = N_\Phi^{(0)} z^{2\mp\alpha}. \tag{2.3.15}$$

Comparing with (2.3.12), the tuning condition is given by the relations

$$b = 2 \mp \alpha = 2 \pm \sqrt{4+a}, \tag{2.3.16}$$

where in the last line we have reverted back to the original parameterization of the bulk mass.

For $z_0 \ll z_1$ and $m_n \ll (z_0)^{-1}$, we can expand the Bessel functions to arrive at an approximate expression for the mass spectrum as a function of excitation number n,

$$m_n z_1 \approx \left(n + \frac{\alpha}{2} - \frac{3}{4}\right)\pi. \tag{2.3.17}$$

Finally, let us consider $W(z)$ a function of α as well, i.e. $W = W(z; \pm\alpha)$. Then

$$W(z;\alpha)^2 + W'(z;\alpha) = W(z;\alpha \mp 1)^2 - W'(z;\alpha \mp 1). \tag{2.3.18}$$

where the sign choice corresponds to the choice in (2.3.9). This will be useful when we discuss fermions below. An implication of this is that two fields, 1 and 2, with $\alpha_1 = \alpha_2 \pm 1$ can have identical spectra at the massive level. This will be important during our discussion of supersymmetry in Chapter 5.

[2] The prescription for treating the delta function is to integrate only to one side of the boundary, hence the "missing" factor of 2.

2.3B Gauge Fields

Up to terms quadratic in the gauge fields A_M, the bulk action for a $U(1)$ gauge field is:

$$S_\Phi = -\int d^5x\sqrt{-g}\left(-\frac{1}{4g_5^2}g^{MR}g^{NS}F_{MN}F_{RS}\right), \tag{2.3.19}$$

where $F_{MN} = \partial_M A_N - \partial_N A_M$. To study the KK spectrum, we will work in the gauge $A_5 = 0$. The equations of motion in this gauge are given by:

$$-\eta^{\mu\rho}\eta^{\nu\sigma}\partial_\mu F_{\rho\sigma} + \eta^{\nu\rho}e^{A(z)}\partial_5\left(e^{-A(z)}\partial_5 A_\rho\right) = 0. \tag{2.3.20}$$

We insert the KK-decomposition for the fields $A_\mu(x,y)$:

$$A_\mu(x,y) = \sum_{n=0}^{\infty} A_\mu^{(n)}(x)f_A^{(n)}(z), \tag{2.3.21}$$

where $\partial^\mu F_{\mu\nu}^{(n)} = m_n^2 A_\nu^{(n)}$.[3] The canonical normalization condition is:

$$\int dz\,\sqrt{-g}\,e^{4A}f_A^{(m)}(z)f_A^{(m)}(z) = \int dz\widetilde{f}_A^{(m)}(z)\widetilde{f}_A^{(n)}(z) = \delta^{mn}, \tag{2.3.22}$$

where $\widetilde{f}_A^{(n)} = e^{-A/2}f_A^{(n)}$. The equation of motion for the bulk field $f_A^{(n)}$ becomes:

$$-e^{A(z)}\partial_5\left(e^{-A(z)}\partial_5 f_A^{(n)}\right) = m_n^2 f_A^{(n)}. \tag{2.3.23}$$

The zero-mode is easily found to be constant $f_A^{(0)}(z) = f_A^{(0)} = 1/\sqrt{2\pi R}$ and is trivially consistent with the Neumann boundary condition $(\partial_5 A_\mu)\,|_{z_0,z_1} = 0$. In direct analogy with our treatment of gravitons and scalar fields, it is easy to show that the field $\widetilde{f}_A^{(n)}$ obeys a Schrödinger equation:

$$\left[-\partial_5^2 + W^2 - W'\right]\widetilde{f}_A^{(n)} = m_n^2\widetilde{f}_A^{(n)}, \tag{2.3.24}$$

$$W(z) = \frac{A'}{2}. \tag{2.3.25}$$

The solutions in a slice of AdS are again given by Bessel functions:

$$\widetilde{f}_A^{(n)}(z) = N_A^{(n)}z^{\frac{1}{2}}\left(J_1(m_n z) + b_A^{(n)}Y_1(m_n z)\right). \tag{2.3.26}$$

For the Neumann boundary conditions, we can once again expand and find that the approximate masses for the Kaluza-Klein modes are,

$$m_n z_1 \simeq \left(n - \frac{1}{4}\right)\pi. \tag{2.3.27}$$

[3] Our gauge choice breaks 4D gauge invariance at the massive level; it is possible to choose a more useful gauge for evaluating Feynman diagrams in warped space [81, 82].

2.3C Fermions

Modeling fermions in a warped extra dimension requires machinery beyond what we have already considered [83, 84]. We start with the Clifford algebra in curved space:

$$\{\Gamma^M, \Gamma^N\} = 2g^{MN}. \tag{2.3.28}$$

The upper-case gamma matrices with spacetime indices (see the conventions in the introduction) are related to the lower-case Dirac gamma matrices by the vielbein ("fünfbein" in five dimensions) as $\Gamma^M = e^M_A \gamma^A$, where the γ^A satisfy the usual Clifford algebra in Minkowski space,

$$\{\gamma_M, \gamma_N\} = 2\ \eta_{MN} = 2\ \mathrm{diag}(-,+,+,+,+), \tag{2.3.29}$$

and the definition of the vielbein,

$$\eta^{AB} e^M_A e^N_B = g^{MN}, \tag{2.3.30}$$

leads to their colloquial description as the "square-root" of the metric.

The irreducible spinor representation in five dimensions consists of four-component Dirac fermions, to be contrasted with the two-component Weyl fermions in four dimensions. We take as a basis the following gamma matrices:

$$\gamma^\mu = -i \begin{pmatrix} 0 & \sigma^\mu \\ \overline{\sigma}^\mu & 0 \end{pmatrix}, \qquad \gamma^5 = \begin{pmatrix} 1 & 0 \\ 0 & -1 \end{pmatrix}, \tag{2.3.31}$$

where $\sigma^\mu = (1, \sigma^i)$, $\overline{\sigma}^\mu = (1, -\sigma^i)$, and σ^i are the usual Pauli matrices. Note that with this basis the proper Dirac conjugate is defined as $\overline{\Psi} = \Psi^\dagger i\gamma^0$. The action describing a fermion with bulk mass M_Ψ can be written in the familiar way,

$$S_\Psi = -i \int \mathrm{d}^5 x \sqrt{-g} \left(\overline{\Psi} \Gamma^M D_M \Psi + M_\Psi \overline{\Psi} \Psi \right), \tag{2.3.32}$$

where the covariant derivative is defined as $D_M = \partial_M + \omega_M$ (plus any relevant gauge covariant piece). Here ω_M is the spin connection, defined as:

$$\omega_M = \frac{i}{2} \mathcal{J}_{AB}\ \omega^{AB}_M, \tag{2.3.33}$$

in terms of the Lorentz generators,

$$\mathcal{J}_{AB} = -\frac{i}{4}\ \left[\gamma^A, \gamma^B\right]. \tag{2.3.34}$$

The coefficients $\omega_M{}^A{}_B$ given by,

$$\omega_M{}^A{}_B = e_R^A \; e_B^S \; \Gamma_{MS}^R - e_B^R \; \partial_M e_S^A, \tag{2.3.35}$$

where Γ_{MS}^R is the Christoffel symbol.

These relations simplify greatly in the case of the conformal metric to which we now specialize, $g_{MN} = e^{-2A(z)}\eta_{MN}$. The fünfbein is given by

$$e_M^A = e^{-A(z)}\delta_M^A, \tag{2.3.36}$$

and the spin connection is found to be

$$\omega_M(z) = (\omega_\mu, \omega_5) = \left(-\frac{A'}{2}\gamma_\mu\gamma^5, 0\right). \tag{2.3.37}$$

It is straightforward to transform coordinates using, for example, equation (2.1.5), under which $A'(z) \to e^{-A(y)}A'(y)$:

$$\omega_M(y) = \left(-\frac{A'}{2}e^{-A}\gamma_\mu\gamma^5, 0\right). \tag{2.3.38}$$

However, one may also take into account the spin connection by replacing the Lagrangian density, $\mathcal{L}$, in the action (2.3.32) with the manifestly real density, $(\mathcal{L} + \mathcal{L}^\dagger)/2$:

$$S_\Psi = -i \int \mathrm{d}^5x\sqrt{-g}\left\{\frac{1}{2}\left[\overline{\Psi}\Gamma^M(D_M\Psi) - (D_M\overline{\Psi})\Gamma^M\Psi\right] + M_\Psi\overline{\Psi}\Psi\right\}. \tag{2.3.39}$$

where D_M is now simply a gauge-covariant derivative (i.e. the spin connection can be omitted). This can simplify many calculations and reduce notational clutter.

Note that the orbifold symmetry forbids any Dirac mass term on the boundaries. This is because the parity operator in 5D is $\Psi(-y) = \pm\gamma_5\Psi(y)$, where absent specified fermion interactions the sign is ambiguous. In either case, this implies $\overline{\Psi}\Psi$ is odd and vanishes on the boundary. Accordingly, the mass term M_Ψ must also be odd and can be parameterized as $M_\Psi = ck\ \mathrm{sgn}(y) = ck\ \mathrm{sgn}(z - z_0)$.

The representation (2.3.31) allows for a convenient decomposition of fermions in terms of even and odd fields $\Psi = \Psi_+ + \Psi_-$, or

$$\Psi = \begin{pmatrix} \Psi_+ \\ \Psi_- \end{pmatrix}, \tag{2.3.40}$$

where $\gamma_5\Psi_\pm = \pm\Psi_\pm$. Then choosing either of $\Psi(-y) = \pm\gamma_5\Psi(y)$ is interpreted as defining the chirality of fermions on the boundary at $z = z_0$ ($y = 0$) [78, 85, 86].

As discussed earlier, the orbifold requirements (2.1.1) allow for the possibility of separately defining the chirality of the fermions on the two boundaries at $z = z_0$ and $z = z_1$. This allows for many interesting possibilities. For example, it can provide a mechanism by which supersymmetry is broken [20] similar to the Scherk-Schwarz mechanism in flat space [18, 19], or aid in unification schemes [87].

For now, we consider only fields that are either even on both boundaries, i.e. $\Psi(y) = \Psi(-y)$ and $\Psi(\pi R - y) = \Psi(\pi R + y)$, or odd on both boundaries, i.e. $\Psi(y) = -\Psi(-y)$ and $\Psi(\pi R - y) = -\Psi(\pi R + y)$. The former in particular lead to massless modes that may be identified with the fermions of the standard model.

Into (2.3.39), we insert $\Psi = \Psi_+ + \Psi_-$, where Ψ_+ and Ψ_- are the left- and right-handed components of the Dirac fermion, respectively. Extremizing the action yields a pair of coupled first-order differential equations,

$$\eta^{\mu\nu}\gamma_\mu\partial_\nu\Psi_\mp \pm e^{2A}\partial_5 e^{-2A}\Psi_\pm + e^{-A}M_\Psi\Psi_\pm = 0, \tag{2.3.41}$$

which may be simplified by rewriting in terms of the transformed field, $\widetilde{\Psi} = e^{-2A}\Psi$:

$$\eta^{\mu\nu}\gamma_\mu\partial_\nu\widetilde{\Psi}_\mp \pm \partial_5\widetilde{\Psi}_\pm + e^{-A}M_\Psi\widetilde{\Psi}_\pm = 0. \tag{2.3.42}$$

Inserting the KK decomposition for $\widetilde{\Psi}$,

$$\widetilde{\Psi}_\pm(x,z) = \sum_{n=0}^{\infty}\psi_\pm^{(n)}(x)\widetilde{f}_{\Psi\pm}^{(n)}(z), \tag{2.3.43}$$

and applying the 4D Dirac equation $\gamma^\mu\partial_\mu\psi_\pm = -m_n\psi_\mp$, yields a 5D analog of the Dirac equation for $\widetilde{f}_{\Psi\pm}$:

$$\left(\pm\partial_5 + e^{-A}M_\Psi\right)\widetilde{f}_{\Psi\pm} = m_n\widetilde{f}_{\Psi\mp}. \tag{2.3.44}$$

The system is easily decoupled by converting to a second order system. The equations for the fields $\widetilde{f}_\pm$ may be written as a pair of Schrödinger equations with "supersymmetric partner potentials" [67],

$$\left(-\partial_5^2 + V_\pm\right)\widetilde{f}_{\Psi\pm} = m_n^2\widetilde{f}_{\Psi\pm}, \tag{2.3.45}$$

where $V_\pm = W^2 \mp W'$ (note the sign difference) and $W(z) = M_\Psi e^{-A(z)}$. In AdS, $W(z) = c/z$ with our parameterization of the bulk mass.

Note that in AdS, the form of the superpotential is exactly the same as that introduced for scalar fields above in Section 2.3A if we identify $\alpha \leftrightarrow c + 1/2$. Therefore, the solution for the fields $\widetilde{f}_{\Psi+}$ is the same as (2.3.11) up to a simple relabeling. Furthermore, since $\alpha - 1 \leftrightarrow c - 1/2$, we can automatically generate the solutions for the fields $f_{\Psi-}$ using the rule (2.3.18). The result is,

$$\widetilde{f}^{(n)}_{\Psi\pm}(z) = N^{(n)}_{\Psi\pm} z^{\frac{1}{2}} \left(J_{c\pm\frac{1}{2}}(m_n z) + b^{(n)}_{\Psi} Y_{c\pm\frac{1}{2}}(m_n z) \right), \tag{2.3.46}$$

subject to the canonical normalization condition,

$$\int dz \sqrt{-g}\, e^A f^{(m)}_{\Psi\pm}(z) f^{(n)}_{\Psi\pm}(z) = \int dz\, \widetilde{f}^{(m)}_{\Psi\pm}(z) \widetilde{f}^{(n)}_{\Psi\pm}(z) = \delta_{mn}. \tag{2.3.47}$$

The boundary contribution to the action is extremized only when one of the fields $\Psi_\pm$ vanishes there–i.e., it satisfies a Dirichlet boundary condition. This is equivalent to fixing the behavior of Ψ under the $\mathbb{Z}_2$ reflection. Applying a Dirichlet condition to $\widetilde{f}_\pm$ corresponds to applying a modified Neumann condition to $\widetilde{f}_\mp$ due to the equations of motion (2.3.44). When $\Psi_\pm$ obeys Dirichlet boundary conditions, the mass spectrum is given approximately by:

$$m_n z_1 \approx \left(n + \frac{|2c \pm 1|}{4} - \frac{1}{4} \right) \pi. \tag{2.3.48}$$

Both modes $\widetilde{f}_\pm$ admit zero-mode solutions,

$$\widetilde{f}^{(0)}_{\pm} = N^{(0)}_{\Psi\pm} e^{\mp \int^z W(z')\mathrm{d}z'} = N^{(0)}_{\Psi\pm} z^{\mp c}, \tag{2.3.49}$$

however only the modified Neumann condition is consistent with the zero-mode solution (2.3.49), implying that the Dirichlet condition kills the other mode entirely. Thus, in the effective 4D theory, we get a Kaluza-Klein tower of massive Dirac fermions, but at the massless level there is a single chiral fermion with the opposite chirality mode projected out of the theory. This is the mechanism by which the $\mathbb{Z}_2$ orbifold is able to recover the chiral fermions of the standard model.

2.3D Bulk Fields Summary

In a slice of AdS, the bulk scalar, gauge, and fermion wavefunctions f_Φ, f_A and $f_{\Psi\pm}$, as well as the graviton wavefunction f_h, can be concisely described in terms of factorizable

Schrödinger equations:

$$(-\partial_5 + W_\phi)(\partial_5 + W_\phi)\widetilde{f}_\phi^{(n)} = m_n^2 \widetilde{f}_\phi^{(n)}, \tag{2.3.50}$$

for $\phi \in \{h,\ A,\ \Phi, \Psi_\pm\}$ where $\widetilde{f}_\phi = e^{\frac{s_\phi}{2}A(z)} f_\phi$ and

$$W_\phi(z) = \tfrac{2\alpha_\phi - 1}{2z}, \tag{2.3.51}$$

$$\begin{aligned} &\alpha_h = 2, \quad \alpha_A = 1, \quad \alpha_\Phi = \pm\sqrt{4+a}, \quad \alpha_{\Psi\pm} = c \pm \tfrac{1}{2}, \\ &s_h = 3, \quad s_A = 1, \qquad s_\Phi = 3, \qquad s_{\Psi\pm} = 4. \end{aligned} \tag{2.3.52}$$

If the bosonic fields satisfy a modified Neumann condition,

$$(\partial_5 + W_\phi)\widetilde{f}_\phi^{(n)}\big|_{z_0,z_1} = 0, \tag{2.3.53}$$

there exists a zero-mode solution given by

$$\widetilde{f}_\phi^{(0)} \sim e^{-\int^z W_\phi(z')dz'} \sim z^{\frac{1-2\alpha_\phi}{2}}. \tag{2.3.54}$$

Otherwise they must obey a a Dirichlet condition and there is no massless mode.

One of the fermion fields $f_\pm$ must satisfy a Dirichlet condition, which corresponds to a modified Neumann condition on the other field through the first-order equations of motion:

$$\widetilde{f}_{\Psi\mp}\big|_{z_0,z_1} = (\pm\partial_5 + W_{\Psi+})\widetilde{f}_\pm\big|_{z_0,z_1} = 0. \tag{2.3.55}$$

Then the corresponding zero-mode solution is given by

$$\widetilde{f}_{\Psi\pm}^{(0)} \sim e^{\mp\int^z W_{\Psi+}(z')dz'} \sim z^{\mp c}. \tag{2.3.56}$$

That the compact notation (2.3.50) can describe both fermion modes is peculiar to the slice of AdS and follows from the relation (2.3.18).

The massive modes for all fields are given in terms of Bessel functions as

$$\widetilde{f}_\phi^{(n)}(z) = N_\phi^{(n)} z^{\frac{1}{2}} \left(J_{\alpha_\phi}(m_n z) + b_\phi^{(n)} Y_{\alpha_\phi}(m_n z) \right). \tag{2.3.57}$$

while the mass spectrum is given approximately by

$$m_n \simeq \begin{cases} \left(n + \frac{\alpha}{2} - \frac{3}{4}\right)\frac{\pi}{z_1} = \left(n + \frac{\alpha}{2} - \frac{3}{4}\right)\pi k e^{-\pi k R} & \text{for bosons,} \\ \left(n + \frac{\alpha}{2} - \frac{1}{4}\right)\frac{\pi}{z_1} = \left(n + \frac{\alpha}{2} - \frac{1}{4}\right)\pi k e^{-\pi k R} & \text{for fermions.} \end{cases} \tag{2.3.58}$$

Thus all particles have KK-towers starting at the TeV scale and growing linearly in mass with excitation number, n.

Wavefunction Localization Properties

The localization properties of wavefunctions are most apparent when the wavefunctions are written with respect to the flat coordinate, y. Using (2.1.5), we define a rescaled function, $\widehat{f}_\phi^{(n)}(y) = e^{A(y)/2}\widetilde{f}_\phi^{(n)}(y)$ such that

$$\int dz\, \widetilde{f}_\phi^{(m)}(z)\widetilde{f}_\phi^{(n)}(z) = \int dy\, \widehat{f}_\phi^{(m)}(y)\widehat{f}_\phi^{(n)}(y). \tag{2.3.59}$$

The localization properties are then manifest in the functional form of $\widehat{f}_\phi^{(n)}(y)$. The rescaled zero-mode profiles are then:

$$\widehat{f}_\phi^{(0)}(y) = e^{\frac{ky}{2}}\widetilde{f}_\phi^{(0)} \sim e^{(1-\alpha_\phi)ky}, \tag{2.3.60}$$

for $\phi \in \{h, A, \Phi, \Psi_+\}$, while

$$\widehat{f}_{\Psi_-}^{(0)}(y) \sim e^{(\alpha_{\Psi_+})ky}. \tag{2.3.61}$$

For bosons, $\alpha_\phi > 1$ corresponds to a UV-localized field with respect to the flat metric, while $\alpha_\phi < 1$ corresponds to an IR-localized field. Thus, the graviton zero-mode ($\alpha_h = 2$) is UV-localized, which we can interpret as resulting in the apparent weakness of gravity on the IR brane,[4] while the gauge boson zero-modes ($\alpha_A = 1$) are not localized at all. The scalar zero-mode, on the other hand, can be localized anywhere in the bulk dependent on the bulk mass parameter a. The fermion zero-modes can also be localized anywhere. When $c > 1/2$ ($c < -1/2$), Ψ_+ (Ψ_-) has a UV-localized zero-mode , while for $c > 1/2$ ($c > -1/2$), the mode is IR-localized.

The KK-modes, on the other hand, are all peaked in the IR. To illustrate this, we have included in Figure 2.1 a plot of the first several gauge boson KK-modes. The plots for other fields are similar.

2.4 Standard Model Couplings

2.4A Yukawa Couplings

We have seen how the orbifold boundary conditions lead to massless, chiral fermions in the free theory. In this section, we will describe how hierarchical fermion masses can be

[4] Note however that gravity couples equally to all bulk fields, regardless of localization, as 4D coordinate invariance and thus the equivalence principle is not broken.

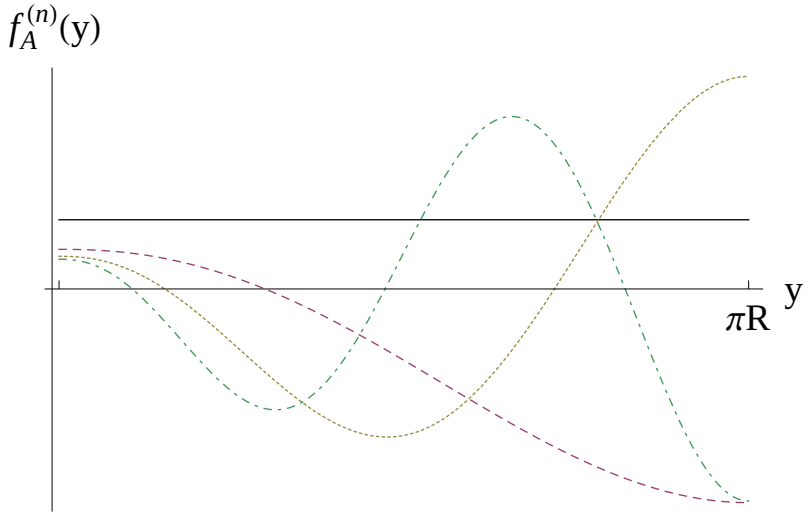

Figure 2.1: The first several Kaluza-Klein gauge boson profiles in the Randall-Sundrum background, coresponding to excitation numbers $n = 0$ (solid line), $n = 1$ (dashed), $n = 2$ (dotted), and $n = 3$ (dot-dashed).

obtained through Yukawa interactions, following the approaches of Refs. [79, 78]. For simplicity, we will only consider a single fermion generation here and will treat the full case in Chapter 4.

We begin by introducing two fermion fields in the bulk, $\Psi_L = \Psi_{L+} + \Psi_{L-}$ and $\Psi_R = \Psi_{R+} + \Psi_{R-}$. The subscripts L and R are labels indicating the types of boundary conditions imposed on each field. At the massless level, Ψ_L is a left-handed field while Ψ_R is right-handed. The corresponding boundary conditions are:

$$\Psi_{L-}(z_0) = \Psi_{L-}(z_1) = 0, \qquad \Psi_{R+}(z_0) = \Psi_{R+}(z_1) = 0. \tag{2.4.1}$$

In a realistic model, the labels would also specify the group transformation properties of the field. For example, if the fields are to be associated with a charged lepton, Ψ_L (Ψ_R) would transform as a doublet (singlet) under $SU(2)_L$.

To lift the zero-modes, we introduce a scalar field $H(x, z)$ that couples the left- and right-handed fields. For simplicity, we will consider a field localized on the IR brane $N_H H(x, z) = 2H(x)e^{A(z)}\delta(z - z_1)$, as in Section 2.2B. Then the 5D Yukawa coupling

takes the form

$$S_{\text{Yukawa}} = \int d^5x\sqrt{-g}\lambda_5 \left[\overline{\Psi}_L\Psi_R + \overline{\Psi}_R\Psi_L\right] \frac{H(x)}{N_H} e^{A(z)}\delta(z-z_0) \tag{2.4.2}$$

$$\to \lambda_4 \int d^4x \left(\overline{\psi}_{L+}\psi_{R-} + \overline{\psi}_{R-}\psi_{L+}\right) H(x). \tag{2.4.3}$$

where λ_5 is assumed to be $\mathcal{O}(1/k)$ and the effective 4D Yukawa coupling is given by:

$$\lambda_4 \equiv \frac{1}{N_H}\int dz e^{-5A(z)}\lambda_5 f^{(0)}_{L+}(z) f^{(0)}_{R-}(z) e^{A(z)}\delta(z-z_1) \tag{2.4.4}$$

$$= \lambda_5 \frac{e^{-4A(z_1)}}{N_H} f^{(0)}_{L+}(z_1) f^{(0)}_{R-}(z_1) = \frac{\lambda_5}{N_H}\widetilde{f}^{(0)}_{L+}(z_1)\widetilde{f}^{(0)}_{R-}(z_1). \tag{2.4.5}$$

The Higgs normalization follows from canonical normalization of the 4D kinetic term. For an IR localized Higgs, $N_H = e^{A(z_1)}$ as in (2.2.19).

In an AdS background, the properly normalized fermion zero-modes are given by

$$f^{(0)}_{L+/R-}(z_1) = \sqrt{\frac{\left(1/2 \mp c_{L/R}\right)k}{(kz_1)^{1\mp 2c_{L/R}} - 1}}(kz)^{\mp c_{L/R}} \tag{2.4.6}$$

$$= \sqrt{\frac{\left(1/2 \mp c_{L/R}\right)}{e^{(1\mp 2c_{L/R})\pi kR} - 1}} e^{\mp c_{L/R} ky}. \tag{2.4.7}$$

Assuming $c_L = -c_R = c$ and $c > 1/2$, we see that the 4D Yukawa coupling

$$\lambda_4 \simeq \lambda_5 k \left(c - \frac{1}{2}\right) e^{(1-2c)\pi kR} \tag{2.4.8}$$

drops off exponentially with the $\mathcal{O}(1)$ localization parameter, c. Indeed, when the Higgs VEV on the IR brane is of order $ke^{-\pi kR} \sim$ TeV and $k \sim M_P \sim 10^{15}$ TeV, the electron Yukawa coupling of $\mathcal{O}(10^{-6})$ is obtained for $c \simeq 0.6$. As we saw in the previous section, there is a simple geographic interpretation to this behavior. The realm $c_L > 1/2$ ($c_R < -1/2$) corresponds to UV-localized fermions. That is, their wavefunctions are peaked near the UV brane as can be seen in (2.3.60) and (2.3.61). Thus, the fermion wavefunctions are exponentially suppressed on the IR brane. The small overlap with the IR-localized Higgs field is the reason for the sharp suppression of the effective 4D Yukawa couplings.

On the other hand, when $c < 1/2$, the fermions are IR localized and there is no large suppression:

$$\lambda_4 \simeq \lambda_5 k \left(\frac{1}{2} - c\right). \tag{2.4.9}$$

Thus, the full range of Yukawa couplings from the electron to the top quark is easily explained in terms of $\mathcal{O}(1)$ 5D parameters.

To describe multiple generations of fermions, the fields are promoted to vectors in flavor space $\Psi^i_{L/R}$ while λ_5 and λ_4 are promoted to matrices λ_5^{ij} and λ_4^{ij}. Doing so necessarily introduces new flavor structure to the standard model, and has therefore been studied by a number of authors [88, 89, 90, 91, 92, 93, 94, 95].

2.4B Fermion Gauge Couplings & Flavor Protection

The calculation of gauge couplings follows a similar recipe. The contribution to the bulk action is given by a familiar gauge term. We will again limit our attention to a $U(1)$ gauge field and a single generation of fermions. The gauge coupling term in the bulk action is:

$$S_{\text{int}} = i \int d^5x \, \sqrt{-g} \, g_5 \left(\overline{\Psi}(x,z) \Gamma^M A_M \Psi(x,z) \right) \tag{2.4.10}$$

We again work in the gauge $A_5 = 0$ and insert the KK expansions for the fields Ψ and A_M. Let us focus on the coupling of a zero-mode gauge boson to the tower of fermions:

$$\begin{aligned} S_{\text{int}} \quad &\Rightarrow \quad \sum_{m,n=0}^{\infty} i \int d^5z e^{-5A} g_5 \left(\overline{\psi}^{(m)} e^A \gamma^\mu A_\mu^{(0)} \psi^{(n)} \right) \left(f_A^{(0)} f_\Psi^{(m)} f_\Psi^{(n)} \right) && (2.4.11) \\ &= \quad \sum_{m,n=0}^{\infty} \frac{g_5}{\sqrt{2\pi R}} i \int d^4x \left(\overline{\psi}^{(m)} \gamma^\mu A_\mu^{(0)} \psi^{(n)} \right) \int dz \, e^{-4A} \left(f_\Psi^{(m)} f_\Psi^{(n)} \right) && (2.4.12) \\ &\equiv \quad \sum_{n=0}^{\infty} g_4 i \int d^4x \left(\overline{\psi}^{(n)} \gamma^\mu A_\mu^{(0)} \psi^{(n)} \right) && (2.4.13) \end{aligned}$$

where $g_4 \equiv g_5/\sqrt{2\pi R}$ and the last equality follows from the orthonormality condition (2.3.47). Thus, the gauge couplings are universal and 4D gauge invariance is preserved.

Next, of considerable importance is the couplings of the fermion zero-modes to the KK gauge bosons. Generically, these couplings would be expected to introduce large contributions to flavor changing amplitudes through, for example, KK gluon exchange. This would result in an extremely high lower bound for the Kaluza-Klein scale, so that the hierarchy problem is no longer solved. However, in practice things are not so severe.

Near the UV brane, the modified Neumann boundary condition on the gauge boson wavefunctions forces the KK-mode profiles to be approximately constant. This can be

seen in the plots in Figure 2.1, for example. As a result, fermions that are peaked strongly toward UV brane inherit couplings that are essentially independent of the localization parameter c, due to the same orthonormality condition. More specifically, whenever $c > 1/2$ ($c < -1/2$) for the fermion zero-mode $f_+^{(0)}(z)$ ($f_-^{(0)}(z)$), the gauge couplings become very nearly constant with varying c. Since the couplings are universal, they are also diagonal in any basis, and therefore there is only a very small contribution to new flavor changing neutral currents. Moreover, from (2.4.8), we can see that this is precisely the region of parameter space for which the effective 4D Yukawa couplings are small. We will return to this issue in more detail during our discussion of soft-wall models in Chapter 4, where we will show that this "GIM-like" mechanism is preserved.

Chapter 3

The Soft-Wall Warped Dimension

3.1 Motivation

The original Randall-Sundrum model [36] has undergone a series of generalizations and extensions since its original introduction over a decade ago. The warped extra dimension framework has grown such that it can now provide a compelling geometrical understanding of a number of mysteries left unexplained by the Standard Model (SM). By the AdS/CFT correspondence [38, 39, 40, 41, 42, 43], these models also admit weakly-coupled holographic descriptions of electroweak symmetry breaking and flavor physics arising from the dynamics of a strongly coupled conformal field theory.

In the original model a slice of AdS bounded by ultraviolet (UV) and infrared (IR) branes was used to solve the hierarchy problem. The exponential dependence of energy scales on position along the extra dimension provided a simple explanation for the low scale of electroweak symmetry breaking provided that all standard model particles were localized on the IR brane. Later, a number of authors began removing the standard model fields from the brane, allowing them to propagate in the bulk of spacetime. This was first done with the gauge fields [74, 75] and later the fermion fields as well [79, 77, 78]. With the gauge bosons and fermions in the bulk, fermion mass hierarchies result from the wavefunction overlap of SM fermions with an IR localized Higgs [79, 78, 80], leading to a fermion geography in the fifth dimension which explains the Yukawa coupling hierarchy and also naturally suppresses the scale of higher-dimension operators that can mediate dangerous processes [78, 80]. Furthermore, since the couplings between

fermions and Kaluza-Klein (KK) gauge modes are nearly universal, there exists a built-in "GIM" mechanism that avoids disastrously large contributions to flavor changing neutral current (FCNC) amplitudes.

A common feature of these extensions is the existence of an IR brane at which the warped dimension abruptly ends. This breaks the conformal symmetry of the theory, generating towers of four-dimensional (4D) particle states with KK mass spectra growing as $m_n^2 \sim n^2$. However, this "hard-wall" picture of the IR brane represents just one way to break conformal symmetry. A more general approach is to replace the IR brane with a so-called "soft wall," in which the departure from conformal symmetry progresses smoothly with position along the extra dimension. With the IR brane removed, all IR fields must reside in the bulk, and their wavefunctions and spectra are thus non-trivially altered by the presence of the soft wall. Given the range of potential functional shapes the soft-wall can take, a variety of KK mass spectra may be generated by considering this more general picture. This allows for a potentially greater phenomenological reach for the warped extra-dimension framework. The greater flexibility can be viewed from the dual holographic description as well; any operator of finite dimension responsible for conformal (or other) symmetry breaking can be modeled in the soft-wall background. In particular, placing the entire Standard Model in a soft-wall warped dimension offers an interesting framework for modeling the possible underlying dynamics of electroweak physics. Furthermore, it has been shown that the soft-wall background itself can arise dynamically from underlying physics [62], suggesting a possible route toward developing a more complete theory.

In this chapter, we describe the construction of a concrete 5D gravity model as a starting point to address the hierarchy problem and stability in the soft-wall framework. To this end, we will first review the background necessary to study physics in the soft-wall background. This includes a brief discussion of the possible dynamical origin of the model using the techniques of Ref. [62]. We will then discuss the phenomenology of gravitons and bulk fields in the model. Even though the fifth dimension is infinite, the KK spectrum can be discrete, with a variety of spacing between resonances. The discussion of bulk fermions is particularly involved. Specifically, it is necessary to move beyond the perturbative zero-mode approximation typically employed in hard-wall calculations and fully account for the 5D Yukawa interactions that generate position-dependent fermion

mass terms and lead to "twisting" of the standard model flavors in the extra space. For this reason, we devote the entire next chapter to the treatment of fermions. The final portion of this chapter is devoted to describing a concrete model of electroweak physics with custodial symmetry, including a description of the dynamics leading to an IR-peaked bulk Higgs condensate responsible for spontaneously breaking elecroweak symmetry. The experimental constraints are discussed and shown to be less stringent than in hard-wall models, suggesting the possibility of observing KK resonances at the TeV scale.

3.2 The Soft-Wall Background

3.2A Overview

The basic feature which distinguishes the soft-wall warped dimension from the usual hard-wall slice of AdS is the replacement of the IR brane with a smooth spacetime cutoff. This can be modeled in different ways. For example one can begin in the "string frame" by considering the background metric as being pure AdS, as in the original Randall-Sundrum scenario. Using the conformal coordinate z, this can be written as

$$ds^2 = g_{MN}dx^M dx^N = e^{-2A(z)}\eta_{MN}dx^M dx^N, \tag{3.2.1}$$

where $A(z) = \log kz$, k is the AdS curvature scale, and $\eta_{MN} = \text{diag}(-,+,+,+,+)$. Without either an IR brane or soft cutoff, a pure AdS spacetime results in a continuous spectra for all particles [37, 41]. In this picture, the soft-wall arises due to the presence of the "dilaton," Φ. The action then takes the form:

$$S = \int d^5x\sqrt{-g}\, e^{-\Phi}\mathcal{L}_{\text{String}}, \tag{3.2.2}$$

where $\mathcal{L}_{\text{String}}$ is the matter field Lagrangian in the string frame. In contrast to hard-wall models, the coordinate z extends to infinity, but the action remains finite assuming suitable conditions on Φ.

Alternatively, one can work in the "Einstein frame," where the cutoff arises as a result of a departure from pure AdS in the IR. From this point of view, the metric (3.2.1) is modified as follows:

$$A(z) \to \widetilde{A}(z) = \log kz + \widetilde{a}(z), \tag{3.2.3}$$

so that the action may be generally written:

$$S = \int d^5x \sqrt{-\widetilde{g}}\, \mathcal{L}_{\text{Einstein}}. \tag{3.2.4}$$

Both approaches have been used in the literature [62, 60, 61, 96, 63, 66, 97].

Importantly, it is possible to translate between the pictures using conformal coordinate transformations. Thus, for calculations we are free to work in whichever picture is most convenient. Although we are taking a phenomenological approach, we have in mind that Φ is to be identified with the string theory dilaton and the action (3.2.2) may originate from some particular D-brane construction [60]. Therefore, for most purposes, we will stick to the string frame picture. However, when discussing the dynamical origin of the background and gravitational fluctuations, it will be useful to employ the Einstein frame where Einstein's equations are considerably simpler.

In the holographic picture, Φ is responsible for the confining dynamics at infrared energy scales. Indeed, in this picture one can identify an effective running coupling that grows in the IR, $g_5^2 e^{\Phi} \sim e^{\Phi}/N_c$, with N_c the number of colors in the dual theory. Correspondingly, sources located at large z will be strongly coupled, and processes involving exchange of IR localized bulk KK modes can become nonperturbative at high energies [60, 61]. However, for UV localized matter, as in the electroweak models that we will present, the effective description will remain perturbative sufficiently far into the infrared region.

We will present the most general analytic results whenever possible. However there are many possible behaviors for the dilaton, and it is not possible to obtain closed form solutions for arbitrary profiles. For concreteness we will at times consider power-law behavior $\Phi(z) = (\mu z)^{\nu}$. The eigenfunctions of bosonic bulk fields with a power-law dilaton satisfy an analog 1D "Schrödinger" equation with a power-law potential. A simple WKB approximation then shows that for large mode number n the KK mass spectrum follows

$$m_n^2 \sim \mu^2\, n^{2-2/\nu}. \tag{3.2.5}$$

so that μ is roughly analogous to $(z_1)^{-1}$ in hard-wall models. Even though the conformal coordinate z extends to infinity, for $\nu > 1$ we obtain a discrete mass spectrum. In particular, for the case $\nu = 2$ the spectrum exhibits linear "Regge" behavior. Later we will specialize to this case as it allows for analytic results. As $\nu \to \infty$ we recover

the usual hard-wall mass spectrum $m_n^2 \sim n^2$. The dilaton power-law exponent, ν, therefore provides a continuous parameter in which the KK mass spectrum varies from a continuum to that associated with a compact extra dimension. As discussed in [61], there are other interesting but qualitatively distinct behaviors possible if $\nu \leq 1$. For example, a constant dilaton [37] leads to "unparticles" [98] from a 4D perspective, while "hidden valley" models [99] are obtained when $\nu = 1$ [100].

Though an IR brane is no longer needed, a UV boundary at small z is still required in order to obtain the zero modes identified with the SM fields, which otherwise would not be normalizable. This also follows from holography, because typically the zero modes are (primarily) elementary fields associated with "sources" on the UV brane, rather than composites emerging from the dual gauge theory. As in hard-wall models, the UV brane will be located at a position $z_0 = 1/k$.

3.2B A Concrete Dynamical Model

Though it is possible to study certain aspects of soft-wall phenomenology from a purely bottom-up approach, a number of important questions cannot be addressed without reference to an underlying gravity theory. A dynamical gravitational model is required, for example, to address issues regarding generation of hierarchies and stability. In this section we present a dynamical 5D gravitational model which leads to a soft-wall warped dimension. The model is the same as that in Ref. [62] with modifications to accommodate a UV boundary.

We start with the Einstein frame action describing gravity and two scalar fields, the "dilaton" ϕ and the "tachyon" T:

$$\begin{aligned} S &= \int d^5x\sqrt{-\widetilde{g}}\,\left(M^3R - \frac{1}{2}\widetilde{g}^{MN}\partial_M\phi\partial_N\phi - \frac{1}{2}\widetilde{g}^{MN}\partial_M T\partial_N T - V(\phi,T)\right) \\ &\quad - \int d^4x\sqrt{-\widetilde{g}_{UV}}\;\lambda_{UV}(\phi,T), \end{aligned} \tag{3.2.6}$$

where M is the 5D Planck scale. The relationship between ϕ and the dilaton Φ defined above will be described later. The bulk action contains a scalar potential $V(\phi,T)$, and there is UV boundary located at $z_0 = 1/k$. The induced metric on the boundary is denoted g_{UV} and there is a boundary potential λ_{UV}.

To solve (3.2.6), we introduce a "superpotential", $W(\phi,T)$, to convert the system

into a set of first-order differential equations [101, 102]. Using this procedure, we can write the bulk and boundary potentials in the simple form

$$V(\phi,T) = 18\left[\left(\frac{\partial W}{\partial \phi}\right)^2+\left(\frac{\partial W}{\partial T}\right)^2\right]-\frac{12}{M^3}W^2, \tag{3.2.7}$$

$$\lambda_{UV}(\phi,T) = 6\left[W(\phi_0,T_0)+\partial_\phi W(\phi_0,T_0)(\phi-\phi_0)+\partial_T W(\phi_0,T_0)(T-T_0)+\dots\right], \tag{3.2.8}$$

where ϕ_0, T_0 are the boundary values at $z = z_0$. The extra terms in the boundary potential may contain higher powers of $(\phi - \phi_0)$ and $(T - T_0)$ without affecting the background solution.

There exists a solution to the 5D gravity-dilaton-tachyon equations of motion with the metric $\widetilde{g}_{MN} = e^{-2\widetilde{A}(z)}\eta_{MN}$ and the background solutions [62]

$$\widetilde{A}(z) = \frac{2}{3}(\mu z)^\nu + \log kz\,, \tag{3.2.9}$$

$$\phi(z) = \sqrt{\frac{8}{3}}M^{3/2}(\mu z)^\nu\,, \tag{3.2.10}$$

$$T(z) = \pm 4\sqrt{1+1/\nu}\,M^{3/2}(\mu z)^{\nu/2}\,, \tag{3.2.11}$$

where the tilde in (3.2.9) distinguishes the Einstein frame from the "string" frame. Note also that there are additive constants in the solutions (3.2.10) and (3.2.11), which we have set to zero. The superpotential that gives rise to this solution is

$$W(\phi,T) = M^3 k\left[(\nu+1)e^{T^2/(24(1+1/\nu)M^3)}-\nu\left(1-\frac{\phi}{\sqrt{6}M^{3/2}}\right)e^{\phi/(\sqrt{6}M^{3/2})}\right], \tag{3.2.12}$$

from which the scalar potential can be obtained using Eq. (3.2.7).

The parameter μ is an integration constant in the solution and sets the IR scale of the soft wall. This is analogous to the radius in RS1, which is also identified as a modulus field. Without stabilization of the scale μ, there should exist a massless radion associated with this modulus. However, we will see next that the UV boundary potential can in fact stabilize μ, and we therefore expect that the radion becomes massive. A complete answer to this question can only be obtained by analyzing the fluctuations of the background solutions, which is beyond the scope of the present work (but see Ref. [103]).

The UV boundary conditions are found to be

$$M^3 e^{\widetilde{A}} \frac{\partial \widetilde{A}}{\partial z}\bigg|_{z_0} = W(\phi_0, T_0), \tag{3.2.13}$$

$$e^{\widetilde{A}} \frac{\partial \phi}{\partial z}\bigg|_{z_0} = 6\,\partial_\phi W(\phi_0, T_0), \tag{3.2.14}$$

$$e^{\widetilde{A}} \frac{\partial T}{\partial z}\bigg|_{z_0} = 6\,\partial_T W(\phi_0, T_0), \tag{3.2.15}$$

which imply that

$$\phi_0 = \sqrt{\frac{8}{3}} M^{3/2} (\mu z_0)^\nu\,, \tag{3.2.16}$$

$$T_0 = \pm 4\sqrt{(1+1/\nu)}\, M^{3/2} (\mu z_0)^{\nu/2}\,. \tag{3.2.17}$$

Taking $z_0 = 1/k$, Eqs. (3.2.16) and (3.2.17) fix the soft-wall scale to be

$$\mu = k \left(\sqrt{\frac{3}{8}} \frac{\phi_0}{M^{3/2}} \right)^{1/\nu} = k \left(\frac{1}{\pm 4\sqrt{1+1/\nu}} \frac{T_0}{M^{3/2}} \right)^{2/\nu}. \tag{3.2.18}$$

Note that (3.2.18) also implies a tuning between ϕ_0 and T_0. Clearly, a large hierarchy cannot be generated between the UV scale k and the soft-wall IR scale μ for $\nu > 1$ if natural values are assumed for the boundary values, $\phi_0 \sim T_0 \sim M^{3/2}$, as this implies $\mu \lesssim k$, with a larger hierarchy for smaller values of ν. In the case $\nu = 2$ on which we will focus later, it is clearly not possible to generate the Planck-weak scale hierarchy without a significant amount of tuning. Interestingly, the hierarchy $\mu/k \sim 10^{-16}$ can be naturally generated for $\phi_0 \sim 0.1\, M^{3/2}$ and $\nu \sim 1/13$, but this does not give rise to a discrete KK particle spectrum. A more involved discussion of naturalness in this model can be found in [103]. Their discussion can be related to the above construction by making the simple replacement $\eta_0 = T_0/\sqrt{2}$.

While the boundary action (3.2.8) fails to naturally generate a large hierarchy between k and μ, an alternative way to satisfy the boundary conditions for ϕ and T is to let

$$\lambda_{UV}(\phi, T) = 6W(\phi, T). \tag{3.2.19}$$

The boundary conditions following from the variational principle do not then fix the IR scale μ. With this assumption other stabilization mechanisms can then be explored.

For example, we might consider an additional scalar field S, as in the Goldberger-Wise mechanism [71], with a small amplitude so that the backreaction on the metric can be neglected. If the field has a profile $S(z) \sim M^{3/2}(\mu z)^{\beta}$, and boundary condition analogous to those in (3.2.14) and (3.2.15), this would suggest $\mu/k \sim \left(S_0/M^{3/2}\right)^{1/\beta}$. A large hierarchy between k and μ would be obtained if $0 < \beta < 1$.

Although our main application of the soft-wall background will be to model electroweak physics, one can ask whether ordinary 4D gravity can be incorporated naturally into our model. The 4D Planck mass is given by

$$\begin{aligned} M_P^2 &= M^3 \int_{z_0}^{\infty} dz\, e^{-3\widetilde{A}(z)}, \\ &= \frac{2^{2/\nu}}{\nu} \frac{M^3\mu^2}{k^3}\, \Gamma\left(-\frac{2}{\nu}, 2\left(\frac{\mu}{k}\right)^{\nu}\right) \simeq \frac{M^3}{2k}, \end{aligned} \tag{3.2.20}$$

where $\Gamma(n,x)$ is the incomplete Gamma function, and we have used $z_0 = 1/k$ and assumed $\mu/k \ll 1$ in the last step. We can see that there is a problem because we would like to have $\mu \sim$ TeV to model electroweak physics. Lacking a robust mechanism that generates a hierarchy between μ and k means that $k \sim \mu \sim$ TeV. If we take as usual $k \lesssim M$, then according to (3.2.20) we cannot account for the weakness of gravity.

With these considerations, there are two possible cases for the UV scale $k \lesssim M$: (i) $k \ll M_P$, i.e. there is no large hierarchy and we project out the zero-mode graviton with Dirichlet conditions (for concreteness we will take $k \sim 1000\mu$ as in [104]); (ii) $k \sim M_P$, i.e. we assume a suitable stabilization mechanism may be found and apply Neumann conditions to allow a massless graviton.

Note that the metric (3.2.1) and action describing matter fields (3.2.2) is defined in the string frame, which is obtained by rescaling the dilaton $\phi = \sqrt{8/3}M^{3/2}\Phi$ and performing a conformal transformation $g_{MN} \to e^{-4\Phi/3} g_{MN}$. In the string frame, the background solutions for the metric and dilaton become

$$A(z) = \log kz, \tag{3.2.21}$$

$$\Phi(z) = (\mu z)^{\nu}. \tag{3.2.22}$$

We have a pure AdS metric and power-law dilaton as advertised in Section 3.2A. Unless otherwise specified we will now restrict to $\nu = 2$. This will give rise to a linear Regge-like mass spectrum and will enable analytic solutions to be obtained. Other values of ν will lead to qualitatively similar features.

3.2C Gravity in the Soft-Wall

To study the graviton modes, we examine fluctuations of the background metric in the Einstein frame, $\widetilde{g}_{MN}$. The most general expression for the perturbed metric leading to 4D graviton modes takes the form of (2.2.1):

$$ds^2 = e^{-2\widetilde{A}(z)}\big[\,(\eta_{\mu\nu} + h_{\mu\nu}(x,z))\,dx^\mu dx^\nu + dz^2\big]. \tag{3.2.23}$$

Thus, it is straightforward to adapt the results of Sections 2.2A and 2.3D. In the transverse-traceless gauge $\partial_\mu h^{\mu\nu} = h^\mu_\mu = 0$ and using the KK expansion (2.2.8), the equations of motion for the z-dependent piece $f_h^{(n)}(z)$ becomes

$$\partial_5(e^{-3\widetilde{A}}\partial_5 f_h^{(n)}(z)) + m_n^2 e^{-3\widetilde{A}} f_h^{(n)}(z) = 0. \tag{3.2.24}$$

The redefinition $f_h^{(n)}(z) = e^{3\widetilde{A}(z)/2}\widetilde{f}_h^n(z)$ brings the equation of motion into the form of a factorizable 1D Schrödinger equation with potential $V(z) = W^2 - W'$,

$$(-\partial_5 + W(z))\,(\partial_5 + W(z))\,\widetilde{f}_h^{(n)}(z) = m_n^2 \widetilde{f}_h^{(n)}(z), \tag{3.2.25}$$

where

$$W(z) = \frac{3}{2}\widetilde{A}', \tag{3.2.26}$$

$$V(z) = 4\mu^4 z^2 + 4\mu^2 + \frac{15}{4z^2}, \tag{3.2.27}$$

and the solutions are normalized as

$$M^3 \int_{z_0}^{\infty} dz\, \widetilde{f}_h^{(n)}(z)\widetilde{f}_h^{(n)}(z) = \delta^{mn}. \tag{3.2.28}$$

With a Neumann UV boundary condition $\partial_5 f_h^{(n)}|_{z_0} = 0$, we can see that a massless mode $f_h^{(0)}(z) = 1/M_P$ still exists, where M_P is defined in (3.2.20). This is expected since we have not broken 4D coordinate invariance.

Next we turn to $m_n \neq 0$. The potential is familiar as the radial equation for a two-dimensional harmonic oscillator. Redefining $\xi = \sqrt{2}\mu z$, the Schrödinger equation is now

$$\left(-\partial_\xi^2 + \xi^2 + \frac{m^2 - 1/4}{\xi^2}\right)\widetilde{f}_h^n(z) = \widehat{E}_n \widetilde{f}_h^n(z), \tag{3.2.29}$$

where $\widehat{E}_n = \left(m_n^2 - 4\mu^2\right)/2\mu^2$ and $m = 2$. In the limit $z_0 \to 0$, the solution will match the well-known result from quantum mechanics, for which the eigenvalues take on integer values $\widehat{E}_n = 4n + 2m + 2$ for $n = 0, 1, 2, \ldots$ and the wavefunctions are given in terms of associated Laguerre polynomials as $f_h^{(n)} \sim e^{-\xi^2/2}\xi^{m+1/2}L_n^m(\xi^2)$. However, imposing a Neumann or Dirichlet boundary condition at $z_0 > 0$ changes the energy levels such that they no longer take on integer values, and the solutions are no longer simple polynomials. The normalizable solutions are instead given by

$$\widetilde{f}_h^{(n)}(z) = N_h^{(n)} e^{-3\widetilde{A}(\xi/\sqrt{2}\mu)/2}\, U\left(-\frac{1}{4}(\widehat{E}_n + 2)\ , -1\ , \xi^2\right), \tag{3.2.30}$$

where $U(a, b, y)$ is the Tricomi confluent hypergeometric function. The profiles $f_h^n(z)$ are therefore

$$f_h^{(n)}(z) = N_h^{(n)}\, U\left(-\frac{m_n^2}{8\mu^2}\ , -1\ , 2\mu^2 z^2\right). \tag{3.2.31}$$

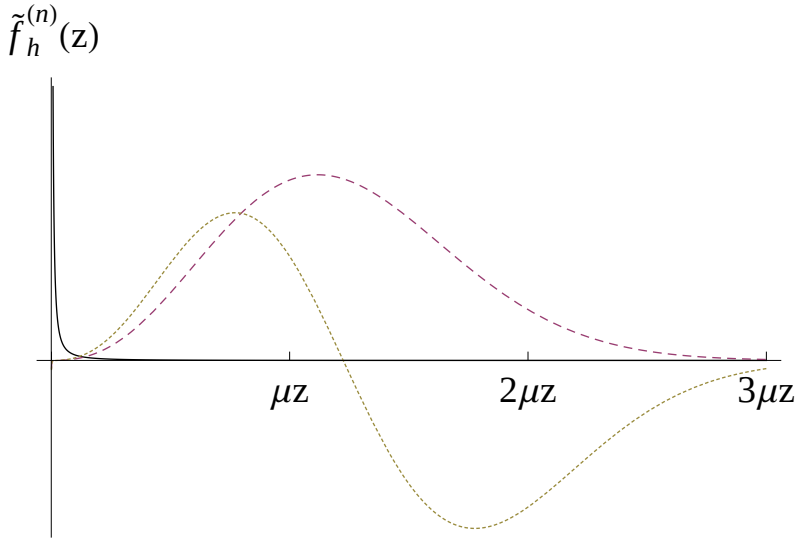

Figure 3.1: KK graviton profiles: The zero mode (solid), $n = 1$ (dash), and $n = 2$ (dot), for $\mu = 1$ TeV and $k = 1000$ TeV. If k and μ have a Planck-weak scale separation, then the zero mode is further separated from the KK modes.

The KK mass spectrum can be found by applying the UV boundary condition. In the limit $\mu z_0 \ll 1$, the KK modes follow approximate linear trajectories:

$$m_n^2 \simeq 8\mu^2(n + 2), \qquad n = 0, 1, 2 \ldots. \tag{3.2.32}$$

The approximate mass formula (3.2.32) is valid for both Neumann and Dirichlet conditions. This is because the mass spectrum is largely determined by IR dynamics and is not overly sensitive to the UV boundary condition. The first few modes have been plotted in Figure 3.1.

For $z \gg z_0$, the wavefunctions (3.2.31) are well approximated by the Laguerre polynomial solutions,

$$f_h^n(z) \simeq N_h^n (-1)^n (n)!\; 4(\mu z)^4 L_n^2\left(2\mu^2 z^2\right). \tag{3.2.33}$$

Using (3.2.33), we can derive an approximate expression for the normalization:

$$N_h^n \simeq \frac{(-1)^n}{(n+2)!}\frac{k}{\mu}\left[\frac{M^3}{k}\sum_{j,k=0}^{n}\frac{(-n)_j}{j!\;(j+2)!}\;\frac{(-n)_k}{k!\;(k+2)!}\;(j+k+2)!\right]^{-1/2}, \tag{3.2.34}$$

where the Pochhammer symbol $(n)_j$ is defined as

$$(n)_j = \prod_{k=0}^{j-1}(a+k) = \begin{cases} \frac{(n+j-1)!}{(n-1)!} & \text{for n} \in \mathbb{Z}_+, \\ (-1)^j \frac{(-n)!}{(-n-j)!} & \text{for n} \in \mathbb{Z}_-. \end{cases} \tag{3.2.35}$$

The sum can be performed,

$$\sum_{j,k=0}^{n-1}\frac{(-n)_j}{j!\;(j+2)!}\;\frac{(-n)_k}{k!\;(k+2)!}\;(j+k+2)! = \frac{1}{(n+1)(n+2)}, \tag{3.2.36}$$

and using (3.2.20), we can write the normalization as

$$N_h^n \simeq \frac{(-1)^n}{M_P}\frac{k}{\mu}\sqrt{\frac{2}{(n+2)!(n)!}}. \tag{3.2.37}$$

As in hard-wall models, the couplings of the KK gravitons depend on where matter is located in the extra dimension. Later we will examine electroweak models with UV localized fermions. In this case the KK mode gravitons couple with a strength $f_h^{(n)}(z_0) \sim \mu/(kM_P)$, which is extremely suppressed and not likely to have observable consequences. This of course will change if fermions propagate in the bulk.

3.3 Bulk fields

We will now consider bulk gauge and fermion fields in the soft-wall background. As motivated in Section 3.2A, the starting point will be the action (3.2.2) with an appropriate matter Lagrangian.

3.3A Gauge Fields

Consider the simple case of a U(1) gauge field $A_M(x,z)$ in the bulk. The gauge field dynamics are described by the action

$$S = \int d^4x dz \sqrt{-g}\, e^{-\Phi} \left(-\frac{1}{4} F_{MN} F^{MN} \right). \tag{3.3.1}$$

Performing a KK decomposition,

$$A_\mu(x,z) = \sum_{n=0}^{\infty} A_\mu^n(x) f_A^n(z), \tag{3.3.2}$$

the wavefunctions obey the equation of motion

$$-e^{(A+\Phi)} \partial_5 (e^{-(A+\Phi)} \partial_5 f_A^{(n)}) = m_n^2 f_A^{(n)}, \tag{3.3.3}$$

and are normalized according to

$$\int_{z_0}^{\infty} dz\, e^{-(A+\Phi)} f_A^n(z) f_A^m(z) = \delta^{nm}. \tag{3.3.4}$$

These relationships are exactly the same as (2.3.22) and (2.3.23) up to the redefinition $A \to A + \Phi$. Therefore, the discussion of Sections 2.3B and 2.3D are easily applied. A massless mode persists due to the unbroken gauge symmetry. It is constant:

$$f_A^{(0)}(z) = \sqrt{-\frac{2k}{\mathrm{Ei}\,(-\mu^2/k^2)}} \simeq \sqrt{\frac{k}{\log(k/\mu) - \gamma/2}}\,, \tag{3.3.5}$$

where $\mathrm{Ei}(x)$ is the exponential integral function, $\gamma \approx 0.577$ is the Euler-Mascheroni constant, and we have used $z_0 = 1/k$ and $\mu/k \ll 1$. The Schrödinger potential following from (2.3.24) with $W(z) = (A' + \Phi')/2 = \mu^2 z + 1/(2z)$ is now given by

$$V(z) = W^2 - W' = \mu^4 z^2 + \frac{3}{4z^2}. \tag{3.3.6}$$

Using the same techniques as for the graviton above, the wavefunctions of the massive modes are found to be

$$f_A^{(n)}(z) = N_A^{(n)}\; U\left(-\frac{m_n^2}{4\mu^2}\;, 0\;, \mu^2 z^2 \right). \tag{3.3.7}$$

Applying the Neumann condition to the wavefunctions at the UV boundary determines the mass spectrum of the excited vector modes. We find that in the limit $\mu/k \ll 1$, the gauge boson masses follow approximate linear trajectories:

$$m_n^2 \simeq 4\mu^2(n+1), \qquad n = 0, 1, 2 \ldots . \tag{3.3.8}$$

For large z, the wavefunctions reduce to Laguerre polynomials:

$$f_A^{(n)}(z) \simeq N_A^{(n)}(-1)^n(n)!\ \mu^2 z^2 L_n^1\left(\mu^2 z^2\right). \tag{3.3.9}$$

Similarly, as for the graviton wavefunction case, this form of the wavefunction can be used to derive an approximate expression for the normalization:

$$N_A^{(n)} \simeq \frac{(-1)^n}{(n+1)!}\sqrt{2(n+1)k}\,. \tag{3.3.10}$$

3.3B Fermions

While the analysis of bulk gauge fields in the soft-wall background is straightforward, this is not the case for fermions. We will postpone a detailed discussion of the full treatment of fermions until Chapter 4. Our purpose here is to highlight the issues involved.

As was discussed in Chapter 2, fermions are typically analyzed using the zero-mode approximation, treating Yukawa interactions with the Higgs as perturbations and obtaining fermion masses from wavefunction overlap integrals [79, 80, 78]. The simplification thereby introduced is considerable: modes of opposite chirality can be treated completely separately. However, this approach is not valid for the soft-wall scenario. Unlike in hard-wall models with an IR brane, the Higgs boson in a soft-wall background must necessarily propagate in the bulk. Since the Higgs profile should be peaked in the IR (to be dual to a composite electroweak symmetry breaking sector), the backreaction of the Higgs vacuum expectation value (VEV) on the bulk fermion equations of motion at large z cannot be neglected. The proper approach is to diagonalize the bulk equations of motion and obtain the SM fermion masses from the boundary conditions.[1] Attempting to treat the Yukawa interaction perturbatively necessarily introduces problems with

[1] Note that in general any model with a bulk Higgs condensate and bulk fermions should be analyzed in this way. However with a hard wall cutting off the extra dimension, it may be reasonable to treat the bulk Yukawa interaction as a perturbation and use the zero-mode approximation for fermions (although, see also [93]).

strong coupling and normalizability. To see this, we will consider fermions in a soft-wall background modeled first by a dilaton and second by a deformed AdS metric.

Dilaton soft wall

First, we can imagine the dilaton providing the soft wall, with $\Phi(z) = \mu^2 z^2$ and a pure AdS metric $A(z) = \log kz$. Inserting the prefactor $e^{-\Phi}$ into the fermion action (2.3.39) results in an equation of motion analogous to (2.3.41):

$$\eta^{\mu\nu}\gamma_\mu\partial_\nu\Psi_\mp \pm e^{(2A+\frac{\Phi}{2})}\partial_5\left(e^{-(2A+\frac{\Phi}{2})}\Psi_\pm\right) + e^{-A}M_\Psi\Psi_\pm = 0, \tag{3.3.11}$$

Inserting the KK-decomposition (2.3.43), the equations of motion for the transformed field $\widetilde{\Psi} = e^{-(2A+\Phi/2)}\Psi$ becomes identical to (2.3.44):

$$\left(\pm\partial_5 + e^{-A}M_\Psi\right)\widetilde{f}_\pm^{(n)}(z) = m_n\widetilde{f}_\mp^{(n)}(z). \tag{3.3.12}$$

Moreover, the normalization condition is identical (2.3.47). The remarkable fact is that the transformed functions depend only on the metric and not on the dilaton profile, a result of the fact that the equations of motion are first order in derivatives. The zero modes have the same power-law profile as in hard-wall models:

$$f_\pm^{(0)}(z) \propto z^{\mp c}. \tag{3.3.13}$$

Since the extra space extends to $z \to \infty$, these modes are normalizable if $1 \mp 2c < 0$, meaning only UV localized zero modes are allowed. Additionally, while it would appear that the Kaluza-Klein spectrum is unchanged, in fact the spectrum is no longer discrete but instead becomes continuous. The wavefunctions given by (2.3.46) asymptotically approach plane wave solutions. This is similar to the behavior of gravitons in the Randall-Sundrum model when the IR brane is removed [37], however there is no normalizable mode in the absence of boundary mass terms.

Let us examine the gauge coupling between a zero-mode fermion f_+ and a KK gauge boson. The gauge boson wavefunction is given in given in Eq. (3.3.7). Inserting the appropriate functions into the Lagrangian (see (2.4.10)), we find that the effective 4D coupling behaves as:

$$\begin{aligned} g^n &\propto g_5\int_{z_0}^{\infty} dz\, z^{-2c}\, U\left(-\frac{m_n^2}{4\mu^2}\,, 0\,, \mu^2 z^2\right), \\ &\simeq g_5\int_{z_0}^{\infty} dz\, z^{-2c} z^{m_n^2/2\mu^2}, \end{aligned} \tag{3.3.14}$$

where we have used the asymptotic large z behavior of the hypergeometric function,

$$U(a, b, y) \sim y^{-a}, \tag{3.3.15}$$

in the final step. Noting the mass spectrum (3.3.8), this coupling becomes

$$g^{(n)} \propto \int_{z_0}^{\infty} dz\, z^{2n-2c}, \tag{3.3.16}$$

which diverges for $n > c - 1/2$. Therefore, once a particular c value is chosen, the coupling $g^{(n)}$ diverges for sufficiently large gauge boson KK mode number n.

Metric soft wall

It is also possible to model the soft wall with an exponentially decaying metric, with $\widetilde{A}(z) = 2\mu^2 z^2/3 + \log kz$. Again, we can follow the analysis above, this time setting $\Phi = 0$, and replacing $A(z) \to \widetilde{A}(z)$. We then obtain the equation of motion for the fermion profiles:

$$\big(\pm \partial_5 + e^{-\widetilde{A}} M_\Psi \big) \widetilde{f}_{\pm}^{(n)}(z) = m_n \widetilde{f}_{\mp}^{(n)}(z). \tag{3.3.17}$$

The massless mode solutions can be obtained straightforwardly by integrating Eq. (3.3.17), leading to

$$\widetilde{f}_{\pm}^{(0)}(z) \propto e^{\mp c\ \mathrm{Ei}\left(-2\mu^2 z^2/3\right)/2}. \tag{3.3.18}$$

However, this solution is not normalizable. The exponential integral function vanishes as $z \to \infty$, and thus the profile $g_{\pm}^{(0)}(z)$ approaches a constant at large z. Noting the normalization condition (2.3.47), we see that the zero mode is not normalizable, and is therefore absent from the theory.

The problems discussed above are ultimately related to the fact that the fifth dimension extends to $z \to \infty$, and their origin is easily understood by considering the the Schrödinger potentials in the second-order equations for the fields. The potentials vanish as $z \to \infty$. If we consider Yukawa interactions with a bulk Higgs, it is easy to see that the perturbabive approximation is invalid. The large addition to the potential due to the IR peaked Higgs profile cannot be treated as a perturbation upon a vanishing potential! We therefore endeavor to fully account for the Higgs feedback on the fermion equations of motion. This is the subject of Chapter 4. For the time being, we will simply assume that there exist fermion solutions that are UV-localized.

3.4 Electroweak models

In this section we investigate models of electroweak symmetry breaking with a soft-wall background. For simplicity, we will consider SM fermions localized on the UV brane, which are interpreted as elementary states in the holographic theory. It is possible to generalize these models to include bulk fermions based on the analysis presented in Chapter 4. We will focus on bulk gauge fields interacting with a Higgs field peaked at large z, which is interpreted in the dual theory as electroweak symmetry breaking due to strong dynamics.

We start by considering a model with a bulk custodial isospin gauge symmetry, so as to protect the model from excessive contributions to precision electroweak observables [89], namely the Peskin-Takeuichi T parameter [48, 49]. The bulk gauge group is $\mathrm{SU}(2)_L \times \mathrm{SU}(2)_R \times \mathrm{U}(1)_X$. On the UV boundary the gauge symmetry is broken via boundary conditions to the electroweak subgroup $\mathrm{SU}(2)_L \times \mathrm{U}(1)_Y$. In the IR region, the custodial symmetry is broken to the vector subgroup via a bulk Higgs condensate. In the usual hard-wall setups, this symmetry breaking is achieved via a Higgs localized on the IR brane [89] or via IR-brane boundary conditions as in Higgsless models [105, 106]. In fact, our setup is very similar to the "gaugephobic Higgs" model [107], though with a different background geometry and no IR brane.

The Lagrangian of the model is given by

$$\begin{aligned} S &= \int d^5x\sqrt{-g}\, e^{-\Phi}\Bigg[-\frac{1}{4g_5^2}L^a_{MN}L^{aMN} - \frac{1}{4g_5^2}R^a_{MN}R^{aMN} - \frac{1}{4g_5'^2}X_{MN}X^{MN} \\ &\qquad - \mathrm{Tr}|D_M H|^2 - V(H)\Bigg] - \int d^4x\sqrt{-g_{UV}}e^{-\Phi}\, V_{UV}(H), \end{aligned} \tag{3.4.1}$$

where $L^a_M(x,z)$, $R^a_M(x,z)$, and $X_M(x,z)$ represent $\mathrm{SU}(2)_L$, $\mathrm{SU}(2)_R$, and $\mathrm{U}(1)_X$ gauge fields, respectively. In addition there is a bulk Higgs boson $H(x,z)$ with bulk and boundary potentials $V(H)$ and $V_{UV}(H)$, respectively. We have chosen the right- and left-handed gauge couplings to be equal for simplicity.

We break $SU(2)_R \times U(1)_X \to U(1)_Y$ through boundary conditions on the UV brane.

The gauge fields satisfy the following UV boundary conditions,

$$\begin{aligned} \partial_5 L_\mu^a\Big|_{z_0} &= 0, & R_\mu^{1,2}\Big|_{z_0} &= 0, \\ \partial_5\left(\tfrac{1}{g_5^2}X_\mu + \tfrac{1}{g_5^2}R_\mu^3\right)\Big|_{z_0} &= 0, & (X_\mu - R_\mu^3)\Big|_{z_0} &= 0, \end{aligned} \tag{3.4.2}$$

which break $SU(2)_R \times U(1)_X \to U(1)_Y$. The four would-be massless directions are indicated by the Neumann conditions.

The bulk Higgs field is a bidoublet under $\mathrm{SU}(2)_L \times \mathrm{SU}(2)_R$ transforming as:

$$H \to U_L H U_R^\dagger. \tag{3.4.3}$$

We define vector and axial-vector fields $V_M^a, A_M^a = (L_M^a \pm R_M^a)/\sqrt{2}$ as the Higgs field only couples to the axial mode through the covariant derivative. After the Higgs acquires a non-trivial profile along the fifth direction,

$$\langle H(z)\rangle = \frac{h(z)}{\sqrt{2}}\begin{pmatrix} 1 & 0 \\ 0 & 1 \end{pmatrix}, \tag{3.4.4}$$

the gauge symmetry is broken down to the vector subgroup $SU(2)_L \times SU(2)_R \to SU(2)_V$. The vector and axial modes can be analyzed using the methods of Sections 2.3B and 3.3A. We refer to the z-dependent pieces in the KK decompositions (see (3.3.2)) for V_M^a and A_M^a as $v(p,z)$ and $a(p,z)$, respectively, where $p = \sqrt{p^2}$ is the 4-momentum. The functions satisfy the equations of motion,

$$e^{(A+\Phi)}\partial_5\left(e^{-(A+\Phi)}\partial_5 v(p,z)\right) = p^2 v(p,z), \tag{3.4.5}$$

$$e^{(A+\Phi)}\partial_5\left(e^{-(A+\Phi)}\partial_5 a(p,z)\right) - e^{-2A}g_5^2 h^2(z)a(p,z) = p^2 a(p,z). \tag{3.4.6}$$

The vector profile $v(p,z)$ is obtained from (3.3.7), while the exact form of the axial-vector profile can only be determined after specifying the Higgs VEV $h(z)$. We will next consider two simple cases which allow for an analytical determination of $a(p,z)$. Note that the X gauge boson profile is also given by $v(p,z)$.

From a 4D perspective, the theory contains a massless photon, a KK tower of charged W bosons, and a KK tower of neutral Z bosons with the lightest states in these towers identified with the SM W and Z bosons, respectively. To determine the mass spectra,

we apply the UV boundary conditions in Eq. (3.4.2). For the W tower, the spectrum (with $m_n^2 = -p^2$) is determined by the following equation:

$$v(p, z_0)a'(p, z_0) + a(p, z_0)v'(p, z_0) = 0, \tag{3.4.7}$$

while for the photon and neutral Z boson tower we find

$$v'(p, z_0)\left[g_5^2(v(p, z_0)a'(p, z_0) + a(p, z_0)v'(p, z_0)) + 2g_5'^2 v(p, z_0)a'(p, z_0)\right] = 0. \tag{3.4.8}$$

The prime ($'$) symbol in Eqs. (3.4.7) and (3.4.8) denotes differentiation with respect to z. Note that of the two equations in (3.4.8), one equation ($v'(p, z_0) = 0$) corresponds to the excited modes of the photon, while the other equation determines the KK spectrum of the Z boson.

To match the 5D theory to the 4D effective theory, we can relate the parameters g_5, g_5', and μ to, for instance, the electric charge and the masses of the W and Z bosons determined from (3.4.7) and (3.4.8). Note that the massless mode is always of the form:

$$A_M \propto \frac{V_M}{g_5^2} + \frac{X_M}{g_5'^2} \equiv \frac{A_M}{\widetilde{g}_5^2}. \tag{3.4.9}$$

From this and the normalization (3.3.5), the electric charge is computed to be

$$e^2 \simeq \frac{g_5^2 g_5'^2}{g_5^2 + 2g_5'^2} \frac{k}{\log(k/\mu) - \gamma/2}\ . \tag{3.4.10}$$

The W and Z boson masses will be computed for specific Higgs profiles below, but first we consider the dynamics of the Higgs sector and present a simple model leading to an IR-peaked Higgs background profile.

3.4A Higgs dynamics

We now analyze the dynamics leading to a bulk Higgs condensate. An understanding of the Higgs dynamics is important for more than just aesthetic reasons; any realistic phenomenological study requires a concrete dynamical model to analyze the Higgs fluctuations and determine, for example, the mass of the physical Higgs scalar and its couplings to SM fields.

The bulk Higgs potential in (3.4.1) is assumed to have the form

$$V(H) = m_H^2(z)\mathrm{Tr}|H|^2, \tag{3.4.11}$$

where we have defined a z-dependent effective mass

$$m_H^2(z) = k^2\left[\alpha(\alpha-4) - 2\alpha\mu^2 z^2\right]. \tag{3.4.12}$$

According to the AdS/CFT dictionary, the particular constant mass-squared in (3.4.12) corresponds to an operator with dimension $\Delta_H = |\alpha - 2| + 2$ in the dual theory. The z-dependent mass term is assumed to arise from a coupling to another scalar field which obtains a background VEV. In fact, in our gravity model there are two candidates for these scalar fields, the dilaton Φ and tachyon T. Interaction terms like $\Phi|H|^2$ or $T^2|H|^2$ can provide the z^2 part of the mass term, although we do not need to specify the precise origin of this term for the phenomenological analysis. Note also that there is a tuning between the different terms in (3.4.12).

Inserting the background (3.4.4), we find the following equation of motion for $h(z)$:

$$e^{(3A+\Phi)}\partial_5(e^{-(3A+\Phi)}\partial_5 h) - e^{-2A}m_H^2(z)h = 0. \tag{3.4.13}$$

The general solution to this equation is

$$h(z) = z^\alpha\left(c_0 + c_1\Gamma\left(2-\alpha, -\mu^2 z^2\right)\right), \tag{3.4.14}$$

where c_0, c_1 are arbitrary constants. Demanding finiteness of this solution in the soft-wall background implies $c_1 = 0$, which leads to

$$h(z) = c_0 z^\alpha. \tag{3.4.15}$$

We must add a UV boundary potential to ensure that the solution (3.4.15) can non-trivially satisfy the boundary condition. An appropriate choice is

$$V_{UV}(H) = \frac{\lambda_0}{k^2}\left(\mathrm{Tr}|H|^2 - v_0^2\right)^2, \tag{3.4.16}$$

which leads to the UV boundary condition

$$\left(\partial_5 h - \frac{2\lambda_0}{k^2}h(h^2 - v_0^2)\right)\Bigg|_{z_0} = 0. \tag{3.4.17}$$

Substituting (3.4.15) into this boundary condition gives rise to two possible solutions, a trivial solution $c_0 = 0$, as well as a non-trivial solution:

$$c_0^2 = k^{3+2\alpha}\left(\frac{v_0^2}{k^3} + \frac{\alpha}{2\lambda_0}\right). \tag{3.4.18}$$

The energy density per unit brane volume, $\mathcal{H}$, can be calculated as in Ref. [108]. The difference between the trivial and non-trivial solution energy densities is found to be

$$\mathcal{H}(h=0) - \mathcal{H}(h = c_0 z^\alpha) = \frac{1}{\lambda_0} k^4 e^{-\mu^2 z_0^2} \left(\frac{\lambda_0 v_0^2}{k^3} + \frac{\alpha}{2} \right)^2 . \tag{3.4.19}$$

Therefore, the non-trivial Higgs background (3.4.15) will be the ground state provided that this difference is positive, which occurs when $\lambda_0 > 0$. Incidentally the energy density of the non-trivial solution is of order $k^4 + v_0^2 k$, so provided $v_0^2 \lesssim k^3$ and $k \lesssim M$ the backreaction on the gravitational background can be neglected.

In order to trigger electroweak symmetry breaking at a scale of order μ, the bulk Higgs VEV should become appreciable near $z \sim 1/\mu$, suggesting that $c_0 \propto k^{3/2} \mu^\alpha$. We thus require that

$$\frac{v_0^2}{k^3} + \frac{\alpha}{2\lambda_0} \sim \left(\frac{\mu}{k} \right)^{2\alpha} . \tag{3.4.20}$$

This is clearly tuned, since the quantity on the left hand side is naturally of order one. The need for this tuning is due to the fact that the stabilizing potential is located on the UV brane. Eq. (3.4.20) suggests two possible situations: either v_0^2 is small and λ_0 is large, or a partial cancellation occurs between the two terms on the left-hand side of (3.4.20), in which case both v_0^2 and λ_0 can have perturbative values. To determine which case can be realized we need to consider the spectrum of fluctuations about the Higgs background.

To study the Higgs fluctuations, we write $h(z) \to h(z) + \widetilde{h}(x,z)$. The equation of motion for $\widetilde{h}$ is

$$\Box \widetilde{h} + e^{(3A+\Phi)} \partial_5 (e^{-(3A+\Phi)} \partial_5 \widetilde{h}) - e^{-2A} m_H^2 \widetilde{h} = 0. \tag{3.4.21}$$

Due to the boundary quartic potential (3.4.16), the UV boundary condition for the fluctuation is a nonlinear equation that does not admit an analytic solution for the eigenvalues. An approximate solution can be found by performing a linearized fluctuation analysis. In this case the boundary condition for the fluctuation becomes

$$\left(\partial_5 - \frac{2\lambda_0}{k^2} \left((h^2 - v_0^2) + 2h^2 \right) \right) \widetilde{h} \Big|_{z_0} = 0. \tag{3.4.22}$$

The KK-expansion is

$$\widetilde{h}(x,z) = \sum_{n=0}^{\infty} \widetilde{h}^{(n)}(x) f_{\widetilde{h}}^{(n)}(z). \tag{3.4.23}$$

Transforming the functions in our accustomed way, $f_{\widetilde{h}}^{(n)}(z) = e^{(3A+\Phi)/2}\,\widetilde{f}_{\widetilde{h}}^{(n)}(z)$, the profiles $\widehat{g}_{\widetilde{h}}^{n}(z)$ satisfy a Schrödinger equation with the potential

$$V_{\widetilde{h}}(z) = \left(\frac{3A'+\Phi'}{2}\right)^2 - \left(\frac{3A''+\Phi''}{2}\right) + e^{-2A}m_H^2(z) \tag{3.4.24}$$

$$= \mu^4 z^2 + 2(1-\alpha)\mu^2 + \frac{(\alpha-2)^2 - 1/4}{z^2}, \tag{3.4.25}$$

which is of the same form as the potential in (3.2.29) with $m = \alpha - 2$. The solutions for the untransformed profiles are then

$$f_{\widetilde{h}}^{(n)}(z) = N_{\widetilde{h}}^{n} z^{\alpha} U\left(-\frac{m_n^2}{4\mu^2}\ , \alpha - 1\ , \mu^2 z^2\right), \tag{3.4.26}$$

where $N_{\widetilde{h}}^{n}$ is a normalization factor. Applying the boundary conditions, the Higgs mass spectrum is determined by the equation

$$m_n^2 z_0^2\, U\left(-\frac{m_n^2}{4\mu^2}+1\ , \alpha\ , \mu^2 z_0^2\right) - 4\,\zeta\, U\left(-\frac{m_n^2}{4\mu^2}\ , \alpha-1\ , \mu^2 z_0^2\right) = 0, \tag{3.4.27}$$

where $\zeta = \alpha + 2\lambda_0 v_0^2/k^3 \sim 2\lambda_0(\mu/k)^{2\alpha}$. In the limit $|\zeta| \ll 1$ the Higgs (lowest lying mode) mass-squared is $m_0^2 \simeq 2\zeta k^2/\log(k/\mu)$. For $\zeta < 0$ we find a tachyon mode, and a zero mode at $\zeta = 0$, so we restrict to $\zeta > 0$. The Higgs mass increases as we increase ζ. Note that these results are at the linearized level and the nonlinear terms in the UV boundary condition have been neglected.

Earlier we argued that $\lambda_0 > 0$ if the non-trivial Higgs profile is to be the vacuum state of the theory. Now we see that this condition also implies that there are no tachyon modes provided $v_0^2/k^3 > -\alpha/(2\lambda_0)$. In particular, for $v_0^2/k^3 = -\alpha/(2\lambda_0)+\epsilon$ then (3.4.20) can be satisfied with $\epsilon \sim (\mu/k)^{2\alpha}$, implying that v_0^2 and λ_0 can have perturbative values. Thus, a perturbative solution describing electroweak symmetry breaking with a light Higgs boson can be found. However, for large enough ζ, corresponding to a heavy Higgs or technicolor limit, the theory becomes nonperturbative.

3.4B Electroweak constraints

With fermions localized on the UV brane and a bulk custodial symmetry, the most important constraint on this model comes from the S parameter [48, 49]. Of course, one would like to extend fermions into the bulk in a realistic manner to understand the

SM flavor structure. In this case, there are other constraints that arise from loop level contributions to the T parameter from KK mode fermions and nonuniversal corrections to the $Z\bar{b}b$ coupling [89, 109], as well as stringent constraints from flavor violation [110, 111, 112]. Mechanisms to weaken these constraints have been developed recently, (e.g. using different custodial representations for third generation fermions [113]), and there is no reason to expect such mechanisms cannot be implemented in the soft-wall warped framework. Nevertheless, the constraint from S is still fairly restrictive in hard-wall models, forcing the KK scale to be around 3 TeV [89]. It is thus interesting to see whether or not the constraint from S can be weakened in a soft-wall background.

Recently, Ref. [61] found that the KK scale can indeed be lowered depending on the assumptions regarding the type of soft wall and Higgs condensate. In particular, they considered an example with a "linear" soft wall ($\nu = 2$ in our notation) with a quadratic Higgs profile, finding that the KK scale can be around 2 TeV. We will verify this result, and present another example for the linear soft wall in which the constraints are even less severe.

To calculate the S parameter we will use the boundary effective action approach [114] which is particularly convenient when fermions are UV localized. Following [114, 115], the general expression for the vector and axial-vector self energies is

$$\Sigma_V = -\frac{1}{g_5^2} e^{-(A+\Phi)} \frac{\partial_5 v}{v}\bigg|_{z_0}, \tag{3.4.28}$$

$$\Sigma_A = -\frac{1}{g_5^2} e^{-(A+\Phi)} \frac{\partial_5 a}{a}\bigg|_{z_0}. \tag{3.4.29}$$

The S parameter is defined as

$$S = 8\pi(\Sigma_V'(0) - \Sigma_A'(0)) \ . \tag{3.4.30}$$

From the exact expression for the vector profile given in (3.3.7), the vector self energy is

$$\Sigma_V(p^2) = \frac{e^{-\mu^2 z_0^2}}{2g_5^2 k} p^2 \frac{U\left(1+\frac{p^2}{4\mu^2}, 1, \mu^2 z_0^2\right)}{U\left(\frac{p^2}{4\mu^2}, 0, \mu^2 z_0^2\right)}. \tag{3.4.31}$$

In the limit $\mu z_0 \ll 1$ we find

$$\Sigma_V'(0) \approx \frac{1}{2g_5^2 k} \left(-\gamma - 2\log \mu z_0\right). \tag{3.4.32}$$

We now examine two explicit examples of profiles $h(z)$ which allow for an analytic determination of the axial-vector profile $a(p,z)$ and S, finding in each case that the KK scale can be lowered.

Linear VEV

Assuming $\nu = 2$ the first case we consider is when the Higgs VEV is linear in z, so that

$$g_5^2 h^2(z) = \xi k^2 \mu^2 z^2, \tag{3.4.33}$$

where ξ is a dimensionless parameter. This requires choosing $\alpha = 1$ or $m_H^2(z) = -3k^2 - 2\mu^2 z^2$. In the dual holographic theory this corresponds to electroweak symmetry breaking with an operator of dimension $\Delta_H = 3$. From the equation of motion (3.4.6), we find the axial-vector profile $a(z)$:

$$a(p,z) = U\left(\frac{p^2}{4\mu^2} + \frac{\xi}{4}\ , 0\ , \mu^2 z^2\right). \tag{3.4.34}$$

By expanding the spectrum equations (3.4.7) and (3.4.8) in the limit $\mu z_0 \ll 1$, $\xi \ll 1$ we find two light modes that can be identified with the W and Z bosons, with masses:

$$m_W^2 \approx \frac{1}{2}\xi\mu^2, \tag{3.4.35}$$

$$m_Z^2 \approx \frac{1}{2}\frac{g_5^2 + 2g_5'^2}{g_5^2 + g_5'^2}\xi\mu^2. \tag{3.4.36}$$

We can see the custodial symmetry at work in the relationship between the W and Z masses [105, 106]. The ratio $m_W^2/m_Z^2 \approx (g_5^2 + g_5'^2)/(g_5^2 + 2g_5'^2) \simeq g^2/(g^2 + g'^2)$, where g, g' are the $\mathrm{SU}(2)_L$, $\mathrm{U}(1)_Y$ gauge couplings, respectively.

The closed form expression for the axial-vector self energy is

$$\Sigma_A(p^2) = \frac{e^{-\mu^2 z_0^2}}{2g_5^2 k}(p^2 + \xi\mu^2)\frac{U\left(1 + \frac{p^2}{4\mu^2} + \frac{\xi}{4}, 1, \mu^2 z_0^2\right)}{U\left(\frac{p^2}{4\mu^2} + \frac{\xi}{4}\ , 0\ , \mu^2 z_0^2\right)}. \tag{3.4.37}$$

Taking the limit $\mu z_0 \ll 1$, $\xi \ll 1$ the derivative becomes

$$\Sigma_A'(0) \approx \frac{1}{2g_5^2 k}\left(-\gamma - 2\log\mu z_0 - \frac{\pi^2}{12}\xi\right). \tag{3.4.38}$$

Combining 3.4.38 with (3.4.32), we find the S parameter for the case of a linear Higgs VEV:

$$S \approx \frac{\pi^3 \xi}{3 g_5^2 k} \simeq \frac{2\pi^3}{3g^2(\log(k/\mu) - \gamma/2)} \frac{m_W^2}{\mu^2}. \tag{3.4.39}$$

Requiring $S < 0.2$ implies that when the UV scale is 1000 TeV, the IR scale $\mu \leq 0.5\,\text{TeV}$. Thus, the first KK gauge boson resonances have masses of order 1 TeV. If we choose the UV scale to be of order M_P then the constraint is even weaker, and the first KK modes can be quite light, of order 300-500 GeV! Also, since the spacing between successive modes is 2μ, in this scenario it may actually be possible to observe the linear trajectory at the LHC.

Quadratic VEV

Next for $\nu = 2$ we consider a quadratic profile for the Higgs,

$$g_5^2 h^2(z) = \xi k^2 \mu^4 z^4. \tag{3.4.40}$$

This requires choosing $\alpha = 2$ or $m_H^2(z) = -4k^2 - 4\mu^2 z^2$. In the dual holographic theory this corresponds to electroweak symmetry breaking with an operator of dimension $\Delta_H = 2$. The axial-vector profile is then

$$a(p,z) = e^{\mu^2 z^2 (1-\sqrt{1+\xi})/2}\, U\left(\frac{p^2}{4\mu^2\sqrt{1+\xi}}\,, 0\,, \sqrt{1+\xi}\,\mu^2 z^2\right). \tag{3.4.41}$$

Expanding (3.4.7) and (3.4.8) in the limit $\mu z_0 \ll 1$, $\xi \ll 1$, the masses of the W and Z bosons are found to be

$$m_W^2 \approx \frac{1}{4}\frac{1}{\log(k/\mu) - \gamma/2}\xi\mu^2, \tag{3.4.42}$$

$$m_Z^2 \approx \frac{1}{4}\frac{g_5^2 + 2g_5'^2}{g_5^2 + g_5'^2}\frac{1}{\log(k/\mu) - \gamma/2}\xi\mu^2. \tag{3.4.43}$$

The axial-vector self energy can then be computed and is given by,

$$\Sigma_A(p^2) = \frac{e^{-\mu^2 z_0^2}}{2g_5^2 k}\left[p^2 \frac{U\left(1 + \frac{p^2}{4\mu^2\sqrt{1+\xi}}\,, 1\,, \sqrt{1+\xi}\mu^2 z_0^2\right)}{U\left(\frac{p^2}{4\mu^2\sqrt{1+\xi}}\,, 0\,, \sqrt{1+\xi}\mu^2 z_0^2\right)} - 2\mu^2(1 - \sqrt{1+\xi})\right], \tag{3.4.44}$$

which leads to the expression for $\Sigma'(0)$ in the limit $\mu z_0 \ll 1$:

$$\Sigma_A'(0) \approx \frac{1}{2g_5^2 k}\left(-\gamma - 2\log\mu z_0 - \log\sqrt{1+\xi}\right). \tag{3.4.45}$$

The S parameter is therefore given by

$$S \approx \frac{2\pi}{g_5^2 k} \log(1+\xi) \simeq \frac{8\pi}{g^2} \frac{m_W^2}{\mu^2}. \tag{3.4.46}$$

In the case when the Higgs VEV is quadratic in z, the constraint $S < 0.2$ translates into an upper bound of $\mu \leq 1.3$ TeV, which is very similar to the result obtained in Ref. [61] for the same mass term (using their $\epsilon = 1$). There is some weak dependence on the ratio k/μ in S, and taking $k \sim M_p$, the lower bound on μ becomes approximately 1.2 TeV.

Chapter 4

Fermions in the Soft-Wall

In Chapter 2, we reviewed the treatment of bulk fields in a hard-wall background, In particular, in Section 2.4A we discussed how to obtain hierarchical fermion masses in hard-wall setups. The perturbative approach we employed is a familiar technique useful for solving many problems in physics. We started with the free theory of two chiral fermion fields absent Yukawa interactions and found the fermion wavefunction profiles along the extra spatial direction. Next, we accounted for the Yukawa interaction between the fermions by using elementary perturbation theory to calculate the resulting contribution to 4D particle masses. Although that is as far as we went in Chapter 2, it is also possible to calculate first-order corrections to the wavefunctions resulting from the interaction, or to fit to known flavor physics observables [93, 94].

When we examined soft-wall models in Chapter 3, we found that this approach is ill-suited. The ultimate reason for the difficulty was discussed in Section 3.3B. The Higgs interaction is expected to take place in the IR (so as to trigger electroweak symmetry breaking at the TeV scale), where the effective Schrödinger potentials in the fermion equations of motion vanish. In such a scenario, the familiar perturbative approach is invalid.

Thus, we are seemingly left with no choice but to approach the full problem, coupling the fermions in the bulk and solving the resulting system of equations. As we will see, this is made difficult because modeling just a single generation of fermions requires solving a fourth-order system–significantly more complicated than the first-order zero-mode equations of motion we found in Chapter 2. Moreover, with interactions throughout the

bulk, it becomes extremely cumbersome to discuss any flavor physics effects whatsoever absent unjustified assumptions regarding the structure of the 5D Yukawa couplings.

In this chapter we present a comprehensive analysis of bulk fermions in a soft-wall background. We document several analytical solutions for special cases of the single generation problem in the context of the electroweak model of Section 3.4. Our results show that many of the attractive features of hard-wall models, including the natural suppression of flavor violation through a GIM-like mechanism are retained. We also cover several approximation methods that allow for the analysis of fermions in an arbitrary background. Finally, we attack the complete three-generation case using a non-iterative numerical routine. We present the full dependence of SM fermion masses on the masses in the bulk and compare the results to a typical hard-wall model. We find that the behavior is very different in the phenomenologically interesting region of the parameter space, where the bulk $SU(2)_L$ doublet and singlet fermions have opposite bulk masses. We then present results for the case of three generations with substantial mixing between bulk profiles. We find example spectra resembling the up- and down-type quarks in the spirit of Ref. [116].

Our discussion follows closely the work of Ref. [66]. Other approaches to this problem can be found in Refs. [65, 64, 117]. An iterative numerical approach may also be found in Ref. [118]; the iterative method offers improved stability when there are extremely large scale hierarchies in the model, however it does not extend readily to the three-generation problem as our approach does.

4.1 Fermions in the Soft-Wall Background

4.1A The Fermion Lagrangian and Equations of Motion

We work in the setup described in detail in Chapter 3. The spacetime is parameterized by (x^μ, z) with conformal coordinate z and metric:

$$ds^2 = e^{-2A(z)}\eta_{MN}dx^M dx^N \ , \tag{4.1.1}$$

where $\eta_{MN} = \text{diag}(-,+,+,+,+)$. In particular we will consider a pure AdS metric, i.e. $A(z) = \log kz$ with k the AdS curvature scale. The spacetime is defined on the interval $z \in [z_0, \infty)$, where z_0 is the location of the UV brane. The spacetime extends

to $z \to \infty$, and we will therefore consider a soft-wall setup in which the dilaton, Φ obtains a background value and provides a dynamical cutoff to spacetime. The gauge and matter fields are described by the action,

$$S = \int d^5x\sqrt{-g}\, e^{-\Phi}\mathcal{L}, \tag{4.1.2}$$

where $\mathcal{L}$ is the 5D Lagrangian. While much of our discussion of fermions in this chapter is valid in general, for the sake of concreteness we will specifically consider the dilaton profile used during our analysis of gauge, scalar, and graviton flucutations in Chapter 3:

$$\Phi(z) = (\mu z)^2, \tag{4.1.3}$$

where the soft-wall mass scale $\mu \sim 1$ TeV.

Consider 5D Dirac fermions, Ψ_L^i (Ψ_R^i) which transform as a doublet (singlet) under $SU(2)_L$. It is straightforward to embed our setup in a theory with a bulk custodial $SU(2)_L \times SU(2)_R$ symmetry as in Section 3.4, but this will not be essential for our discussion. In the absence of Yukawa interactions, the fermion action is given by:

$$\begin{aligned} S &= -\int d^5x\sqrt{-g}\; e^{-\Phi}\left[\frac{1}{2}\left(\bar{\Psi}_L^{ai}e_A^M\gamma^A D_M\Psi_L^{ai} - D_M\bar{\Psi}_L^{ai}e_A^M\gamma^A\Psi_L^{ai}\right) + M_L^{ij}\bar{\Psi}_L^{ai}\Psi_L^{aj}\right. \\ &\qquad \left. + \frac{1}{2}\left(\bar{\Psi}_R^{i}e_A^M\gamma^A D_M\Psi_R^{i} - D_M\bar{\Psi}_R^{i}e_A^M\gamma^A\Psi_R^{i}\right) + M_R^{ij}\bar{\Psi}_R^{i}\Psi_R^{j}\right], \end{aligned} \tag{4.1.4}$$

where $e_A^M = e^A\delta_A^M$ is the vielbein and $D_M = \partial_M + \omega_M$ is the covariant derivative with spin connection ω_M. The index a is an $SU(2)$ label, while i, j are 5D flavor indices.

The projections of the Dirac spinors are given by $\Psi_{L\pm}^{ai} = \pm\gamma^5\Psi_{L\pm}^{ai}$ and similarly for Ψ_R^i. Dirichlet conditions are imposed on the fields Ψ_{L-}^{ia} and Ψ_{R+}^i at the UV boundary:

$$\begin{aligned} \Psi_{L-}^{ai}(x,z)\Big|_{z_0} &= 0, \\ \Psi_{R+}^{i}(x,z)\Big|_{z_0} &= 0. \end{aligned} \tag{4.1.5}$$

This choice of boundary conditions is familiar from our discussion of hard-wall models in Chapter 2, as it gives rise to massless chiral fermions from the 4D point of view. As we saw in Chapter 3, for a soft-wall model we instead get a continuum of modes in the AdS background. Introducing a Yukawa coupling to a bulk Higgs, whose vacuum

expectation value (VEV) is z-dependent, will result in a discrete spectrum and raise the would-be zero-mode. The Yukawa interaction contribution to the action is:

$$\begin{aligned} S_{Yukawa} &= -\int d^5x\sqrt{-g}e^{-\Phi}\Big[\frac{\lambda_5^{ij}}{\sqrt{k}}\bar{\Psi}_L^{ai}(x,z)H^a(x,z)\Psi_R^j(x,z)+\text{h.c.}\Big], \\ &\equiv -\int d^5x\sqrt{-g}e^{-\Phi}\Big[m^{ij}(z)\,\bar{\Psi}_L^i(x,z)\Psi_R^j(x,z)+\text{h.c.}\Big], \end{aligned} \tag{4.1.6}$$

where we have substituted the background value for the Higgs field:

$$H(x,z)\to H(z)=\frac{h(z)}{\sqrt{2}}\begin{pmatrix}0\\1\end{pmatrix}, \tag{4.1.7}$$

and dropped the $SU(2)$ labels $\Psi_L\equiv\Psi_L^2$. Note that we have dropped the $SU(2)_L\times SU(2)_R$ custodial symmetry requirement here, as it is not relevant to our discussion. The effective z-dependent bulk mass term arising from the Yukawa interaction is simply:

$$m^{ij}(z)\equiv\frac{\lambda_5^{ij}}{\sqrt{2\,k}}h(z). \tag{4.1.8}$$

To ensure a discrete spectrum of fermion masses, the Higgs VEV must grow faster than the metric factor, $e^{A(z)}=1/(kz)$, decays. Namely,[1]

$$\lim_{z\to\infty}\frac{h(z)}{z}\to\infty. \tag{4.1.9}$$

Varying the action with respect to $\bar{\Psi}_{L,R}$, we find the equations of motion:

$$\gamma^\mu\partial_\mu\psi_{L\pm}^i\mp\partial_5\psi_{L\mp}^i+e^{-A}M_L^{ij}\psi_{L\mp}^j+e^{-A}m^{ij}\psi_{R\mp}^j = 0, \tag{4.1.10}$$

$$\gamma^\mu\partial_\mu\psi_{R\pm}^i\mp\partial_5\psi_{R\mp}^i+e^{-A}M_R^{ij}\psi_{R\mp}^j+e^{-A}m^{\dagger ij}\psi_{L\mp}^j = 0, \tag{4.1.11}$$

where we have defined $\Psi=e^{2A+\Phi/2}\psi$. This transformation shows that the fermion mass spectra do not depend on the presence of the dilaton. Rather, it is the Higgs VEV that sets the fermion spacing, in contrast to the case of bosonic fields.

We seek solutions to these equations of motion that satisfy separation of variables. The KK expansion for the fields $\psi_{L,R\pm}$ is assumed to be:

$$\psi_{L\pm}^i(x,z) = \sum_{n,\alpha}\widetilde{f}_{L\pm}^{i\alpha(n)}(z)\psi_\pm^{\alpha(n)}(x), \tag{4.1.12}$$

$$\psi_{R\pm}^i(x,z) = \sum_{n,\alpha}\widetilde{f}_{R\pm}^{i\alpha(n)}(z)\psi_\pm^{\alpha(n)}(x), \tag{4.1.13}$$

[1] Other possiblities may also be considered. For example, if $\lim_{z\to\infty}h(z)/z\to\mu>0$, there can exist discrete low-lying modes with a continuous spectrum above a "mass gap," as in Refs. [65, 96].

where $\gamma^\mu \partial_\mu \psi_\pm^{\alpha(n)} = -m_n^\alpha \psi_\mp^{\alpha(n)}$ (no sum over α). Similar to the conventions of Ref. [116] we have introduced separate Latin and Greek indices labelling the 5D and 4D flavor, respectively. In this way, n is analagous to a principal quantum number while α runs over states with degenerate principal quantum numbers and split energy levels. Note that this KK-expansion is designed to diagonalize the 4D mass matrix. Defining the vectors:

$$\widetilde{f}_\pm^{i\alpha(n)} = \begin{pmatrix} \widetilde{f}_{L\pm}^{i\alpha(n)} \\ \widetilde{f}_{R\pm}^{i\alpha(n)} \end{pmatrix}, \tag{4.1.14}$$

allows the equations of motion for the 5D fields to be written in the form:

$$\left[\pm\partial_5 \delta^{ij} + \mathcal{M}^{ij}\right] \widetilde{f}_\pm^{j\alpha(n)}(z) = m_n^\alpha \widetilde{f}_\mp^{i\alpha(n)}, \tag{4.1.15}$$

where the mixing matrix is defined as

$$\mathcal{M} = e^{-A} \begin{pmatrix} M_L^{ij} & m^{ij}(z) \\ m^{\dagger ij}(z) & M_R^{ij} \end{pmatrix}. \tag{4.1.16}$$

Note that α, i, j run from $1, \ldots N_F$, where N_F is the number of fermion generations. Thus $\mathcal{M}^{ij}$ is a $2N_F \times 2N_F$ matrix, and equation (4.1.15) represents a coupled system of $4N_F$ differential equations for each α. The 4D fermion fields $\psi_\pm^{\alpha(n)}(x)$ are canonically normalized by requiring that:

$$\int_{z_0}^{\infty} dz \ \left((f_{L\pm}^{i\alpha(n)})^\dagger f_{L\pm}^{i\beta(m)} + (f_{R\pm}^{i\alpha(n)})^\dagger f_{R\pm}^{i\beta(m)} \right) = \delta^{nm} \delta^{\alpha\beta}. \tag{4.1.17}$$

Note that the index i is to be summed over in this expression.

Before ending our general discussion of the fermion setup, let us count and discuss the parameters involved in the problem. There are $4N_F$ integration constants to be fixed. Of these, $2N_F$ are fixed explicitly by the boundary conditions (4.1.5). The remaining $2N_F$ constants are fixed by the normalization condition (4.1.17). One of these constants corresponds to an overall scale, while the other $2N_F - 1$ constants may be recast as the ratios of the various non-vanishing field components at the boundary. A consistent solution can only exist for certain values of the m_n^α. In general, however, it is not possible to determine the masses or normalization constants independently. This is the source of difficulty in solving the problem.

4.2 Fermion Spectrum

The coupled equations (4.1.15) cannot be solved analytically except for a few special single-generation cases, depending upon the particular form of the Higgs VEV and the relative bulk masses for the fermions. We first review the single generation case in detail. We begin very generally, emphasizing that these methods apply to a wide variety of soft-wall models in AdS. We then specialize to a quadratic VEV and find the explicit solutions to the equations of motion for the special cases. The analytic solutions allow us to verify the results of the numerical routine we present in Section 4.3 (as well as the numerical treatment of Ref. [64] in which the Yukawas are treated perturbatively).

4.2A Single Generation

For a single generation of fermions, equation (4.1.15) becomes:

$$[\pm\partial_z + \mathcal{M}]\, \widetilde{f}_{\pm}^{(n)}(z) = m_n \widetilde{f}_{\mp}^{(n)}(z), \tag{4.2.1}$$

where $\mathcal{M}$ is a 2×2 mixing matrix:

$$\mathcal{M} = e^{-A} \begin{pmatrix} M_L & m(z) \\ m(z) & M_R \end{pmatrix}. \tag{4.2.2}$$

The equations for $\widetilde{f}_{+}^{(n)}$ and $\widetilde{f}_{-}^{(n)}$ can be decoupled by deriving a second-order equation from (4.2.1). The fields $\widetilde{f}_{\pm}^{(n)}$ obey a Schrödinger-like equation:

$$\left(-\partial_z^2 + \mathcal{V}_{\pm}\right) \widetilde{f}_{\pm}^{(n)} = m_n^2 \widetilde{f}_{\pm}^{(n)}, \tag{4.2.3}$$

where the "potentials" are given by:

$$\mathcal{V}_{\pm}(z) = \mathcal{M}^2 \mp \mathcal{M}'. \tag{4.2.4}$$

This is of the same apparent form as the superpotentials we introduced previously, only now the potential is a matrix. The difficulty in solving (4.2.3) is due to the fact that the mixing matrix generally cannot be diagonalized through global transformations of the functions, $\widetilde{f}_{L\pm,R\pm}$. However, there are special cases for which the second-order equations can be decoupled further. They occur whenever:

$$\begin{aligned} M_L &= M_R, && \text{“degenerate”} \\ M_L + M_R &\pm \partial_z e^{A(z)} = 0. && \text{“split”} \end{aligned} \tag{4.2.5}$$

The "degenerate" case is separable in any background. The "split" cases are separable regardless of the Higgs VEV *in AdS*, where the split-case condition simply becomes $M_L + M_R \pm k = 0$.

For generic forms of the Higgs VEV, it is most useful to work with transformed fields,

$$g_{\pm}^{(n)} = \begin{pmatrix} g_{L\pm}^{(n)} \\ g_{R\pm}^{(n)} \end{pmatrix} = U f_{\pm}^{(n)} = \frac{1}{\sqrt{2}} \begin{pmatrix} 1 & 1 \\ 1 & -1 \end{pmatrix} \begin{pmatrix} \widetilde{f}_{L\pm}^{(n)} \\ \widetilde{f}_{R\pm}^{(n)} \end{pmatrix}. \tag{4.2.6}$$

In this basis the equations of motion are given by,

$$\left[\pm\partial_z + \widehat{\mathcal{M}}\right] g_{\pm}^{(n)}(z) = m_n g_{\mp}^{(n)}(z), \tag{4.2.7}$$

where

$$\widehat{\mathcal{M}} = U^{\dagger}\mathcal{M}U = \frac{e^{-A}}{2} \begin{pmatrix} 2m(z) + M_L + M_R & M_L - M_R \\ M_L - M_R & -2m(z) + M_L + M_R \end{pmatrix}, \tag{4.2.8}$$

while the boundary conditions (4.1.5) become:

$$g_{L\pm}^{(n)}\Big|_{z_0} = \pm g_{R\pm}^{(n)}\Big|_{z_0}. \tag{4.2.9}$$

We may also define transformed potentials, $\widehat{\mathcal{V}}_{\pm}$, in direct analogy with (4.2.4). For the degenerate case, both of the potentials $\widehat{\mathcal{V}}_{+}$ and $\widehat{\mathcal{V}}_{-}$ are simultaneously diagonal in this basis. In the split cases, only one of the potentials $\widehat{\mathcal{V}}_{\pm}$ will be diagonal. After solving the corresponding pair of decoupled second-order equations, the first-order equations (4.2.7) can be used to generate the remaining solutions.

Below, we consider the degenerate case and one of the two split cases, $M_L + M_R + k = 0$, assuming the following form for the Higgs VEV:

$$h(z) = \eta k^{3/2} \mu^2 z^2, \tag{4.2.10}$$

giving $m(z) = bk(\mu z)^2$ where $b = \lambda_5 \eta/\sqrt{2}$, as in [63]. We also parameterize the bulk masses in units of the AdS curvature, $M_{L,R} = c_{L,R}k$, where $c_{L,R}$ are dimensionless coefficients.

Degenerate Bulk Masses

The solution to the degenerate bulk mass case $c_L = c_R = c$ was first presented in detail in [63]. It is fairly straightforward to solve. The Schrödinger potentials are given by

$$\widehat{\mathcal{V}}_{\pm} = \begin{pmatrix} \frac{c(c\pm 1)}{z^2} + (2c \mp 1) b\mu^2 + b^2\mu^4 z^2 & 0 \\ 0 & \frac{c(c\pm 1)}{z^2} - (2c \mp 1) b\mu^2 + b^2\mu^4 z^2 \end{pmatrix}, \quad (4.2.11)$$

and admit the following solutions in terms of confluent hypergeometric functions:[2]

$$g^{(n)}_{L+}(z) = N^n_{L+}\, e^{-b\,\mu^2 z^2/2} z^{-c}\, U\left(-\frac{m_n^2}{4b\mu^2}\ ,\ \frac{1}{2} - c\ ,\ b\,\mu^2 z^2\right), \quad (4.2.12)$$

$$g^{(n)}_{L-}(z) = N^n_{L-}\, e^{-b\,\mu^2 z^2/2} z^{1-c}\, U\left(-\frac{m_n^2}{4b\mu^2} + 1\ ,\ \frac{3}{2} - c\ ,\ b\,\mu^2 z^2\right), \quad (4.2.13)$$

$$g^{(n)}_{R+}(z) = N^n_{R+}\, e^{-b\,\mu^2 z^2/2} z^{1+c}\, U\left(-\frac{m_n^2}{4b\mu^2} + 1\ ,\ \frac{3}{2} + c\ ,\ b\,\mu^2 z^2\right), \quad (4.2.14)$$

$$g^{(n)}_{R-}(z) = N^n_{R-}\, e^{-b\,\mu^2 z^2/2} z^{c}\, U\left(-\frac{m_n^2}{4b\mu^2}\ ,\ \frac{1}{2} + c\ ,\ b\,\mu^2 z^2\right). \quad (4.2.15)$$

The fermion mass spectrum is obtained by applying the boundary conditions (4.2.9) and demanding consistency of the first order equations (4.2.7). These requirements can be shown to result in a single equation describing the spectrum:

$$\frac{1}{4} m_n^2 z_0^2\, U\left(-\frac{m_n^2}{4b\mu^2} + 1\ ,\ \frac{3}{2} - c\ ,\ b\,\mu^2 z_0^2\right) U\left(-\frac{m_n^2}{4b\mu^2} + 1\ ,\ \frac{3}{2} + c\ ,\ b\,\mu^2 z_0^2\right)$$
$$- U\left(-\frac{m_n^2}{4b\mu^2}\ ,\ \frac{1}{2} - c\ ,\ b\,\mu^2 z_0^2\right) U\left(-\frac{m_n^2}{4b\mu^2}\ ,\ \frac{1}{2} + c\ ,\ b\,\mu^2 z_0^2\right) = 0. \quad (4.2.16)$$

The first massive mode is to be identified with the SM fermion, so it is of interest to determine its mass. In the limit $\mu z_0 \ll 1$, and assuming the first mode is light $m_0^2/(4b\mu^2) \ll 1$, an expansion of Eq. (4.2.16) reveals a very light mode for $|c| > 1/2$:

$$m_0^2 \simeq \frac{2b\mu^2}{\Gamma(-1/2 + |c|)} (b\mu^2 z_0^2)^{-1/2+|c|}. \quad (4.2.17)$$

In the regime $-1/2 < c < 1/2$, we find instead that the fermion mass is of order $b\mu^2$:

$$m_0^2 \simeq \frac{4b\mu^2}{\pi \sec c\pi - \psi(1/2 - c) - \psi(1/2 + c)}\ , \quad (4.2.18)$$

[2] These Schrödinger potentials are easily related to the radial equation for a two-dimensional harmonic oscillator. See the discussion in Section 3.2C or [60].

where ψ is the digamma function. Thus we see that it is possible to generate a small fermion mass (e.g. electron) or a large mass (e.g. top quark) by choosing different values of the bulk mass parameter c, at least in this simple case of one generation.

Split Localizations

Next we consider one of the "split" cases, $c_L+c_R+1=0$. The other case, $c_L+c_R-1=0$, is very similar. With this choice, the transformation (4.2.6) will diagonalize the potential $\widetilde{\mathcal{V}}_+$ for any Higgs VEV in AdS. However, for our choice, $h(z)\sim z^2$, the untransformed potential $\mathcal{V}_-$ happens to be diagonal,

$$\mathcal{V}_- = \begin{pmatrix} \frac{c(c-1)}{z^2}+b^2\mu^4z^2 & 0 \\ 0 & \frac{(c+1)(c+2)}{z^2}+b^2\mu^4z^2 \end{pmatrix}, \tag{4.2.19}$$

so we will work in this basis.

A consistent solution requires that either $\widetilde{f}^{(n)}_{L-}=0$ or $\widetilde{f}^{(n)}_{R-}=0$. This is a peculiarity of the particular choice of the Higgs VEV and will not be true for other forms. The result is that the full tower of orthogonal solutions is most easily described in terms of two "distinct" KK towers of solutions. The first solution is:

$$\widetilde{f}^{(n)}_{L-}(z) = N^{(n)}_{L-}e^{-b\mu^2z^2/2}z^c\ U\left(\frac{1}{4}+\frac{c}{2}-\frac{m_n^2}{4b\mu^2},\frac{1}{2}+c,b\mu^2z^2\right), \tag{4.2.20}$$

$$\widetilde{f}^{(n)}_{R+}(z) = \frac{b\mu^2z}{m_n}f^{(n)}_{L-}, \tag{4.2.21}$$

$$\widetilde{f}^{(n)}_{L+}(z) = \frac{1}{m_n}\left(\frac{c}{z}f^{(n)}_{L-}-f^{(n)\prime}_{L-}\right), \tag{4.2.22}$$

$$\widetilde{f}^{(n)}_{R-}(z) = 0, \tag{4.2.23}$$

where $N^{(n)}_{L-}$ is a normalization constant. For this tower, the boundary conditions $\widetilde{f}^{(n)}_{R+}\big|_{z_0}=0$ and $\widetilde{f}^{(n)}_{L-}\big|_{z_0}=0$ are equivalent. The orthonormality condition for all fields may be written compactly as,

$$\int_{z_0}^{\infty}dz\ \widetilde{f}^{(n)}_{L-}\widetilde{f}^{(m)}_{L-}=\delta^{nm}, \tag{4.2.24}$$

as this in fact implies the correct orthonormality condition for the remaining fields,

$$\int_{z_0}^{\infty}dz\ \left[\widetilde{f}^{(n)}_{L+}\widetilde{f}^{(m)}_{L+}+\widetilde{f}^{(n)}_{R+}\widetilde{f}^{(m)}_{R+}\right]=\delta^{nm}. \tag{4.2.25}$$

The other KK tower is given by:

$$\widetilde{f}^{(n)}_{R-}(z) = N^{(n)}_{R-} e^{-b\mu^2 z^2/2} z^{2+c}\, U\left(\frac{5}{4}+\frac{c}{2}-\frac{m_n^2}{4b\mu^2}, \frac{5}{2}+c, b\mu^2 z^2\right), \quad (4.2.26)$$

$$\widetilde{f}^{(n)}_{L+}(z) = \frac{b\mu^2 z}{m_n} f^{(n)}_{R-}, \quad (4.2.27)$$

$$\widetilde{f}^{(n)}_{R+}(z) = -\frac{1}{m_n}\left(\frac{1+c}{z} f^{(n)}_{R-} + f^{(n)\prime}_{R-}\right), \quad (4.2.28)$$

$$\widetilde{f}^{(n)}_{L-}(z) = 0, \quad (4.2.29)$$

where $N^{(n)}_{R-}$ is a normalization constant. The spectrum for this tower is found by imposing the boundary condition $\widetilde{f}^{(n)}_{R+}\big|_{z_0} = 0$, while the normalization condition is,

$$\int_{z_0}^{\infty} dz\, \widetilde{f}^{(n)}_{R-} \widetilde{f}^{(m)}_{R-} = \delta^{nm}. \quad (4.2.30)$$

The second tower in fact admits a very light ground state, however approximating the mass requires some care. Note that it was possible to derive the approximation (4.2.17) for the degenerate case because the first argument of the hypergeometric functions in (4.2.12) – (4.2.15) was small. We do not have such luxury in this case.

Instead, for $m_0^2 \ll b\mu^2$ we can expand the functions using techniques of so-called boundary perturbation theory of quantum mechanics [119, 120]. We start by considering the Schrödinger-like equation for $\widetilde{f}^{(n)}_{R-}$,

$$-\partial_z^2 \widetilde{f}^{(n)}_{R-} + \left[\frac{(c+1)(c+2)}{z^2} + b^2\mu^4 z^2\right] \widetilde{f}^{(n)}_{R-} = m_n^2 \widetilde{f}^{(n)}_{R-}. \quad (4.2.31)$$

As we are seeking solutions with small m_0^2, we begin by writing $\widetilde{f}^{(0)}_{R-}$ as a product of the zero-mode solution and a correction:

$$\widetilde{f}^{(0)}_{R-} = \zeta(z) F(z), \quad (4.2.32)$$

where $\zeta(z)$ is chosen so as to satisfy the zero-mode equation

$$-\partial_z^2 \zeta + \left[\frac{(c+1)(c+2)}{z^2} + b^2\mu^4 z^2\right] \zeta = 0. \quad (4.2.33)$$

The solution to this equation may be written as,

$$\zeta(z) = N^{(0)}_{R-} z^{1/2} K_\nu(b\mu^2 z^2/2),$$

where $N_{R-}^{(0)}$ is a constant, K_ν is the modified Bessel function and $\nu = 3/4 + c/2$. The function $F(z)$ obeys the second-order equation,

$$\left[\zeta^{-2}\partial_z(\zeta^2\partial_z) + m_0^2\right] F(z) = 0$$

and may be expanded in powers of m_0^2. The resulting expansion for $\widetilde{f}_{R-}^{(0)}$ is,

$$\widetilde{f}_{R-}^{(0)} \simeq \zeta(z)\left[1 + m_0^2\int_{z_0}^{z} \mathrm{d}z'\zeta^{-2}\int_{z'}^{\infty}\mathrm{d}z''\zeta^2 + \mathcal{O}(m_0^4)\right]. \tag{4.2.34}$$

Such an expansion has also been used in Ref. [61] to approximate wavefunctions in soft-wall models. In contrast, here we are using it to solve the boundary value problem itself. The UV boundary condition,

$$\widetilde{f}_{R+}^{(0)}\Big|_{z_0} = \left(\widetilde{f}_{R-}^{(0)\prime} + \frac{1+c}{z}\widetilde{f}_{R-}^{(0)}\right)\Big|_{z_0} = 0, \tag{4.2.35}$$

can now be applied to the expansion (4.2.34). Notice that at the boundary $z = z_0$, the $\mathcal{O}(m_0^2)$ correction vanishes while its derivative is given by a single integral over Bessel functions. Using well-known known rules for differentiation and integration of Bessel functions (c.f. [121]), we can thus derive the following approximate expression for m_0^2:

$$m_0^2 \simeq \frac{K_{1-\nu}(b\mu^2 z_0^2/2)}{K_\nu(b\mu^2 z_0^2/2)\mathcal{I}(z_0)}z_0, \tag{4.2.36}$$

where

$$\mathcal{I}(z) \equiv \int_z^\infty dz'\,\zeta^2(z'). \tag{4.2.37}$$

The expression (4.2.36) can now be expanded for small z_0. For $c > -1/2$ we find,

$$m_0^2 \simeq \frac{2(c/2+3/4)}{\Gamma\left(c/2+3/4\right)}\left(\frac{b^2\mu^4 z_0^2}{4}\right)\left[\left(\frac{b\mu^2 z_0^2}{4}\right)^{c-1/2}\Gamma\left(-c/2+1/4\right) + \Gamma\left(c/2-1/4\right)\right]. \tag{4.2.38}$$

In the limit $c \gg 1/2$, this expression simplifies further to

$$m_0^2 \simeq \left(1 + \frac{1}{c-1/2}\right)b^2\mu^4 z_0^2. \tag{4.2.39}$$

This expression reveals a lower bound on the fermion mass in this region of the bulk mass parameter space,

$$m_{\min} = (\mu z_0)b\mu. \tag{4.2.40}$$

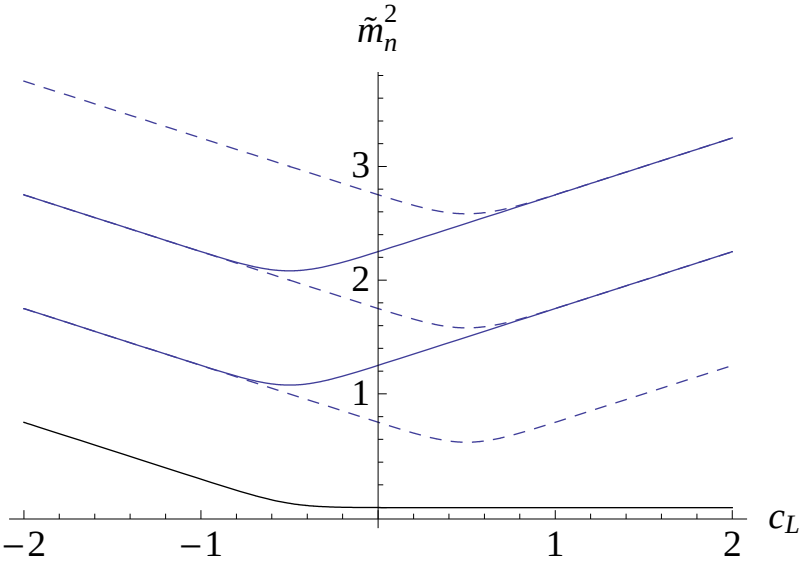

Figure 4.1: The first several masses in the split case plotted as a function of c_L. The spectrum is composed of two "separate" towers (dashed and solid lines), which coincide for large negative and positive values of c_L. Here, $\widetilde{m}_n^2 = m_n^2/b\mu^2$ and $\mu z_0 \ll 1$.

For $c \ll -1/2$, the above expansions are poor approximations because the mass becomes $\mathcal{O}(b\mu)$. To deal with this regime, we can apply mathematical techniques from "supersymmetric quantum mechanics" to determine the mass [67]. As we have observed frequently in previous chapters, quantum mechanical system for which the Hamiltonian may be factorized as,

$$[-\partial_z + W(z)]\,[\partial_z + W(z)]\,\psi = m_n^2\psi. \tag{4.2.41}$$

admit zero-mode solutions $\psi \sim e^{-\int W}$ satisfying boundary conditions that are trivially consistent with the equations of motion,

$$[\partial_z + W(z)]\,\psi\big|_{\mathcal{B}} = 0. \tag{4.2.42}$$

Thus we consider the particular "superpotential,"

$$W(z) = \frac{1+c}{z} + b\mu^2 z, \tag{4.2.43}$$

which gives rise to the "ordinary" potential:

$$V(z) = W^2 - W' = \frac{(c+1)(c+2)}{z^2} + b^2\mu^4 z^2 + (2c+1)b\mu^2. \tag{4.2.44}$$

which is equivalent to the potential in (4.2.31) up to a constant shift of the reference potential. Next, we note that the boundary conditions in (4.2.35) are equivalent to $[\partial_z + W(z)]\widetilde{f}^{(0)}_{R-}|_{z_0} = 0$ in the limit $\mu z_0 \to 0$. We can conclude then that the solution $\psi \sim e^{-\int W}$ is in fact a good approximation for $\widetilde{f}^{(0)}_{R-}$ provided the mass eigenvalue is given by

$$m_0^2 \simeq (-1-2c)b\mu^2. \tag{4.2.45}$$

This is clearly only valid when $c < -1/2$. We have checked that the expressions (4.2.39) and (4.2.45) match the exact results well in the appropriate regions. The full spectrum is plotted in Fig. 4.1. The distinctive KK tower structure of the split case suggests the possibility of novel KK physics unlike that found in hard-wall models and may be interesting to study in other soft-wall bulk Higgs models as well.

4.2B Comparison with Perturbative Expansions

The possibility of modeling fermions by introducing non-constant bulk Dirac mass terms has been considered in Ref. [64]. For a single generation setup with quadratic bulk mass terms, the equations of motion are the same as (4.2.1), but now the mixing matrix (4.1.16) can be written effectively as,

$$\mathcal{M} = e^{-A}\begin{pmatrix} c_L^0 k + c_L^1 k\mu^2 z^2 & bk\mu^2 z^2 \\ bk\mu^2 z^2 & c_R^0 k + c_R^1 k\mu^2 z^2 \end{pmatrix}, \tag{4.2.46}$$

where $c^0_{L,R}, c^1_{L,R}$ are constant coefficients. The effect of this non-constant bulk mass is that normalizable zero-modes persist (depending on the choice of the signs of $c^1_{L,R}$) even in the limit $b \to 0$. For small values of b, the spectrum may be found by treating the bulk Yukawa interaction as a perturbation on the $b = 0$ solutions.

Such an approach can be related to ours in some cases. For example, in the case of degenerate constant mass pieces, $c_L^0 = c_R^0$, global unitary transformations may still be used to diagonalize the mass matrix when the bulk masses have the same functional form as the Higgs VEV. Thus, the introduction of non-constant bulk masses can be viewed as effectively changing the boundary conditions on the fields in such cases.

It is interesting to note that the case considered in [64] is similar to our "split" case. In particular, they examine $c_L^1 = -c_R^1$ and $c_L^0 = -c_R^0$ in detail. In the slightly different split configuration for the constant pieces of the bulk mass, $c_L^0 = \pm 1 - c_R^0$, analytical

solutions can be obtained in a similar fashion to our earlier analysis. For $c_L^0 = -1 - c_R^0$, we find the lowest lying KK tower to be:

$$f_{R-}^{(n)}(z) = N_{R-}^{(n)} e^{-\widetilde{b}\mu^2 z^2/2} z^{2+c_L^0}\, U\left(\frac{5}{4} + \frac{c_L^0}{2} - \frac{\widetilde{m}_n^2}{4\widetilde{b}\mu^2}, \frac{5}{2} + c_L^0, \widetilde{b}\mu^2 z^2\right), \quad (4.2.47)$$

$$f_{L+}^{(n)}(z) = \frac{b\mu^2 z}{m_n} f_{R-}^{(n)}, \quad (4.2.48)$$

$$f_{R+}^{(n)}(z) = -\frac{1}{m_n}\left(f_{R-}^{(n)\prime} + \frac{1 + c_L^0}{z} f_{R-}^{(n)} + c_L^1 \mu^2 z f_{R-}^{(n)}\right), \quad (4.2.49)$$

$$f_{L-}^{(n)}(z) = 0, \quad (4.2.50)$$

where we have defined effective parameters, $\widetilde{b}^2 = \left(c_L^1\right)^2 + b^2$, and $\widetilde{m}_n^2 = m_n^2 - c_L^1\left(2c_L^0 + 1\right)$ to make the comparison with (4.2.26)–(4.2.29) clear. Note that there remains a lower bound on the mass for $c_L^0 \gg 1/2$. We have checked that this solution describes the large c_L^0 behavior for the case considered in Ref. [64], $c_L^0 = -c_R^0$. We expect that all of the basic features of the non-constant bulk mass model should be contained within our exact solutions.

Generically the split and degenerate cases allow one to find the spectrum exactly by solving a set of decoupled second-order equations. Even when the equations cannot be solved exactly, approximate methods such as those we have described above may be employed. Additionally, as our numerical results will verify, one can expect the behavior in these special cases to provide a complete qualitative picture of the full parameter space dependence.

4.2C Couplings to Gauge Bosons

Of significant interest in models involving extra dimensions is the coupling of fermions to the KK gauge bosons. When the fermions are localized at different points along the extra dimension, they can obtain non-universal couplings to the excited gauge bosons. Such non-universality will generically lead to large contributions to flavor physics observables, providing very stringent lower bounds on the allowed KK scale [122].

In hard-wall models, the couplings can become universal for certain regions of the parameter space, resulting in a GIM-like suppression of FCNCs [78] and greatly lowering the bound on the allowed KK scale. We therefore would like to see if a similar effect is

present in the soft-wall case. Moreover, we would like to develop our formalism in such a way that multiple fermion generations can be incorporated.

In analogy with the discussion of Section 2.4B, the couplings of the zero mode fermions to the KK gauge bosons are found to be:

$$g_{\pm}^{\alpha\beta(n)} = g_5 \int_{z_0}^{\infty} \mathrm{d}z f_A^{(n)} \left((f_{L\pm}^{i\alpha(0)})^\dagger f_{L\pm}^{i\beta(0)} + (f_{R\pm}^{i\alpha(0)})^\dagger f_{R\pm}^{i\beta(0)} \right), \tag{4.2.51}$$

where $f_A^{(n)}$ is the gauge boson profile along the extra dimension. The gauge boson profiles arising from a quadratic dilaton (4.1.3) were derived in Section 3.3A. The zero-mode couplings $g_{\pm}^{\alpha\beta(0)} \equiv g\delta^{\alpha\beta}$ remain universal due to the orthonormality condition (4.1.17) and the flat zero mode gauge boson profile. This is because the dilaton factor explicitly cancels and plays no role.

The degenerate single-generation case was considered in [63], where it was found that only one of the couplings, g_+ or g_-, can become universal due to the opposite localizations of the fermion modes. In Ref [64], it was seen that opposite constant and non-constant bulk masses led to universal couplings for both g_+ and g_-. This happens as well for the split case solutions. We have plotted the couplings for this case in Figs. 4.2 and 4.3. We find that the couplings g_+ and g_- become universal simultaneously whenever $c \gg 1/2$.

Note that the bounds from flavor physics are generically expected to be more stringent in soft-wall models than in models with a hard wall. This follows from the generically closer spacing of the KK modes in soft-wall models as compared to hard-wall models. For example, we can consider the contribution to Δm_K arising from non-universal couplings. The effective 4D Lagrangian contains operators that are suppressed by the squared masses of the KK gauge bosons mediating the strangeness-changing transitions ($\Delta S = 2$):

$$\mathcal{L}_{\Delta S=2} \supseteq \sum_{n=1}^{\infty} \frac{1}{M_n^2} \left[\bar{d}_L^{\alpha} \widetilde{g}_+^{\alpha\beta(n)} \gamma^\mu d_L^{\beta} + \bar{d}_R^{\alpha} \widetilde{g}_-^{\alpha\beta(n)} \gamma^\mu d_R^{\beta} + \text{ h.c.} \right]^2, \tag{4.2.52}$$

where the sum is over the gauge boson KK modes with KK masses M_n, and $\widetilde{g}_{\pm}^{\alpha\beta(n)} = V_{L,R}^d \, g_{\pm}^{\alpha\beta(n)} V_{L,R}^{d\dagger}$ with $V_{L,R}^d$ generic unitary matrices [122]. Thus, in the presence of non-degenerate couplings to the bulk KK gauge bosons, bounds from flavor experiments may be interpreted as a lower bound on the KK scale.

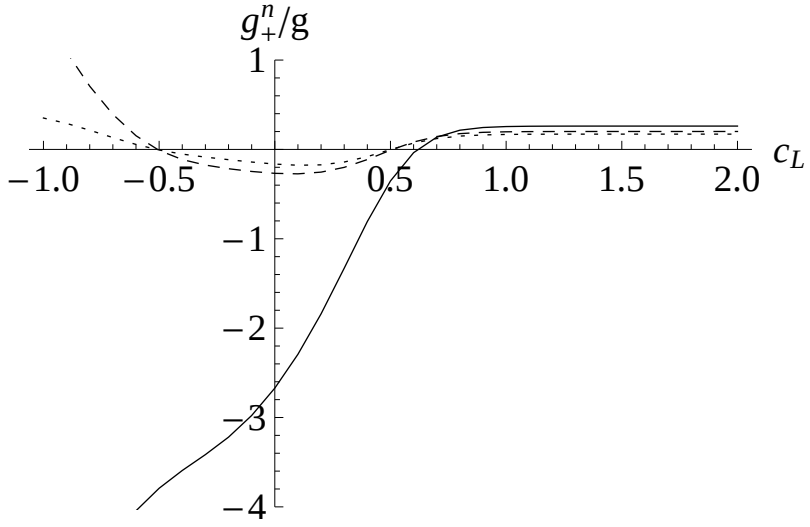

Figure 4.2: The ratio $g_+^{(n)}/g$ for $n = 1$ (solid), $n = 2$ (dashed), and $n = 3$ (dotted) KK gauge modes coupled to the zero-mode fermion in the split case, as calculated using (4.2.51).

The key point is that the total amount of suppression in (4.2.52) depends upon the spacing of the KK tower. In a hard-wall model, for example, $M_n^2 \sim n^2 M_{KK}^2$, where M_{KK} is the KK mass scale. This compares to the soft-wall scenario where it would seem to imply a problem, because the squared mass trajectories grow generically as $m_n^2 \sim n M_{KK}^2$. (Indeed, this spacing was the original motivation for studying the soft-wall [60]). While the sum of $1/n$ diverges as $n \to \infty$, we should of course truncate the sum at some high energy cutoff. Nevertheless, the naive implication is that the constraints on soft-wall models should be considerably tighter.

However, this argument ignores the fact that the gauge bosons become increasingly IR localized with increasing mode number n. Thus, any off-diagonal terms in the gauge coupling matrices are further suppressed for large n. By performing a numerical fit using the first several dozen gauge boson modes and our split case solutions, we find that the couplings fall off as $n^{-0.4}$ to a very good approximation in the region where the couplings are independent of localization. This implies that the terms in the sum (4.2.52) grow as $n^{-1.4}$. All other things being equal, this implies that the constraints from flavor physics are roughly a factor of two more stringent in this model than in hard-wall models.

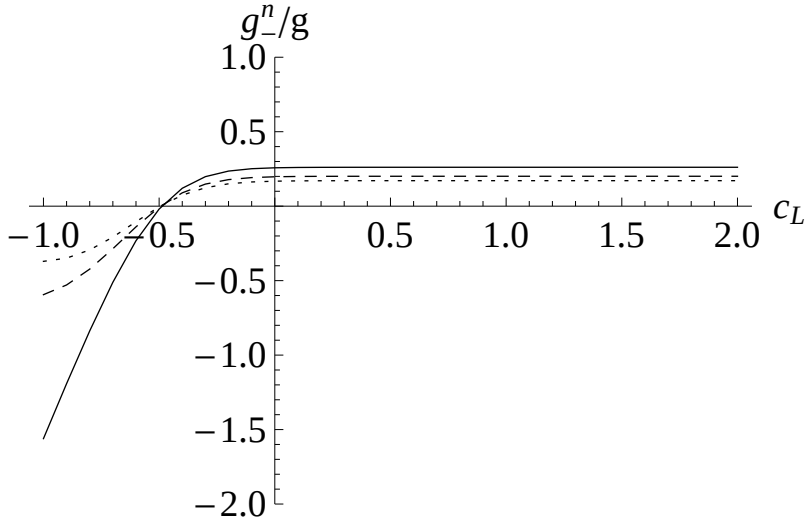

Figure 4.3: The ratio $g_-^{(n)}/g$ for $n = 1$ (solid), $n = 2$ (dashed), and $n = 3$ (dotted) KK gauge modes coupled to the zero-mode fermion in the split case, as calculated using (4.2.51).

While this presents no great problem for the model with a *quadratic* dilaton, for a generic power law behavior in the dilaton, $\Phi \sim z^\alpha$, the spectrum of gauge bosons grows as $m_n^2 \sim n^{2-2/\alpha} M_{KK}^2$ [63]. This means that for less steep potentials, even tiny amounts of non-degeneracy among the bulk couplings has potentially severe implications for flavor physics.

4.3 Numerical Solution

4.3A Routine

The analytical solutions that we have presented, though useful, do not solve the full fermion mass problem including flavor. Our goal is to solve the eigenvalue problem (4.1.15) with mixed boundary conditions. The "initial conditions" (4.1.5) specify half of the boundary values at the UV brane or, equivalently, half of the integration constants for the system. The remaining constants of integration are fixed by the normalization conditions (4.1.17), which can only be satisfied if the eigenvalue, m_n^α, has been chosen correctly. Thus, following our discussion at the end of Section 4.1, it would seem that we

must find the particular coordinates in a $2N_F$-dimensional parameter space that result in a normalizable solution.

In fact, the problem is made considerably simpler by exploiting the linearity of the system. To this end, we first convert the problem to an initial value one by extending and modifying the shooting method [123] to linear boundary value problems of arbitrary order. In this way, the orthonormality requirement (4.1.17) can be viewed as fixing the $2N_F - 1$ ratios of the functions at the boundary at $z = z_0$, plus one irrelevant scale parameter. The remaining degree of freedom corresponds to m_n^α and is fixed by demanding finiteness of the solution in the IR.

Since (4.1.15) is linear, its solutions may be written as:

$$f^{i\alpha(n)}(z) = U(m_n^\alpha; z, z_0)^{ij} f^{j\alpha(n)}(z_0), \tag{4.3.1}$$

where the propagator $U(m_n^\alpha; z, z_0)$ is a linear operator and the $f^{i\alpha(n)}(z)$ are $4N_F \times 4N_F$ matrix-valued functions for N_F fermion generations.

Our approach is to solve for the matrix elements of U by integrating an arbitrary set of $4N_F$ linearly independent basis vectors that span the space of initial values, $f^{i\alpha(n)}(z_0)$, and inverting (4.3.1). Having reconstructed the matrix U, it is straightforward to find the initial value vectors that lead to normalizable solutions by considering the behavior of U acting on such a vector: it transports it to the zero-vector. Therefore, the initial conditions leading to normalizable solutions correspond to eigenvectors of $U(m_n^\alpha; z, z_0)$ with vanishing eigenvalues in the limit $z \to \infty$. There are generally $2N_F$ such eigenvectors. The actual solution will be formed from a sum over these vectors,

$$f_j^{i\alpha(n)}(z) = \sum_{i=1}^{2N_F} a_i F_j^{i\alpha(n)}(z), \tag{4.3.2}$$

where the a_i are constants and the capitalized $F^{i\alpha(n)}(z)$ are $4N_F$-component vector-valued functions ($j = 1, 2, \ldots, 4N_F$) satisfying[3]

$$\lim_{z_1 \to \infty} U(m_n^\alpha; z_1, z)^{ij} F^{j\alpha(n)}(z) = 0. \tag{4.3.3}$$

Numerically, we can estimate the values of these vectors by considering the eigenvectors of $U(m_n^\alpha; z_1, z_0)$, where our cutoff satisfies $z_1 \gg \mu^{-1}$. In practice, results are

[3] Technically, given the orthonormality condition, we should consider the limit of $|UF|^2$, but the distinction is inconsequential.

much more reliable if one starts the forward integration from some intermediate range $z^* \sim \mu^{-1}$ and then integrates the normalizable modes back to z_0. Variations on this theme can be explored, and one of the attractive features of the method is that it does not depend on a particular numerical integration technique.

We scan over m_n^α, at each point integrating the system from an arbitrary set of initial values so as to reconstruct the normalizable solutions. If there exists a linear combination of the solutions that matches the boundary conditions (4.1.5), then m_n^α is a solution to the system. To determine when this occurs, we define a merit function in the following way. Let us arrange the functions $f^{i\alpha(n)}$ such that the functions satisfy Dirichlet conditions for $i = 1, 2, \ldots, 2N_F$. Then from (4.3.2) we have:

$$\sum_{i=1}^{2N_F} a_i F_j^{i\alpha(n)}(z_0) = 0, \qquad \text{for } j = 1, 2, \ldots 2N_F, \tag{4.3.4}$$

which can only be satisfied if they are linearly independent. Thus,

$$\det \begin{pmatrix} F_1^{1\alpha(n)}(z_0) & F_1^{2\alpha(n)}(z_0) & \cdots & F_1^{2N_F\alpha(n)}(z_0) \\ F_2^{1\alpha(n)}(z_0) & F_2^{2\alpha(n)}(z_0) & \cdots & F_2^{2N_F\alpha(n)}(z_0) \\ \vdots & \vdots & \ddots & \vdots \\ F_{2N_F}^{1\alpha(n)}(z_0) & F_{2N_F}^{2\alpha(n)}(z_0) & \cdots & F_{2N_F}^{2N_F\alpha(n)}(z_0) \end{pmatrix} = 0. \tag{4.3.5}$$

Our merit function is simply the absolute value of this determinant, and we search for a minimum.

When the hierarchy between μ and z_0^{-1} is very large, increasingly high precision is necessary to achieve reliable results. Iterative methods may be better suited to the problem in such cases. Our primary goal is to highlight the differences between fermions in soft-wall and hard-wall scenarios, and the speed and simplicity of this technique are its chief advantages. For this reason, we have limited our attention to a modest hierarchy below.

4.3B Results

Single Generation

We first present results for a single generation of fermions, as this case illustrates the essential features of the fermion mass behavior in the soft-wall, and allows us to compare

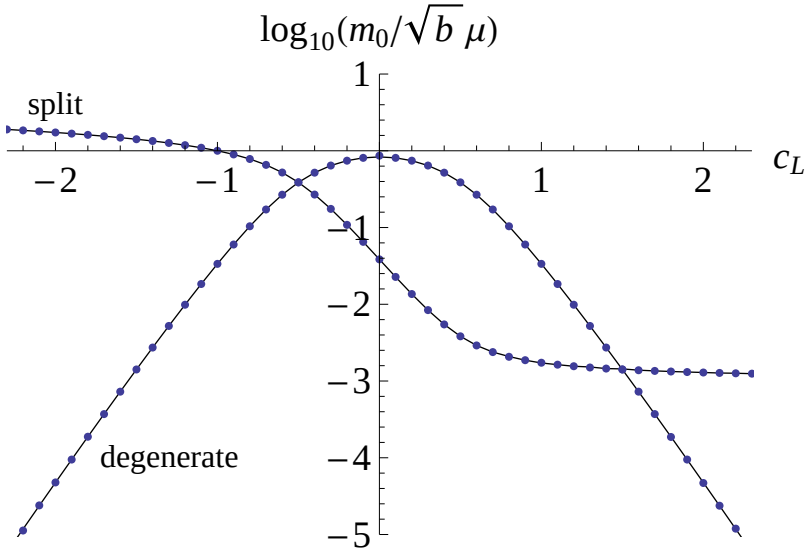

Figure 4.4: Lowest lying masses for the "degenerate" ($c = c_L = c_R$) and "split" ($c = c_L = -1 - c_R$) cases. The solid lines are determined using the exact results from Section 4.2, while the dots represent values obtained using the numerical method of Section 4.3A.

our numerical results with the analytical cases in the appropriate limits as well as to a typical hard-wall setup. We assume the following values of the parameters:

$$\mu = 1 \text{ TeV}; \qquad \mu z_0 = 10^{-3}; \qquad b = 1. \tag{4.3.6}$$

In Figure 4.4, we compare the numerical results to the analytical results from Section 4.2 where it can be seen that the two methods agree very well. In Figure 4.5, we plot the fermion mass contours to show the full dependence on the parameters c_L and c_R. The shape of the plot is easily understood from the analytical results. The numerical solution smoothly interpolates between the solutions along the lines $c_L = c_R$ and $c_L = \pm 1 - c_R$. Because a similar analysis can be repeated for other Higgs VEVs, this provides a natural way to begin studying the qualitative aspects of other models in AdS as well.

We can compare the soft-wall behavior with a typical hard-wall setup. In Figure 4.6 we provide the corresponding contour plot for a hard-wall model in which the SM fermion masses are simply proportional to the values of the wavefunctions at $z = 1/\mu$. The most striking difference between the plots occurs in the lower right-hand corner. This is the region where $c_L > 1/2$ and $c_R < -1/2$.

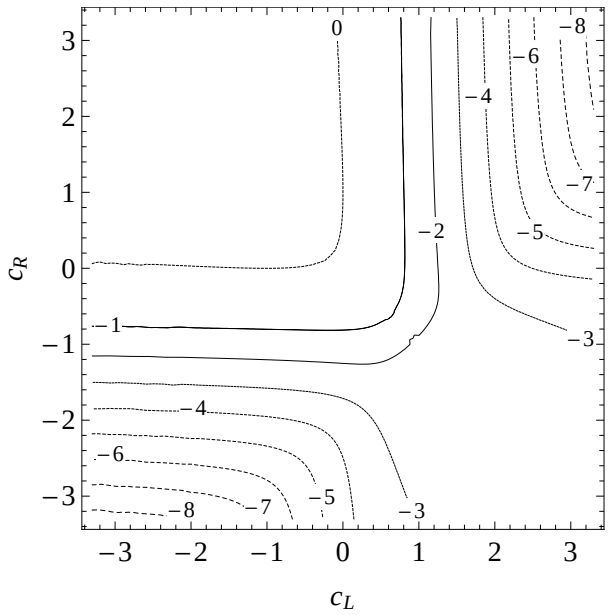

Figure 4.5: Contours of $\log_{10}(m_0/\sqrt{b}\mu)$ for the lowest lying masses in our soft-wall setup with $\sqrt{b}\mu z_0 = 10^{-3}$.

The hard-wall case is characterized by a steep dependence on the bulk mass in this region, where the wavefunctions are proportional to $f^{(0)}_{L+} \sim z^{-c_L}$ and $f^{(0)}_{R-} \sim z^{c_R}$. For $z_0 \ll \mu^{-1}$, the normalization constants become vanishingly small:

$$N^{(0)}_{L,R} \sim z_0^{-1/2 \pm c_{L,R}}. \tag{4.3.7}$$

Thus, the values of the functions in the IR at $z = \mu^{-1}$ are additionally suppressed. This is the well-known mechanism for generating SM mass hierarchies in Randall-Sundrum scenarios with bulk fields [79, 78]. For the soft-wall case, however, we can see the lower bound on the mass in this region,

$$m_0 \sim (\mu z_0)\mu, \tag{4.3.8}$$

as indicated by the approximate expression (4.2.39). This can be understood by noting that the normalization (4.1.17) involves the sum of two types of fermion contributions, which are generically not simultaneously suppressed.

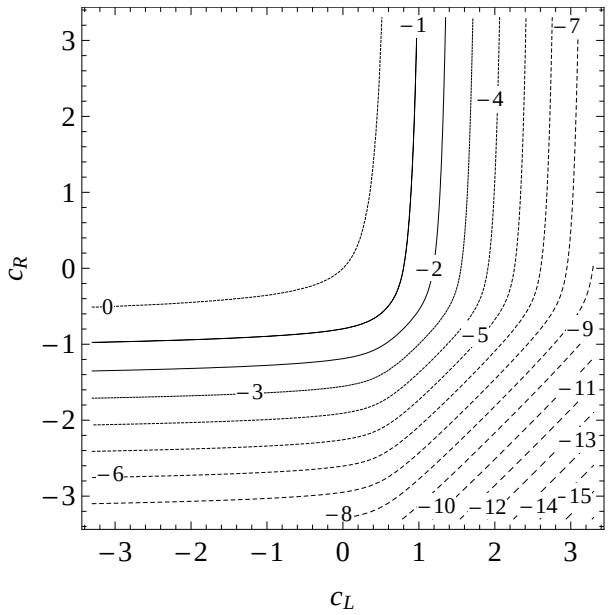

Figure 4.6: Contours of $\log_{10}(m_0/\sqrt{b}\mu)$ for the lowest lying masses in a typical hard-wall setup with $\sqrt{b}\mu z_0 = 10^{-3}$.

Three-Generations

In this section we aim to provide concrete numerical examples involving three generations of fermions that fully take into account the 5D flavor mixing to show that the attractive features of the soft-wall are maintained.

For multiple generations, there are three matrices that parameterize the fermions: two bulk mass matrices M_L and M_R, and the bulk Yukawa matrix, λ_5. We take the action (4.1.4) to be written in an arbitrary basis, for example, the CKM basis. Absent some symmetry, there is no reason to expect any structure relating the entries of the various bulk parameter matrices. We generically expect that the entries of each matrix are all of order unity (in units of the AdS curvature scale, k), and that the various matrices are misaligned. There is of course some basis in which both M_L and M_R are diagonal. Thus, by "misaligned," we mean that this basis is distinct from the one in which the Yukawa matrix is diagonal. Indeed, the typical approach is to work in this basis, treating the Yukawa interactions as perturbations. Such an approach has been used in both hard-wall [79, 78, 116, 80, 93] and even in modified soft-wall setups [64].

In Ref. [64], it was found that one needed to include the first several KK modes in order to achieve reliable results in such a perturbative expansion when including only a single generation. At such a point, the analysis is essentially a numerical exercise. In our view, it is advantageous to include the entire KK tower in the numerical formulation wherever possible. That is to say that it may make the most sense to simply solve the equations of motion (4.1.15), which guarantee the orthogonality of the eigenfunctions due to the Hermiticity of the mixing matrix.

We expect that all other interactions may be treated reliably as perturbations. This is because the Higgs grows unbounded in the IR where it is the dominant contribution to the fermion equations of motion. Other observables may thus be calculated using the usual wavefunction overlap approximation. As an application, we will calculate the couplings to excited gauge bosons for examples involving three generations.

We do not attempt to set precise bounds on soft-wall models here, as doing so goes significantly beyond the scope of this work. Electroweak and flavor constraints have been discussed in the context of soft-wall models in Refs. [63, 64]. Detailed analyses in various hard-wall scenarios can be found in [79, 78, 80, 122, 112, 93] and references therein.

However, we will require that the eigenvalues of the bulk mass matrices satisfy $m_L^i \gtrsim k/2$ and $m_R^i \lesssim -m_L^i$ in order to get nearly degenerate gauge couplings. Because of the lower bound on the fermion masses at $m_0 \sim (\mu z_0)\mu$ in this region, it is clear that the hierarchy considered above, $\mu z_0 = 10^{-3}$ will be inadequate for generating MeV scale masses when $\mu = 1$ TeV, and will only be possible for $\mu z_0 \lesssim 10^{-6}$. Thus we again assume a quadratic Higgs VEV, $h(z) = \eta k^{3/2}\mu^2 z^2$, and the following for our input parameters:

$$\mu = 1 \text{ TeV}; \qquad \mu z_0 = 10^{-6}. \tag{4.3.9}$$

Dealing with much larger hierarchies presents significant numerical challenges. However, the qualitative results of such an analysis should not be substantially different from the results presented here.

First, we present an example resembling down-type quarks (or charged leptons). For simplicity, we take the entries of M_L to be nearly degenerate, but we allow for large non-degeneracy in the matrix M_R as well as in the Yukawa matrix. Specifically, we

consider,

$$\frac{M_L}{k} = \begin{pmatrix} 0.784 & -0.020 & 0.023 \\ -0.020 & 0.808816 & 0.0094 \\ 0.024 & 0.0094 & 0.780 \end{pmatrix}, \qquad \frac{M_R}{k} = \begin{pmatrix} -2.179 & -0.459 & -0.774 \\ -0.459 & -1.073 & -0.354 \\ -0.774 & -0.354 & 0.1218 \end{pmatrix},$$

$$\frac{\eta}{\sqrt{2}}\lambda_5 = \begin{pmatrix} 0.422 & 0.175 & -0.678 \\ -0.007 & 0.928 & 0.348 \\ 0.295 & -0.327 & 0.637 \end{pmatrix}. \tag{4.3.10}$$

We find a spectrum of masses resembling the down-type quarks (or charged leptons):

$$m_0^\alpha = 0.57 \text{ MeV},\ 96.08 \text{ MeV},\ 1.310 \text{ GeV}. \tag{4.3.11}$$

The fermion mass hierarchy is clearly obtained, but due to the complexity of the numerical procedure we do not match the SM masses exactly. The fermion bulk profiles,

$$F_-^\alpha(z) = \sqrt{(f_{L-}^{i\alpha(0)})^\dagger f_{L-}^{i\alpha(0)} + (f_{R-}^{i\alpha(0)})^\dagger f_{R-}^{i\alpha(0)}}, \tag{4.3.12}$$

are plotted in Figure 4.7. The fermion profile overlap with the Higgs VEV, $h(z)$ leads to the fermion mass hierarchy. The corresponding bulk profiles, $F_+^\alpha(z)$ are not plotted because the profile differences between the flavors are not as pronounced. This is due to our choice of UV boundary conditions and bulk masses (4.3.10).

From expression (4.2.51), we can calculate the coupling of the zero mode fermions to the KK gauge bosons (i.e. gluons). The result is a matrix whose off-diagonal entries contribute to flavor violation. We obtain the following results for the first two KK gauge

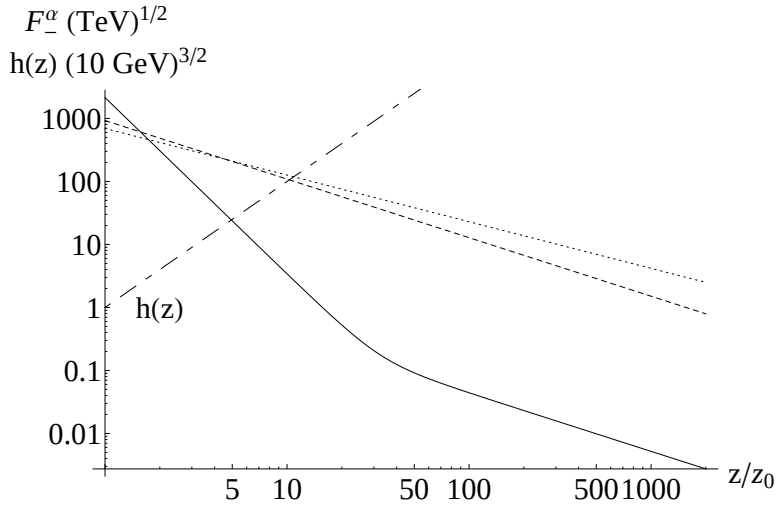

Figure 4.7: The down-type fermion bulk profiles $F_-^\alpha(z)$ for the first generation (solid), second generation (dashed) and third generation (dotted) showing the overlap with the Higgs VEV $h(z)$. Note that $h(z)$ has been rescaled for presentation.

coupling matrices, normalized to the coupling to the massless gauge boson:

$$\begin{aligned}
\frac{g_+^{(1)}}{g} &= \begin{pmatrix} 0.186 & 10^{-4} & 10^{-4} \\ 10^{-4} & 0.187 & 2\times 10^{-4} \\ 10^{-4} & 2\times 10^{-4} & 0.185 \end{pmatrix}, \\
\frac{g_+^{(2)}}{g} &= \begin{pmatrix} 0.140 & 10^{-4} & 10^{-4} \\ 10^{-4} & 0.138 & 10^{-4} \\ 10^{-4} & 10^{-4} & 0.137 \end{pmatrix}; \\
\frac{g_-^{(1)}}{g} &= \begin{pmatrix} 0.188 & \approx 0 & \approx 0 \\ \approx 0 & 0.188 & 10^{-4} \\ \approx 0 & 10^{-4} & 0.184 \end{pmatrix}, \\
\frac{g_-^{(2)}}{g} &= \begin{pmatrix} 0.139 & \approx 0 & \approx 0 \\ \approx 0 & 0.139 & 10^{-4} \\ \approx 0 & 10^{-4} & 0.137 \end{pmatrix}.
\end{aligned} \tag{4.3.13}$$

This behavior is maintained for higher modes as well. For this choice of parameters, the very nearly degenerate couplings imply that μ of order a few TeV will be consistent with flavor constraints [65, 93, 112]. Note that we have assumed no contributions to

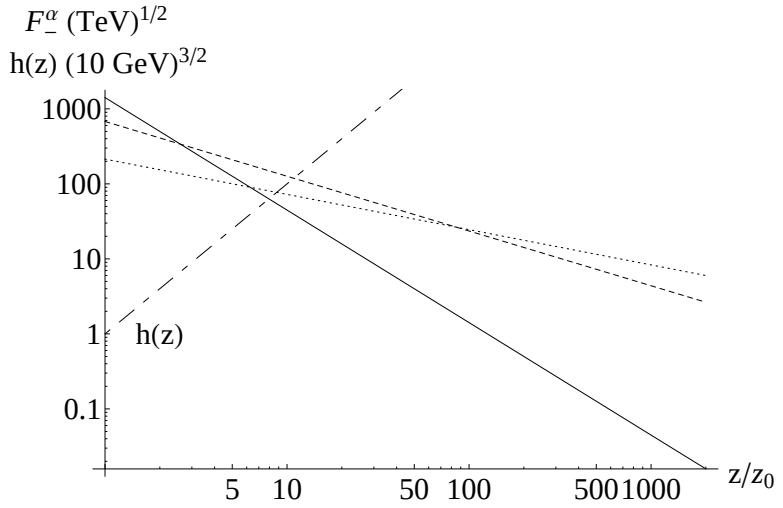

Figure 4.8: The up-type fermion bulk profiles $F_-^\alpha(z)$ for the first generation (solid), second generation (dashed) and third generation (dotted) showing the overlap with the Higgs VEV $h(z)$. Note that $h(z)$ has been rescaled for presentation.

CP violation. Thus the soft-wall model can accommodate the fermion mass hierarchy with large bulk mixing and small flavor violation.

The up-type quarks are only moderately more sensitive to the presence of the top when large bulk mixing is allowed. For the choices, $\mu = 1$ TeV and $\mu z_0 = 10^{-6}$ we obtain

$$\frac{M_L}{k} = \begin{pmatrix} 0.749 & -0.005 & 0.017 \\ -0.005 & 0.785 & 0.066 \\ 0.017 & 0.066 & 0.516 \end{pmatrix}, \qquad \frac{M_R}{k} = \begin{pmatrix} -0.940 & -0.285 & -0.200 \\ -0.285 & -1.103 & -0.338 \\ -0.200 & -0.338 & -0.657 \end{pmatrix},$$

$$\frac{\eta}{\sqrt{2}}\lambda_5 = \begin{pmatrix} 0.700 & -0.352 & -0.193 \\ -0.079 & 0.826 & -0.065 \\ -0.098 & -0.321 & 1.430 \end{pmatrix}, \tag{4.3.14}$$

which gives rise to the following mass spectrum:

$$m_0^\alpha = 2.10 \text{ MeV},\ 129.1 \text{ MeV},\ 151.5 \text{ GeV}. \tag{4.3.15}$$

Again we see that the correct fermion mass hierarchy can be obtained. The fermion bulk profiles, $F_-^\alpha(z) = \sqrt{(f_{L-}^{(0)}(z))^2 + (f_{R-}^{(0)}(z))^2}$ are plotted in Figure 4.8. The fermion

profile overlap with the Higgs VEV, $h(z)$ leads to the fermion mass hierarchy. Similarly to the down-type fermions, the corresponding up-type bulk profiles $F_+^\alpha(z)$ are not plotted because the profile differences are negligible due to the choice of UV boundary conditions and bulk masses (4.3.14). The gauge couplings are nearly universal among the first two generations:

$$\begin{aligned}
\frac{g_+^{(1)}}{g} &= \begin{pmatrix} 0.186 & 2\times10^{-3} & 2\times10^{-3} \\ 2\times10^{-3} & 0.185 & 10^{-6} \\ 2\times10^{-3} & 10^{-6} & -0.05 \end{pmatrix}, \\
\frac{g_+^{(2)}}{g} &= \begin{pmatrix} 0.140 & 10^{-3} & 10^{-3} \\ 10^{-3} & 0.139 & 10^{-3} \\ 10^{-3} & 10^{-3} & -0.05 \end{pmatrix}; \\
\frac{g_-^{(1)}}{g} &= \begin{pmatrix} 0.188 & 2\times10^{-6} & 4\times10^{-4} \\ 4\times10^{-4} & 0.183 & 10^{-3} \\ 2\times10^{-3} & 10^{-3} & -0.17 \end{pmatrix}, \\
\frac{g_-^{(2)}}{g} &= \begin{pmatrix} 0.140 & 10^{-6} & 3\times10^{-4} \\ 10^{-6} & 0.137 & 2\times10^{-3} \\ 3\times10^{-4} & 2\times10^{-3} & -0.140 \end{pmatrix}.
\end{aligned} \tag{4.3.16}$$

Constraints from top quark physics are significantly weaker, so this is not expected to affect the bound on μ.

Chapter 5

Lepton Flavor Violation with Heavy Sleptons and Dirac Gauginos

5.1 Introduction

Extensive effort has been devoted toward solving the supersymmetric flavor conundrum. Supersymmetry provides an elegant and natural solution to the hierarchy problem, but consistency with flavor physics measurements requires that the off-diagonal elements of the squark and slepton mass matrices be unnaturally small. This has led many physicists to favor flavor-blind features as an essential ingredient in models of supersymmetry breaking. Gauge mediation has become immensely popular in no small part due to its prediction of flavor universal sfermion masses.

However, there are additional possibilities that do not require universal soft masses for the suppression of flavor violation, and it is interesting to consider these possibilities. Three particular mechanisms that have been previously proposed are:

1. Alignment: the fermion and sfermion mass matrices are aligned in some basis, so that the rotations to the gauge eigenstates cancel [124, 125],

2. Hierarchy: the first two generations are heavy while the third (most notably the stop) is light [28], and

3. Extended R-Symmetry: the absence of certain MSSM diagrams (such as those involving Majorana gauginos) results in a much reduced flavor violation effect [30].

In this chapter, we consider lepton flavor violation under these scenarios, focusing on models with both sfermion mass hierarchy and an extended R-symmetry. As we will describe, this can arise naturally in phenomenological models of supersymmetry breaking from a warped background. In contrast to the original proposal of Randall and Sundrum [36], which solved the hierarchy problem by positing that the Higgs was localized on the infrared brane, we consider an elementary Higgs sector protected by supersymmetry. In this case, the Higgs is peaked in the UV while the warped geometry is used to explain the scale of SUSY breaking.

The generic low energy theory we consider features first-two generation sfermions of order 5 TeV, third generation sfermions of order 500 GeV and Dirac gauginos. While the existence of heavy sparticles is seemingly at odds with one of the primary motivations of supersymmetry—namely, naturalness in the Higgs sector—non-universality actually allows for large first and second generation scalar masses without destabilizing the Higgs due to small Yukawa couplings [29]. This combination prevents excessive rates for flavor violating processes, even when one considers large mixing among the sfermions. In particular, we consider the process $\mu \to e\gamma$, which provides the most stringent constraint on the lepton sector of these models.[1] The light third generation requires the inclusion of second-order mass insertion effects.

After a short review of supersymmetry in AdS in Section 5.2, we describe how supersymmetry breaking from extra dimensions can yield the general low-energy theory we have described in Section 5.3. In Section 5.4, we examine the existing flavor constraints on these models in terms of mass-insertion parameters. We find that LFV constraints can be accommodated for arbitrarily large mixing and gaugino masses no larger than 1.5 TeV. In Section 5.5, we discuss the implications of lepton-slepton alignment, which results in all flavor violation being mediated only by charginos. Finally, in Section 5.6 we compare these results with generic models with off-diagonal slepton mass terms and

[1] Ref. [126] considered $\mu \to e$ conversion in nuclei and found that this process provided the strongest constraints for relatively light sleptons and squarks. With larger sfermion masses, these processes are subdominant.

discuss the implications for the squark sector.

5.2 Supersymmetry in a Slice of AdS

Warped Background

The setup we have in mind is a supersymmetric Randall-Sundrum [36] background. Numerous top-down studies of this scenario have been undertaken [127, 128, 129, 130, 21]. Here we are interested in aspects of flavor in a phenomenological, bottom-up approach. As we are only interested in constraining low energy observables, we will not construct an explicit model, but rather outline the important features and behaviors. However, we will provide some explicit examples from the literature to illustrate our points.

We will be following many of the conventions of Section 2.1A. In particular, our spacetime is described by the conformal metric,

$$ds^2 = g_{MN}dx^M dx^N = e^{-2\widetilde{A}(z)}\eta_{MN}dx^M dx^N, \tag{5.2.1}$$

and is cut off by two three-branes at $z = z_0 = 1/k$ and $z = z_1 = e^{\pi kR}/k$

The standard model fermions, gauge bosons, and their superpartners are assumed to live in the bulk. We will therefore review how supersymmetry can be realized in a slice of AdS, following the work of Refs. [78, 131, 132, 133]. We will limit our attention to the vector supermultiplet and hypermultiplets.

Supersymmetric Bulk Field Content

Since the simplest spinor representation in five dimensions is the four-component Dirac spinor, the minimum number of supercharges is 8. This corresponds to $\mathcal{N} = 2$ SUSY from the 4D point of view. We will focus on the $U(1)$ vector supermultiplet and hypermultiplet representations. The supermultiplet field content is given by:

$$\mathcal{V} = (V_M, \lambda^i, \Sigma) \tag{5.2.2}$$

where V_M is the gauge field, Σ is a real scalar in the adjoint representation, and λ^i for $i = 1, 2$ is a symplectic-Majorana spinor:

$$\lambda^i = \begin{pmatrix} \lambda^i_L \\ \epsilon^{ij}\lambda^*_{Lj} \end{pmatrix}, \tag{5.2.3}$$

obeying $\lambda^i = \mathcal{C}(\overline{\lambda}^i)^T$ where $\mathcal{C}$ is the charge conjugation matrix.

The action is due to the gauge (2.3.19), fermion (2.3.32), and scalar contributions (2.3.1), with modifications to account for a symplectic Majorana spinor and real scalar:

$$S = -\int d^5x\sqrt{-g}\left[\frac{1}{4g_5^2}F_{MN}^2 + (D_M\Sigma)^2 + \frac{1}{2}m_\Sigma^2\Sigma^2 + \frac{i}{2}\overline{\lambda}^i\Gamma^M D_M\lambda^i + \frac{im_\lambda}{2}\overline{\lambda}^i\,(\sigma_3)^{ij}\,\lambda^j\right], \tag{5.2.4}$$

The supersymmetry transformations for each field may be found in Refs. [131, 78]. The gauge supermultiplet Lagrangian will be invariant under these transformations only when the fermion and scalar 5D masses take on particular values. This is in contrast to flat space, in which all particles in the multiplet must have identical masses. The masses compatible with supersymmetry are

$$m_\Sigma^2 = \left((\alpha_\Sigma + \frac{1}{2})(\alpha_\Sigma - \frac{1}{2}) - \frac{15}{4}\right)k^2 = -4k^2, \tag{5.2.5}$$

$$m_\lambda = c_\lambda k\ \mathrm{Sgn}(z - z_0) = \frac{k}{2}\ \mathrm{Sgn}(z - z_0) \tag{5.2.6}$$

Importantly, the tuning relation (2.3.16) between the scalar bulk and boundary masses is also required for the theory to be supersymmetric.

Given our discussion in Section 2.3D, we can see how supersymmetry is realized. With $c_\lambda = 1/2$ and λ^1 even (corresponding to Ψ_+), the λ^1 profiles will match that of the gauge field ($\alpha_A = 1$). Then λ^2 must be odd and $\alpha_{\lambda_2} = 0$. It will not have a zero-mode, but at the massive level it will couple to λ^1 to form a tower of Dirac KK-states. Similarly, the scalar field will have $\alpha_\Sigma = 0$ and odd boundary conditions lead to the same spectrum as the other fields, but the massless mode is projected out. Note that even though the values of α are different, the KK towers are identical. This is due to the relation (2.3.18), which relates the KK-spectra of fields differing in α by 1. Thus, from the 4D point of view, the orbifold boundary conditions have reproduced the massless vector multiplet of $\mathcal{N} = 1$ supersymmetry. At the massive level, there is a KK-tower of

$\mathcal{N}=2$ supermultiplets. with identical masses and couplings. In summary, we have:

$$\alpha = \begin{cases} 1, & \text{for even fields } \mathrm{V_M},\ \lambda^1 \ \Rightarrow \mathcal{N}=1 \text{ multiplet at massless level;} \\ 0, & \text{for odd fields } \Sigma,\ \lambda^2 \ \Rightarrow \text{ no massless modes.} \end{cases} \tag{5.2.7}$$

The story is very similar for the hypermultiplet,

$$\Phi = (H^i, \Psi). \tag{5.2.8}$$

where H^i for $i = 1, 2$ are complex scalars and Ψ is a Dirac fermion. The action is obtained in a straightforward way from (2.3.32) and (2.3.1), and the relevant supersymmetry transformations are again found in Refs. [131, 78]. The required relationship between the scalar masses and the fermion bulk mass is:

$$m_\Psi = ck\ \mathrm{Sgn}(z - z_0) \tag{5.2.9}$$

$$m_H^{1,2} = \left(c^2 \pm c - 15/4\right) k^2 + (3 \mp 2c)\, k e^{A(z)} \left[\delta(z - z_0) - \delta(z - z_1)\right] \tag{5.2.10}$$

Again, the relation is easily understood by the results of Section 2.3D and (2.3.18), as we can identify $\alpha = |c + 1/2|$ for H^1 and $\alpha = |c - 1/2|$ for H^2. With Ψ_+ and H^1 even, they will have zero-modes. Then Ψ_- and H^2 must be odd and their massless modes are projected out. The result is that we regain the $\mathcal{N}=1$ chiral multiplet at the massless level.

We have seen that at the massless level, boundary conditions break the amount of supersymmetry in the low-energy theory down to $\mathcal{N}=1$. The remaining $\mathcal{N}=1$ SUSY is assumed to remain unbroken on the UV brane and softly broken in the IR. By the AdS/CFT correspondence [38, 39, 40, 41, 42, 43], this setup has a dual interpretation in terms of a purely four-dimensional strongly coupled conformal field theory (CFT). In particular, fields that are UV-localized are dual to elementary states of the CFT, while those that are IR localized correspond to composite states.

5.3 Supersymmetry Breaking

At this point, it is natural to ask what we have gained beyond redundancy by considering supersymmetry–a solution to the hierarchy problem–in the context of the Randall-Sundrum solution to the hierarchy problem. The answer lies in the fact that in order for

supersymmetry to be realized, a new hierarchy must be introduced to explain the low scale of supersymmetry breaking. The non-supersymmetric Randall-Sundrum solution to the hierarchy problem requires the Higgs to live on the TeV brane, where the effective cutoff for corrections to the Higgs mass-squared is of order the TeV scale. With a bulk supersymmetry, there is no need to confine the Higgs to the IR, and instead it may live, for example, near the UV brane. Then supersymmetry may provide the solution to the hierarchy puzzle, while the warped model can provide a dual description of low-energy supersymmetry breaking by strong dynamics. Thus, we will consider the up- and down-type Higgs bosons to be UV-localized fields.

5.3A Elementary Higgses and (S)Fermion Mass

Our main interest in the Higgs sector is how it relates to the pattern of sfermion masses. For our purposes, then, we can assume the Higgs sector is completely confined to the UV brane. The reason for this is as follows. As described in Section 2.4A, the standard model fermions arise from the marriage of the massless modes of two bulk fields, $\Psi_L^{(0)i}$ and $\Psi_R^{(0)i}$, where Ψ_L (Ψ_R) is a doublet (singlet) under $SU(2)_L$ and i is a generation index. The boundary conditions are chosen such that $\Psi_L^{(0)i}$ is left-handed while $\Psi_R^{(0)i}$ is right-handed from the 4D point of view. The joining occurs through Yukawa couplings with the Higgs, forming light Dirac fermions in the 4D theory. These couplings are only allowed on either boundary due to the bulk $\mathcal{N} = 2$ SUSY. Assuming no large hierarchies in fundamental Yukawas, we can then relate fermion masses to their couplings at the boundary where the appropriate Higgs is localized. Thus, it is only the boundary value of the appropriate Higgs field that is important in determining any fermion's (and thus sfermion's) localization.

To make the discussion concrete, each member of a 5D $SU(2)_L$ doublet field shares a common localization parameter, c_L^i. For $c_L^i > 1/2$ ($c_L^i < 1/2$), the doublet is UV (IR) localized. Similarly, each right-handed $SU(2)_L$ singlet has localization parameter c_R^i. These fields are UV (IR) localized for $c_R^i < -1/2$ ($c_R^i > -1/2$).

The zero modes obtain masses through wavefunction overlap with the UV localized Higgs fields, with effective 4D Yukawa couplings, Y_Ψ, related to 5D bulk Yukawa

couplings, Y_Ψ^{5D}, by [22]:

$$Y_\Psi = Y_\Psi^{5D} k \sqrt{\frac{1/2 - c_L}{(kz_1)^{1-2c_L} - 1}} \sqrt{\frac{1/2 + c_R}{(kz_1)^{1+2c_R} - 1}}. \tag{5.3.1}$$

A large range of 4D Yukawa couplings is obtained by varying the parameters c_L and c_R of each field over a range of $\mathcal{O}(1)$. To see this, consider $c_L = -c_R = c$. Since $kz_1 \gg 1$, it is clear from (5.3.1) that UV localized fields ($c > 1/2$) obtain order 1 4D Yukawa couplings while IR localized fields ($c < 1/2$) obtain exponentially tiny couplings. As a result, the fermion localizations are expected to follow a distinctive pattern. In particular, the relatively light first-two generations should be somewhat IR localized, while the heavy third-generation fermions should be UV localized.

This is important for the following reason: if supersymmetry is broken at low energy, its effects should be felt predominantly by IR localized fields. Thus, the soft sfermion masses are expected to follow a roughly inverse pattern: the first two generation scalars are heavy while the third is light. To see this explicitly, let us consider two explicit mechanisms that have been proposed in the literature: supersymmetry breaking due to orbifold boundary conditions, and supersymmetry breaking due to a deformed AdS background.

5.3B Supersymmetry Breaking by Orbifold Boundary Conditions

We first consider an analog of the flat-space Scherk-Schwarz mechanism [18, 19] in which "twisted" orbifold boundary conditions are used to break supersymmetry, as in Refs. [78, 134]. The flat-space analog has been considered in numerous studies (see [135, 136, 137, 138, 139] and references therein). Recall from Chapter 2, that the orbifold symmetry can be interpreted as symmetry under two independent transformations, a $\mathbb{Z}_2$ about $y = 0$ and a $\mathbb{Z}_2'$ about $y = \pi R$. Fields that are even under both the $\mathbb{Z}_2$ and $\mathbb{Z}_2'$ (satisfying Neumann boundary conditions at both the UV and IR boundaries) admit massless modes, while fields obeying Dirichlet conditions do not.

To model supersymmetry breaking at the TeV scale, we can impose different boundary conditions on fields within the same multiplet. For example, consider a multiplet for which one field obeys even boundary conditions and therefore has a massless mode, while its superpartner is even under $\mathbb{Z}_2$ but odd under $\mathbb{Z}_2'$ (and thus satisfies a Neumann

condition at the UV boundary but a Dirichlet condition at the IR brane). Then it is not difficult to show that the mass spectrum is found by solving [78]:

$$\frac{J_{\alpha-1}(\frac{m_n}{k})}{Y_{\alpha-1}(\frac{m_n}{k})} = \frac{J_\alpha(e^{\pi kR}\frac{m_n}{k})}{Y_\alpha(e^{\pi kR}\frac{m_n}{k})}. \tag{5.3.2}$$

For $\alpha \notin \mathbb{Z}$, the Neumann functions satisfy:

$$Y_\alpha(x) = \frac{1}{\sin(\alpha\pi)}\left[\cos(\alpha\pi)J_\alpha(x) - J_{-\alpha}(x)\right]. \tag{5.3.3}$$

The connection to Y_α for $\alpha \in \mathbb{Z}$ involves a non-trivial limit, but we will be able to recover the $\alpha = 1$ case in the end. Inserting (5.3.3) into (5.3.2) allows us to eliminate the Neumann functions:

$$J_{-\alpha}(wx)J_{\alpha-1}(x) + J_\alpha(wx)J_{1-\alpha}(x) = 0. \tag{5.3.4}$$

where $x = m_n/k$ and $w = e^{\pi kR}$. To find the lowest lying mode, we assume $m_0/k \ll 1$ and substitute the standard expansion for the Bessel function,

$$J_\alpha(x) = \left(\frac{x}{2}\right)^\alpha \sum_{k=0}^{\infty} \frac{(-1)^k}{k!\Gamma\left(\alpha+k+1\right)}\left(\frac{x}{2}\right)^{2k}. \tag{5.3.5}$$

Expanding to 2nd order in x and solving gives:

$$\frac{m_0}{k} = \frac{2\sqrt{\alpha^2-\alpha}}{\sqrt{e^{2\alpha\pi kR} - e^{2\mathrm{kR}\pi}\alpha + \alpha - 1}} \tag{5.3.6}$$

The limit $\alpha \to 1$ reproduces the result for gauginos found in [78]. The general behavior is as expected from geographical arguments. As $\alpha > 1$ ($\alpha < 1$) corresponds to a UV (IR) localized field, we expect the twisted boundary condition to have a larger effect for small α, because IR-localized fields will be most affected by the different boundary conditions on the IR brane. This is indeed the case, as can be seen in Figure 5.1. Since the light fermions are IR localized when the Higgs lives on the UV brane, their scalar superpartners are heavy, and vice versa.

5.3C Supersymmetry Breaking by Deformed AdS

Another possibilty is that supersymmetry is broken due to the spacetime departing from pure AdS in the IR region. This is similar to the soft-wall setups we discussed

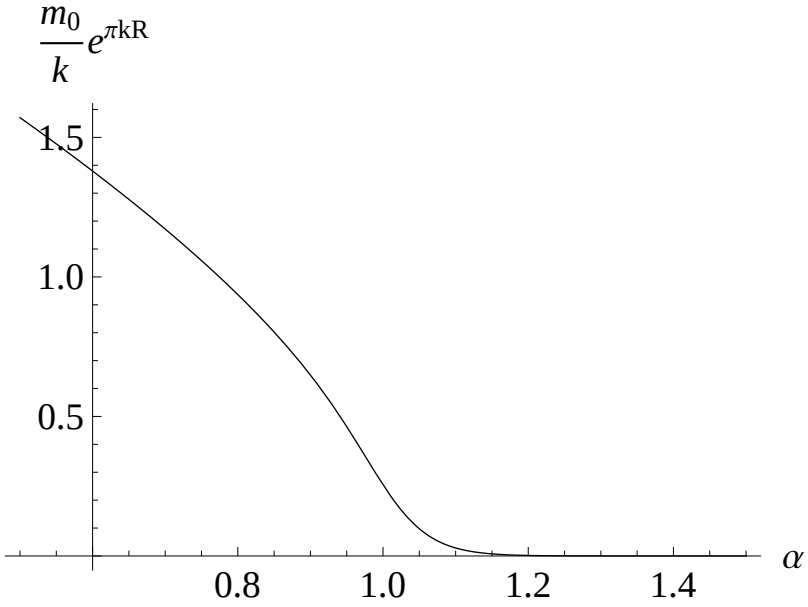

Figure 5.1: Tree level SUSY-breaking mass masses vs. α for $kR = 10$ when SUSY is broken by orbifold boundary conditions.

in Chapter 3. As we saw, the treatment of fermions was particularly involved when the IR brane is removed completely. Therefore, we will consider the concrete model of Ref. [22], which constructed a gravity dual to single-sector SUSY breaking [140] in five dimensions. The background is given by the metric:

$$e^{-2\widetilde{A}(z)} = \frac{1}{(kz)^2}\left[1 - \epsilon\left(\frac{z}{z_1}\right)^4\right]. \tag{5.3.7}$$

The small parameter $\epsilon = 0.05$ arises from an underlying 10D supergravity solution and characterizes the size of the AdS deformation in the IR. For our purposes, its value is taken to be freely chosen (but see Appendix D of [22]). Note that this background can also be modeled using the dynamical setup of Chapter 3, with a perturbed metric given by

$$\widetilde{A} = \log kz + \frac{\epsilon}{2}\left(\frac{z}{z_1}\right)^4, \tag{5.3.8}$$

as the two backgrounds are equivalent to first-order in the small parameter ϵ. The primary difference between this model and the soft-wall models is that there remains an IR brane located at $z = z_1$, so that in essence conformal symmetry breaking in the

IR is due to a hybrid mechanism. With the hard IR brane in place, fermions present no added difficulty. Their massless modes are protected by chiral symmetry while the deformation endows the scalar zero modes with masses.

The model parameters are chosen such that the curvature scale $k \sim M/10$, where M is the five-dimensional Planck scale, implying $k \simeq 10^{-3/2} M_P = 7.7 \times 10^{16}$ GeV. Additionally,

$$\pi kR = 28.42, \qquad z_1 = (ke^{-\pi kR})^{-1} = (35 \text{ TeV})^{-1}.$$

The ratio of the Higgs VEVs is taken to be $\tan\beta = 10$.

Scalar Superpartners & Soft Masses

As we saw in Section 5.2, the localization parameter, $c_{L/R}$, of each fermion is related to that of the scalar partner, $\alpha_{L/R}$, by supersymmetry as:

$$\alpha_{L/R} = |c_{L/R} \pm 1/2|.$$

The localization parameter determines the soft mass of the scalar. In the small ϵ limit [22],

$$\widetilde{m}^2 = \epsilon \frac{(\alpha-1)(12-\alpha)}{(kz_1)^4} \frac{(kz_1)^{3-\alpha} - (kz_1)^{\alpha-1}}{(kz_1)^{\alpha-1} - (kz_1)^{1-\alpha}} k^2 + \mathcal{O}(\epsilon^2). \tag{5.3.9}$$

For the choices of the parameters (5.3.9), scalar masses can be vanishingly small for $\alpha \ll 1$ or $\mathcal{O}(z_1^{-1} = 35 \text{ TeV})$ for $\alpha > 1$. The size of soft masses is thus tied to the localization of the superfield. Because the Higgs is located on the UV brane, the light fermion superpartners will be IR localized and receive large SUSY-breaking masses.

5.3D Generic Spectrum and Features of the Low-Energy Theory

The above examples demonstrate that the basic setup we outlined generically generates a spectrum with heavy, composite first-two generation scalars and light, elementary third generation scalars. Thus, these models are generically dual to single-sector models [140, 141]. The pattern of soft masses has nothing to do with the particular mechanism of supersymmetry breaking (i.e. boundary conditions vs. the deformation of AdS), and only with whether the Higgs is elementary or composite.

Assuming the Kaluza-Klein (KK) scale is high enough that we can neglect effects from KK-mediated processes,[2] we can focus on a low-energy theory with supersymmetric field content and hierarchical sfermion soft masses. However, it is not necessarily the MSSM field content. The reason is that the bulk theory has a continuous $U(1)$ R-symmetry. Assuming this symmetry remains unbroken or approximately unbroken below the IR scale, it will be protected from a number of deleterious effects [30]. For example, Majorana gaugino masses are forbidden, which eliminates many diagrams that give large contributions to flavor violation. In a warped framework, Dirac masses are readily generated by pairing up the massless modes with KK-modes, as occurs for example when SUSY is broken by boundary conditions.[3] These can be heavy or light depending on the nature and scale of the SUSY breaking.

There are a few additional considerations that we incorporate as constraints from the start. Naturalness demands that the scalars should should not be too heavy to avoid unnatural EWSB. This primarily constrains the scale of the stop due to the larger Yukawa couplings, but also implies the other scalars should not be too heavy [29]. Additionally, we assume left-right degeneracy among the first-two generations to avoid large hypercharge Fayet-Iliopoulos (FI) terms [28]. Finally, any explicit model must be checked to ensure that the stop square-mass is not driven negative [142, 143]. We will limit our attention to $\tan\beta$ not too large, in which case we need not worry about the influence of an extended Higgs sector.

In summary, we have a supersymmetric Randall-Sundrum setup with an elementary Higgs sector and bulk gauge and matter supermultiplets. The scale of soft-susy masses is assumed to be consistent with natural EWSB. The important modifications to the MSSM are:

1. heavy first two-generation scalars of up to 5 TeV (we neglect their mass difference),

2. light third generation scalars of under 1 TeV,

3. Dirac gauginos with masses of order 1 TeV.

[2] In Ref. [22], the scale was taken to be of order 100 TeV.

[3] This description might invite objection on the grounds that towers with different boundary conditions are not in the same Hilbert space. Nevertheless, we have Dirac gauginos.

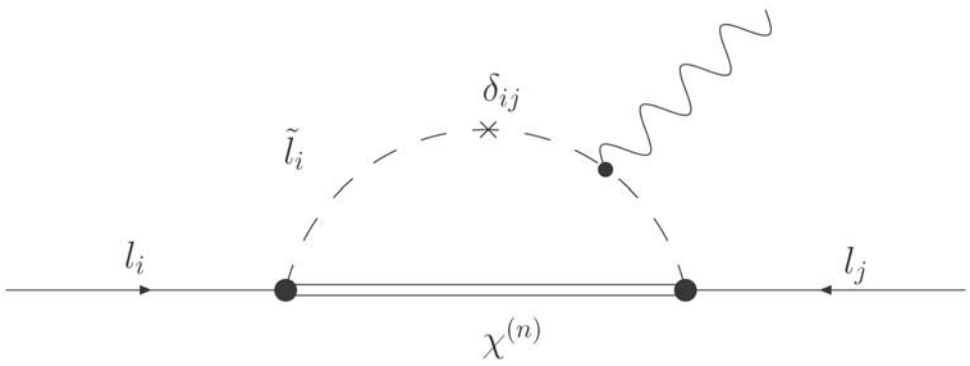

Figure 5.2: Generic Feynman graph leading to lepton decay. With Dirac gauginos, the chirality flip (indicated by arrow direction) can take place on external lines or at the lepton-slepton-higgsino vertex. There are also loops involving sneutrino-chargino exchange (c.f. [145]).

We will also assume $\tan\beta \gtrsim 1$ but not too large to avoid large additional flavor violation [144].

5.4 Lepton Flavor Violation

With Dirac gauginos and light sleptons, flavor constraints are weakened considerably. The gauginos may naturally be significantly heavier than the scalars and dangerous dimension five operators are forbidden. In particular, relatively large mixing in the slepton matrices may be allowed for gaugino masses of order a few TeV with relatively light sleptons [30], however there are important constraints from $\mu \to e$ conversion processes that can dominate when the sfermions are light [126]. In models with heavy first-two generations *and* an extended R-symmetry, the bounds on single insertions are suppressed by the heavy slepton masses. However, the suppression is not as large as one might naively expect unless the gauginos are also made very heavy because the loop functions depend on the ratio of gaugino to slepton masses. Additionally, significant contributions can remain due to second order mixing involving the light third generation sleptons.

With heavy first-two generation sleptons, the most important constraint comes from

the rare decay $\mu \to e\gamma$. The Feynman graphs contributing to $\mu \to e\gamma$ are like those depicted in Fig. 5.2. The loops can involve chargino and sneutrino exchange or neutralino and charged slepton exchange. The branching ratio for the process is given by:

$$\frac{\Gamma(\mu \to e\gamma)}{\Gamma(\mu \to e\bar{\nu}_e\nu_\mu)} = \frac{48\alpha\pi^3}{G_F^2}\left(|A_L^{(n1)} + A_L^{(n2)} + A_L^{(c1)} + A_L^{(c2)}|^2 + |A_R^{(n1)} + A_R^{(n2)}|^2\right) \quad (5.4.1)$$

The notation is chosen to match that of Refs. [145, 30]. The superscripts c (n) indicate chargino (neutralino) exchange. The numbers 1 and 2 indicate the chirality flip occurs on the external and internal lines, respectively. Finally, the L and R indicate whether the insertion of the left- or right-handed type. The internal chirality flip arises only due to Higgsino-gaugino mixing, as we have assumed no left-right mixing terms are generated. Additionally, terms smaller by a factor of the ratio m_e/m_μ have been dropped.

Following Ref. [145], we assume the first-two generation heavy sleptons have approximately degenerate physical masses. Notational clutter is greatly simplified by noting that in the setup we have described, left-handed charged sleptons and sneutrinos should have roughly equal physical masses, although the structure of their mass squared matrices is not necessarily the same. Additionally, for the first two generations, this will also give approximately the physical mass for the right-handed charged slepton due to our assumption of left-right degeneracy for the heavy scalars. We denote this single heavy scale $\widetilde{m}_L$. The mass of the left-handed (right-handed) third generation scalars are $\widetilde{m}_{\tau_L}$ ($\widetilde{m}_{\tau_R}$). The entries of the soft mass-squared matrices in the basis of gauge interactions are labelled by capital letters: $(\widetilde{M}_L^2)_{ij}$ and $(\widetilde{M}_E^2)_{ij}$.

We also define the differences $\Delta\widetilde{m}_L^2 = \widetilde{m}_L^2 - \widetilde{m}_{\tau_L}^2$ and $\Delta\widetilde{m}_R^2 = \widetilde{m}_L^2 - \widetilde{m}_{\tau_R}^2$. Finally, the insertion parameters that enter the amplitude expressions we write as:

$$(\delta_{L/R})_{12} = \frac{(\widetilde{M}_{L/E}^2)_{12}}{\widetilde{m}_L^2}, \qquad (\delta_{L/R})_{i3} = \frac{(\widetilde{M}_{L/E}^2)_{i3}}{\Delta\widetilde{m}_{L/R}^2} \quad (5.4.2)$$

for $i = 1, 2$ in the second expression. Note that these expressions differ somewhat from common definitions in terms of "average slepton mass." Our definitions are related to the terms that directly enter the amplitudes[4] as calculated using the "multi-mass insertion" technique [145], which is easily related to an expansion of loop integrals over rotated mass matrices (as in Ref. [146]). Also, since the 3×3 squark mass-squared

[4] We have approximated $(\Delta\widetilde{m}_L^2)^2 \simeq \Delta\widetilde{m}_L^2\widetilde{m}_L^2$ and similary for $(\Delta\widetilde{m}_R^2)^2$.

matrices can each be diagonalized by unitary transformations, these expressions satisfy $\delta_{ij} \leq 1/2$ when two of the squarks are degenerate.

To first order in the ratios $M_W/M_{\widetilde{B}}$ and $M_W/M_{\widetilde{W}}$ that determine the neutralino and chargino mixing, the amplitudes are given by[5]

$$A_L^{(c1)} = \frac{\alpha_2}{24\pi}\left\{\frac{(\delta_L)_{12}+(\delta_L)_{13}(\delta_L)_{23}}{\widetilde{m}_L^2} g^{(c1)}\left(x_{cL}\right) - \frac{(\delta_L)_{13}(\delta_L)_{23}}{\widetilde{m}_{\tau_L}^2} f^{(c1)}\left(x_{c\tau_L}\right)\right\}, \tag{5.4.3}$$

$$A_L^{(c2)} = -\frac{\alpha_2}{4\pi}\left\{\frac{(\delta_L)_{12}+(\delta_L)_{13}(\delta_L)_{23}}{\widetilde{m}_L^2} g^{(c2)}\left(x_{cL}\right) - \frac{(\delta_L)_{13}(\delta_L)_{23}}{\widetilde{m}_{\tau_L}^2} f^{(c2)}\left(x_{c\tau_L}\right)\right\}, \tag{5.4.4}$$

$$A_L^{(n1)} = -\frac{\alpha_2}{48\pi}\left(1+t_W^2\right)\left\{\frac{(\delta_L)_{12}+(\delta_L)_{13}(\delta_L)_{23}}{\widetilde{m}_L^2} g^{(n1)}\left(x_{nL}\right) - \frac{(\delta_L)_{13}(\delta_L)_{23}}{\widetilde{m}_{\tau_L}^2} f^{(c1)}\left(x_{n\tau_L}\right)\right\}, \tag{5.4.5}$$

$$A_L^{(n2)} = \frac{\alpha_2}{16\pi}\left(1-t_W^2\right)\left\{\frac{(\delta_L)_{12}+(\delta_L)_{13}(\delta_L)_{23}}{\widetilde{m}_L^2} g^{(n2)}\left(x_{nL}\right) - \frac{(\delta_L)_{13}(\delta_L)_{23}}{\widetilde{m}_{\tau_L}^2} f^{(c2)}\left(x_{n\tau_L}\right)\right\}, \tag{5.4.6}$$

$$A_R^{(n1)} = -\frac{\alpha_1}{12\pi}\left\{\frac{(\delta_R)_{12}+(\delta_R)_{13}(\delta_R)_{23}}{\widetilde{m}_L^2} g^{(n1)}\left(x_{nL}\right) - \frac{(\delta_R)_{13}(\delta_R)_{23}}{\widetilde{m}_{\tau_R}^2} f^{(n1)}\left(x_{n\tau_R}\right)\right\}, \tag{5.4.7}$$

$$A_R^{(n2)} = \frac{\alpha_1}{8\pi}\left\{\frac{(\delta_R)_{12}+(\delta_R)_{13}(\delta_R)_{23}}{\widetilde{m}_L^2} g^{(n2)}\left(x_{nL}\right) - \frac{(\delta_R)_{13}(\delta_R)_{23}}{\widetilde{m}_{\tau_R}^2} f^{(n2)}\left(x_{n\tau_R}\right)\right\}, \tag{5.4.8}$$

[5] As all relevant diagrams are proportional to m_μ, the factors appearing in Ref. [145] have been absorbed into the decay rate.

where $t_W = \tan(\theta_W)$ and $x_{ab} = \widetilde{m}_a^2/\widetilde{m}_b^2$ with $\widetilde{m}_c$ and $\widetilde{m}_n$ the mass of the appropriate chargino or neutralino, respectively. The loop functions are given by

$$f_{c1}(x) = \frac{1}{2(1-x)^4}\left(2+3x-6x^2+x^3+6x\log x\right), \tag{5.4.9}$$

$$f_{c2}(x) = -\frac{1}{2(1-x)^3}\left(3-4x+x^2+2\log x\right), \tag{5.4.10}$$

$$f_{n1}(x) = \frac{1}{2(1-x)^4}\left(1-6x+3x^2+2x^3-6x^2\log x\right), \tag{5.4.11}$$

$$f_{c1}(x) = \frac{1}{(1-x)^3}\left(1-x^2+2x\log x\right), \tag{5.4.12}$$

$$g_{ai}(x) = f_{ai}(x) + x f'_{ai}(x). \tag{5.4.13}$$

We have provided contour plots satisfying the present bound $BR(\mu \to e\gamma) = 1.2 \times 10^{-11}$ [147] in Figures 5.3 and 5.4. In Figure 5.3, we have assumed all δ_{ij} entries are of the same size, while in Figure 5.4, we have only included the δ_{12} contribution. There is an apparent large cancellation over much of the parameter space due to a competition between various loop contributions to the amplitudes. In any case, large flavor violating δ_{ij} entries are allowed for gaugino masses in the 1-2 TeV range, and order 0.1-0.2 for the 0.5-1 TeV range.

5.5 Alignment Scenario

Next we consider the alignment scenario discussed in Ref. [124], in which the charged slepton mass eigenstates are aligned with the charged lepton mass eigenstates, and similarly for the sneutrinos and neutrinos. This scenario greatly alleviates neutral current contributions to flavor violation in both the lepton [124] and quark [125] sectors. Note that our assumption is different from a trivial alignment scenario where the sneutrinos, charged sleptons and leptons are all aligned simultaneously.

In this case, all neutralino-mediated contributions to flavor violation vanish. The reason is that the effective mixing matrix for the neutralino couplings is:

$$\widetilde{K}_{e_M\widetilde{e}_M} = U^\dagger_{e_M}\widetilde{U}_{e_M}, \tag{5.5.1}$$

where $M = L, R$ (again, we are neglecting left-right slepton mixing). Since the leptons and charged sleptons are aligned, $U_{e_M} = \widetilde{U}_{e_M}$ and the product is just the unit matrix.

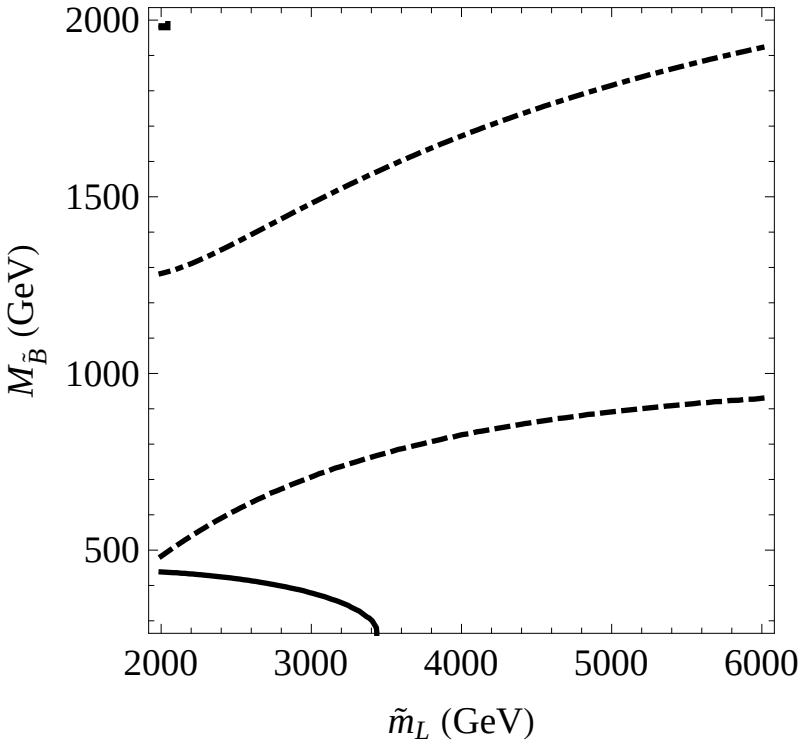

Figure 5.3: Contours for $M_{\widetilde{B}}$ satisfying BR$(\mu \to e\gamma) = 1.2 \times 10^{-11}$ assuming $\delta_{12} = \delta_{13} = \delta_{23} = 0.1$ (solid), 0.25 (dashed), and 0.5 (dot-dashed), $\widetilde{m}_{\tau_L} = \widetilde{m}_{\tau_R} = 500$ GeV, and $M_{\widetilde{W}} = 2M_{\widetilde{B}}$. The area below each curve indicates the excluded region.

In contrast, the chargino mixing matrix is given by:

$$\widetilde{K}_{e_L\widetilde{\nu}_L} = U^{\dagger}_{e_L}\widetilde{U}_{\nu_L} = U_{PMNS} \tag{5.5.2}$$

where the last equality follows from our assumption of neutrino and sneutrino alignment and the measurements of neutrino mixing angles in the Pontecorvo-Maki-Nakagawa-Sakata matrix U_{PMNS}. We take the values for the mixing angles from Ref. [148] and ignore any CP violating or Majorana phases for simplicity. We have listed the angles in Table 5.1. Then the PMNS matrix is:

$$U_{PMNS} = \begin{pmatrix} 0.822 & 0.564 & 0.084 \\ -0.449 & 0.550 & 0.705 \\ 0.351 & -0.617 & 0.705 \end{pmatrix}.$$

Working in a basis in which the lepton masses and chargino vertices are diagonal, the

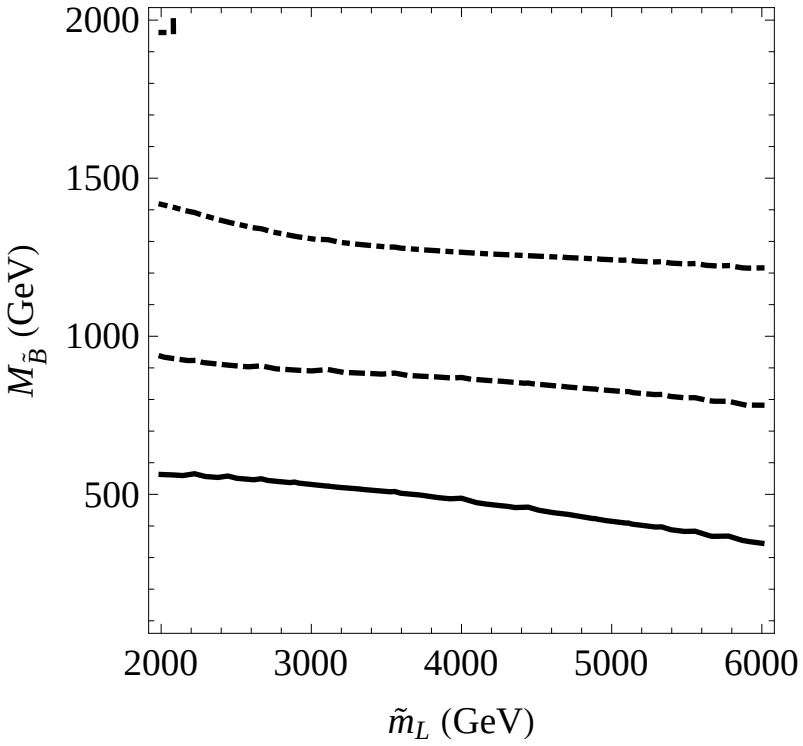

Figure 5.4: Contours for $M_{\widetilde{B}}$ satisfying $\mathrm{BR}(\mu \to e\gamma) = 1.2 \times 10^{-11}$ assuming $\delta_{13} = \delta_{23} = 0$, $\delta_{12} = 0.1$ (solid), 0.25 (dashed), and 0.5 (dot-dashed), $\widetilde{m}_{\tau_L} = \widetilde{m}_{\tau_R} = 500$ GeV, and $M_{\widetilde{W}} = 2M_{\widetilde{B}}$. The area below each curve indicates the excluded region.

flavor violation is moved to the sneutrino mass matrices:

$$\left(\widetilde{M}^2_{\nu_L}\right)_{ij} = \left(U M^{(d)2}_{\nu_L} U^\dagger\right)_{ij}. \tag{5.5.3}$$

where we have dropped the "PMNS" label from U. In the scenario we have outlined with heavy first-two generation charged and neutral sleptons, the 23 mixing is nearly maximal due to the fact that $\theta_{23} \simeq 45^\circ$. For example, given a stau neutrino mass of $\widetilde{m}_{\nu_\tau} = 500$ GeV and selectron and smuon masses of $\widetilde{m} = 5$ TeV, we find:

$$\left(\widetilde{M}^2_{\nu_L}\right) = \widetilde{m}^2 \begin{pmatrix} 0.993 & -0.058 & -0.058 \\ -0.058 & 0.508 & 0.492 \\ -0.058 & 0.492 & 0.508 \end{pmatrix}.$$

The equality of the 13 and 12 entries is due to our assumption of degeneracy between the first two generations. If exact degeneracy is maintained and the mixing angle θ_{13}

Parameter	Best Fit
$\sin^2\theta_{12}$	0.32
$\sin^2\theta_{23}$	0.50
$\sin^2\theta_{13}$	0.007
Δm^2_{12} (10^{-5} eV^2)	7.6
Δm^2_{23} (10^{-3} eV^2)	2.4

Table 5.1: Best-fit values for the neutrino mixing angles as they appear in Ref. [148].

turns out to in fact vanish, then both the 12 and 13 entries would vanish. Then $\mu \to e\gamma$ vanishes and $\tau \to \mu\gamma$ provides the most stringent constraints. In any other case, however, the contributions of both δ_{12} and the product $\delta_{13}\delta_{23}$ can be important.

In Figure 5.5 are contour plots for the branching fraction over a range of heavy sneutrino and gaugino masses when the third generation is 500 GeV. Remarkably the contribution to $\mu \to e\gamma$ is only sensitive to the relative splitting between the heavy sneutrino masses and the chargino mass. Additionally, the rate is within the reach of a experimental searches given reasonable slepton and gaugino masses.

5.6 Discussion

5.6A Comparison with MSSM-like models

We can readily compare these results with those of typical models. With slepton and gaugino masses of order a few hundred GeV, Majorana gauginos, and explicit μ terms, the constraints on LFV for a generic model are very stringent. We have listed the constraints as found in Ref. [33] in Table 5.2. Two of the RR entries lack solid constraints due to cancellations that occur in various regions of the space of MSSM parameters. The orders of magnitude for these bounds are generically expected to be of the same order as the corresponding LL constraint. Furthermore, we are neglecting any LR mixing.

The improvement over such models is apparent. Taking into account only the increased slepton masses (i.e., ignoring the monotonic increase in the loop functions with decreasing $m^2_{\widetilde{c}/\widetilde{n}}/\widetilde{m}^2_L$), one can hope to relax the δ_{12} constraints by up to 2 orders of

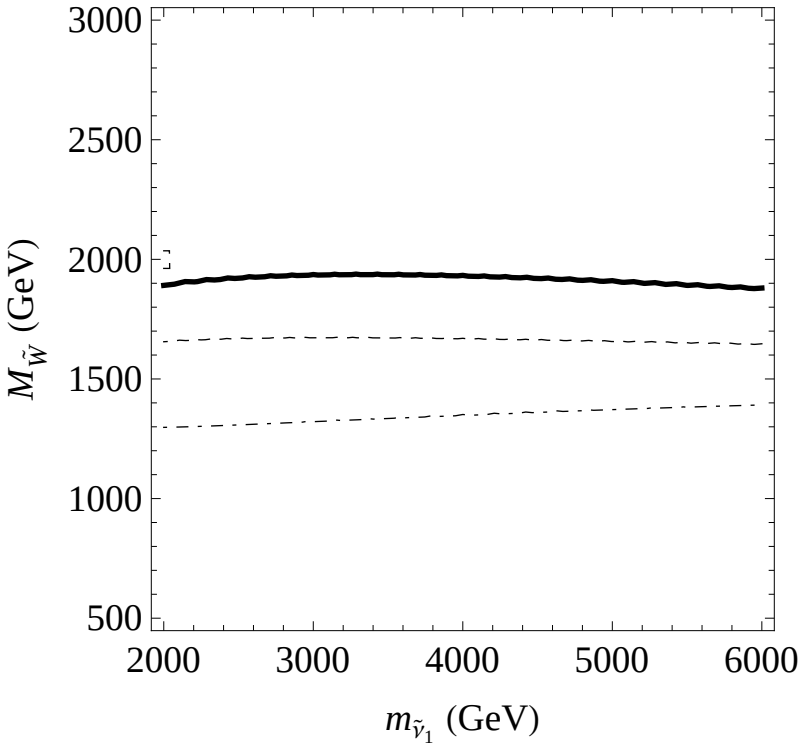

Figure 5.5: Contours satisfying BR($\mu \to e\gamma$) $= 1.2 \times 10^{-11}$ assuming only chargino contributions due to an alignment mechanism and neutrino-like mixing (see text) for $\widetilde{m}_{\nu_2} = 0.9\widetilde{m}_{\nu_1}$ (solid line), $\widetilde{m}_{\nu_2} = \widetilde{m}_{\nu_1}$ (dashed), and $\widetilde{m}_{\nu_2} = 1.1\widetilde{m}_{\nu_1}$ (dot-dashed). The third generation sneutrino is assumed to be 500 GeV.

magnitude to 0.06.[6] The product $\delta_{13}\delta_{23}$ obeys a similar bound. Moreover, the rate for $\mu \to e\gamma$ can be very sensitive to $\tan\beta$ when there are Majorana gauginos and explicit μ terms.

In contrast, the scenario we considered allowed for significantly larger values for δ_{12} with or without large cancellations in the amplitudes. For example, in Figure 5.4 we see that heavy sleptons and gauginos of about 500 GeV are consistent with current measurements of $\mu \to e\gamma$ when the δ_{12} entry is as big as 0.1. With gaugino masses of order $1 - 1.5$ TeV, arbitrarily large δ_{ij} entries are allowed.

[6] The rates are proportional to δ_{12}^2 and inversely proportional to the average slepton mass to the fourth power.

Table 5.2: Bounds on the $(\delta_{AB})_{ij}$ as they appear in Ref. [33].

ij	LL	RR
12	6×10^{-4}	0.09
13	0.15	$\approx 10^{-1}$
23	0.12	$\approx 10^{-1}$

5.6B The (s)quark sector

It would be interesting to complete a similar analysis of flavor violation in the quark sector, namely of the rates for $\Delta F = 2$ processes involving the kaon and D_0 systems. The analysis of Ref. [30] found that explaining the kaon mass difference required gluinos of at least 5 TeV provided there is large mixing in both the left- and right-handed squark mass-squared matrices. A complimentary analysis in the presence of hierarchical soft terms could be completed in the spirt of Ref. [31].

For models with an alignment mechanism as discussed in Section 5.5 above, or at least an approximate alignment mechanism, gluino-mediated flavor violation is significantly suppressed [125], as there is only the much weaker coupling to the charginos, and the quark mixing matrices are small. In such a case, the lepton sector is expected to provide the most severe constraints. Therefore, it would be interesting to explore concrete models like those we have described that feature alignment mechanisms through, e.g., horizontal symmetries.

5.6C Conclusions

We discussed lepton flavor violation in models with hierarchical soft terms and Dirac gauginos. The rates for $\mu \to e\gamma$ are within the bounds provided by experiment with large off-diagonal entries in the slepton mass-squared matrices provided the gauginos are sufficiently heavy ($M_{\widetilde{B}}$ between $500 - 1500$ GeV).

We motivated this discussion by describing how this spectrum can arise in models of SUSY breaking from a warped extra dimension with an elementary Higgs sector, similar to the model of Ref. [22]. We argued that the geographical relation between fermion masses and wavefunction localizations leads to an inverted hierarchy for the sfermion

masses, with the first-two generations being generically heavy and the third generically light, while the bulk R-symmetry indicates that the neutralinos should acquire Dirac masses.

We also considered flavor violation mediated strictly by charginos, as occurs when the slepton masses are aligned with the lepton superpartner masses. When the off-diagonal elements are due to the large neutrino mixing angles, rates for $\mu \to e\gamma$ may remain within reach of future experiments.

In all the cases we considered, the rates for $\mu \to e\gamma$ are such that that they should be detected in future experiments unless there are unnaturally small off-diagonal elements in the slepton mass matrices or the gauginos are very heavy. Assuming neither is true, an experimental signature of this sort of model would be the discovery of a light stau and measurement of $\mu \to e\gamma$ at a rate near the present bound, together of course with sufficiently high lower limits on the masses of the first-two generation sleptons.

References

[1] G. Altarelli and M. W. Grunewald, "Precision electroweak tests of the standard model," *Phys. Rept.* **403-404** (2004) 189–201, arXiv:hep-ph/0404165.

[2] D. J. H. Chung *et al.*, "The soft supersymmetry-breaking Lagrangian: Theory and applications," *Phys. Rept.* **407** (2005) 1–203, hep-ph/0312378.

[3] R. Barbieri, S. Ferrara, and C. A. Savoy, "Gauge Models with Spontaneously Broken Local Supersymmetry," *Phys. Lett.* **B119** (1982) 343.

[4] A. H. Chamseddine, R. L. Arnowitt, and P. Nath, "Locally Supersymmetric Grand Unification," *Phys. Rev. Lett.* **49** (1982) 970.

[5] L. J. Hall, J. D. Lykken, and S. Weinberg, "Supergravity as the Messenger of Supersymmetry Breaking," *Phys. Rev.* **D27** (1983) 2359–2378.

[6] J. R. Ellis, D. V. Nanopoulos, and K. Tamvakis, "Grand Unification in Simple Supergravity," *Phys. Lett.* **B121** (1983) 123.

[7] M. Dine, W. Fischler, and M. Srednicki, "Supersymmetric Technicolor," *Nucl. Phys.* **B189** (1981) 575–593.

[8] S. Dimopoulos and S. Raby, "Supercolor," *Nucl. Phys.* **B192** (1981) 353.

[9] C. R. Nappi and B. A. Ovrut, "Supersymmetric Extension of the SU(3) x SU(2) x U(1) Model," *Phys. Lett.* **B113** (1982) 175.

[10] M. Dine and A. E. Nelson, "Dynamical supersymmetry breaking at low-energies," *Phys. Rev.* **D48** (1993) 1277–1287, arXiv:hep-ph/9303230.

[11] M. Dine, A. E. Nelson, and Y. Shirman, "Low-energy dynamical supersymmetry breaking simplified," *Phys. Rev.* **D51** (1995) 1362–1370, arXiv:hep-ph/9408384.

[12] M. Dine, A. E. Nelson, Y. Nir, and Y. Shirman, "New tools for low-energy dynamical supersymmetry breaking," *Phys. Rev.* **D53** (1996) 2658–2669, arXiv:hep-ph/9507378.

[13] P. Meade, N. Seiberg, and D. Shih, "General Gauge Mediation," *Prog. Theor. Phys. Suppl.* **177** (2009) 143–158, arXiv:0801.3278 [hep-ph].

[14] E. A. Mirabelli and M. E. Peskin, "Transmission of supersymmetry breaking from a 4- dimensional boundary," *Phys. Rev.* **D58** (1998) 065002, arXiv:hep-th/9712214.

[15] D. E. Kaplan, G. D. Kribs, and M. Schmaltz, "Supersymmetry breaking through transparent extra dimensions," *Phys. Rev.* **D62** (2000) 035010, arXiv:hep-ph/9911293.

[16] L. Randall and R. Sundrum, "Out of this world supersymmetry breaking," *Nucl. Phys.* **B557** (1999) 79–118, arXiv:hep-th/9810155.

[17] C. Csaki, J. Erlich, C. Grojean, and G. D. Kribs, "4D constructions of supersymmetric extra dimensions and gaugino mediation," *Phys. Rev.* **D65** (2002) 015003, arXiv:hep-ph/0106044.

[18] J. Scherk and J. H. Schwarz, "Spontaneous Breaking of Supersymmetry Through Dimensional Reduction," *Phys. Lett.* **B82** (1979) 60.

[19] J. Scherk and J. H. Schwarz, "How to Get Masses from Extra Dimensions," *Nucl. Phys.* **B153** (1979) 61–88.

[20] T. Gherghetta and A. Pomarol, "A warped supersymmetric standard model," *Nucl. Phys.* **B602** (2001) 3–22, arXiv:hep-ph/0012378.

[21] C. P. Burgess *et al.*, "Warped supersymmetry breaking," *JHEP* **04** (2008) 053, arXiv:hep-th/0610255.

[22] M. Gabella, T. Gherghetta, and J. Giedt, "A gravity dual and LHC study of single-sector supersymmetry breaking," *Phys. Rev.* **D76** (2007) 055001, arXiv:0704.3571 [hep-ph].

[23] R. Barbieri and R. Gatto, "Conservation Laws for Neutral Currents in Spontaneously Broken Supersymmetric Theories," *Phys. Lett.* **B110** (1982) 211.

[24] S. Dimopoulos and H. Georgi, "Softly Broken Supersymmetry and SU(5)," *Nucl. Phys.* **B193** (1981) 150.

[25] J. R. Ellis and D. V. Nanopoulos, "Flavor Changing Neutral Interactions in Broken Supersymmetric Theories," *Phys. Lett.* **B110** (1982) 44.

[26] F. Gabbiani, E. Gabrielli, A. Masiero, and L. Silvestrini, "A complete analysis of FCNC and CP constraints in general SUSY extensions of the standard model," *Nucl. Phys.* **B477** (1996) 321–352, hep-ph/9604387.

[27] G. F. Giudice and R. Rattazzi, "Theories with gauge-mediated supersymmetry breaking," *Phys. Rept.* **322** (1999) 419–499, hep-ph/9801271.

[28] A. G. Cohen, D. B. Kaplan, and A. E. Nelson, "The more minimal supersymmetric standard model," *Phys. Lett.* **B388** (1996) 588–598, hep-ph/9607394.

[29] S. Dimopoulos and G. F. Giudice, "Naturalness constraints in supersymmetric theories with nonuniversal soft terms," *Phys. Lett.* **B357** (1995) 573–578, hep-ph/9507282.

[30] G. D. Kribs, E. Poppitz, and N. Weiner, "Flavor in supersymmetry with an extended R-symmetry," *Phys. Rev.* **D78** (2008) 055010, arXiv:0712.2039 [hep-ph].

[31] G. F. Giudice, M. Nardecchia, and A. Romanino, "Hierarchical Soft Terms and Flavor Physics," *Nucl. Phys.* **B813** (2009) 156–173, arXiv:0812.3610 [hep-ph].

[32] M. Dine, R. G. Leigh, and A. Kagan, "Flavor symmetries and the problem of squark degeneracy," *Phys. Rev.* **D48** (1993) 4269–4274, arXiv:hep-ph/9304299.

[33] M. Ciuchini *et al.*, "Soft SUSY breaking grand unification: Leptons vs quarks on the flavor playground," *Nucl. Phys.* **B783** (2007) 112–142, hep-ph/0702144.

[34] D. Sword, "Lepton Flavor Violation with Heavy Sleptons and Dirac Gauginos," *Submitted to Phys. Lett. B* (2010) .

[35] N. Arkani-Hamed, S. Dimopoulos, and G. R. Dvali, "The hierarchy problem and new dimensions at a millimeter," *Phys. Lett.* **B429** (1998) 263–272, arXiv:hep-ph/9803315.

[36] L. Randall and R. Sundrum, "A large mass hierarchy from a small extra dimension," *Phys. Rev. Lett.* **83** (1999) 3370–3373, hep-ph/9905221.

[37] L. Randall and R. Sundrum, "An alternative to compactification," *Phys. Rev. Lett.* **83** (1999) 4690–4693, arXiv:hep-th/9906064.

[38] J. M. Maldacena, "The large N limit of superconformal field theories and supergravity," *Adv. Theor. Math. Phys.* **2** (1998) 231–252, arXiv:hep-th/9711200.

[39] S. S. Gubser, I. R. Klebanov, and A. M. Polyakov, "Gauge theory correlators from non-critical string theory," *Phys. Lett.* **B428** (1998) 105–114, arXiv:hep-th/9802109.

[40] E. Witten, "Anti-de Sitter space and holography," *Adv. Theor. Math. Phys.* **2** (1998) 253–291, arXiv:hep-th/9802150.

[41] N. Arkani-Hamed, M. Porrati, and L. Randall, "Holography and phenomenology," *JHEP* **08** (2001) 017, arXiv:hep-th/0012148.

[42] R. Rattazzi and A. Zaffaroni, "Comments on the holographic picture of the Randall-Sundrum model," *JHEP* **04** (2001) 021, arXiv:hep-th/0012248.

[43] M. Perez-Victoria, "Randall-Sundrum models and the regularized AdS/CFT correspondence," *JHEP* **05** (2001) 064, arXiv:hep-th/0105048.

[44] O. Aharony, S. S. Gubser, J. M. Maldacena, H. Ooguri, and Y. Oz, "Large N field theories, string theory and gravity," *Phys. Rept.* **323** (2000) 183–386, arXiv:hep-th/9905111.

[45] S. Weinberg, "Implications of Dynamical Symmetry Breaking," *Phys. Rev.* **D13** (1976) 974–996.

[46] S. Weinberg, "Implications of Dynamical Symmetry Breaking: An Addendum," *Phys. Rev.* **D19** (1979) 1277–1280.

[47] L. Susskind, "Dynamics of Spontaneous Symmetry Breaking in the Weinberg-Salam Theory," *Phys. Rev.* **D20** (1979) 2619–2625.

[48] M. E. Peskin and T. Takeuchi, "A New constraint on a strongly interacting Higgs sector," *Phys. Rev. Lett.* **65** (1990) 964–967.

[49] M. E. Peskin and T. Takeuchi, "Estimation of oblique electroweak corrections," *Phys. Rev.* **D46** (1992) 381–409.

[50] H. Georgi and D. B. Kaplan, "Composite Higgs and Custodial SU(2)," *Phys. Lett.* **B145** (1984) 216.

[51] H. Georgi, D. B. Kaplan, and P. Galison, "Calculation of the Composite Higgs Mass," *Phys. Lett.* **B143** (1984) 152.

[52] D. B. Kaplan, H. Georgi, and S. Dimopoulos, "Composite Higgs Scalars," *Phys. Lett.* **B136** (1984) 187.

[53] D. B. Kaplan and H. Georgi, "SU(2) x U(1) Breaking by Vacuum Misalignment," *Phys. Lett.* **B136** (1984) 183.

[54] R. S. Chivukula, "Technicolor and compositeness," `arXiv:hep-ph/0011264`.

[55] K. Lane, "Two lectures on technicolor," `arXiv:hep-ph/0202255`.

[56] M. A. Luty and T. Okui, "Conformal technicolor," *JHEP* **09** (2006) 070, `arXiv:hep-ph/0409274`.

[57] J. Galloway, J. A. Evans, M. A. Luty, and R. A. Tacchi, "Minimal Conformal Technicolor and Precision Electroweak Tests," *JHEP* **10** (2010) 086, `arXiv:1001.1361 [hep-ph]`.

[58] J. Polchinski and M. J. Strassler, "Hard scattering and gauge / string duality," *Phys. Rev. Lett.* **88** (2002) 031601, arXiv:hep-th/0109174.

[59] J. Erlich, E. Katz, D. T. Son, and M. A. Stephanov, "QCD and a Holographic Model of Hadrons," *Phys. Rev. Lett.* **95** (2005) 261602, arXiv:hep-ph/0501128.

[60] A. Karch, E. Katz, D. T. Son, and M. A. Stephanov, "Linear Confinement and AdS/QCD," *Phys. Rev.* **D74** (2006) 015005, arXiv:hep-ph/0602229.

[61] A. Falkowski and M. Perez-Victoria, "Electroweak Breaking on a Soft Wall," *JHEP* **12** (2008) 107, arXiv:0806.1737 [hep-ph].

[62] B. Batell and T. Gherghetta, "Dynamical Soft-Wall AdS/QCD," *Phys. Rev.* **D78** (2008) 026002, arXiv:0801.4383 [hep-ph].

[63] B. Batell, T. Gherghetta, and D. Sword, "The Soft-Wall Standard Model," *Phys. Rev.* **D78** (2008) 116011, arXiv:0808.3977 [hep-ph].

[64] S. M. Aybat and J. Santiago, "Bulk Fermions in Warped Models with a Soft Wall," arXiv:0905.3032 [hep-ph].

[65] A. Delgado and D. Diego, "Fermion Mass Hierarchy from the Soft Wall," arXiv:0905.1095 [hep-ph].

[66] T. Gherghetta and D. Sword, "Fermion Flavor in Soft-Wall AdS," *Phys. Rev.* **D80** (2009) 065015, arXiv:0907.3523 [hep-ph].

[67] F. Cooper, A. Khare, and U. Sukhatme, "Supersymmetry in quantum mechanics," Singapore, Singapore: World Scientific (2001) 210 p.

[68] C. Csaki, "TASI lectures on extra dimensions and branes," hep-ph/0404096.

[69] S. B. Giddings, E. Katz, and L. Randall, "Linearized gravity in brane backgrounds," *JHEP* **03** (2000) 023, arXiv:hep-th/0002091.

[70] J. Garriga and T. Tanaka, "Gravity in the brane-world," *Phys. Rev. Lett.* **84** (2000) 2778–2781, arXiv:hep-th/9911055.

[71] W. D. Goldberger and M. B. Wise, "Modulus stabilization with bulk fields," *Phys. Rev. Lett.* **83** (1999) 4922–4925, arXiv:hep-ph/9907447.

[72] S. Carroll, *Spacetime and Geometry: An Introduction to General Relativity* Benjamin Cummings, June, 2003.

[73] R. M. Wald, *General Relativity* University of Chicago Press, June, 1984.

[74] H. Davoudiasl, J. L. Hewett, and T. G. Rizzo, "Bulk gauge fields in the Randall-Sundrum model," *Phys. Lett.* **B473** (2000) 43–49, arXiv:hep-ph/9911262.

[75] A. Pomarol, "Gauge bosons in a five-dimensional theory with localized gravity," *Phys. Lett.* **B486** (2000) 153–157, arXiv:hep-ph/9911294.

[76] S. J. Huber and Q. Shafi, "Higgs mechanism and bulk gauge boson masses in the Randall-Sundrum model," *Phys. Rev.* **D63** (2001) 045010, hep-ph/0005286.

[77] S. Chang, J. Hisano, H. Nakano, N. Okada, and M. Yamaguchi, "Bulk standard model in the Randall-Sundrum background," *Phys. Rev.* **D62** (2000) 084025, hep-ph/9912498.

[78] T. Gherghetta and A. Pomarol, "Bulk fields and supersymmetry in a slice of AdS," *Nucl. Phys.* **B586** (2000) 141–162, hep-ph/0003129.

[79] Y. Grossman and M. Neubert, "Neutrino masses and mixings in non-factorizable geometry," *Phys. Lett.* **B474** (2000) 361–371, hep-ph/9912408.

[80] S. J. Huber and Q. Shafi, "Fermion Masses, Mixings and Proton Decay in a Randall- Sundrum Model," *Phys. Lett.* **B498** (2001) 256–262, arXiv:hep-ph/0010195.

[81] L. Randall and M. D. Schwartz, "Quantum field theory and unification in AdS5," *JHEP* **11** (2001) 003, arXiv:hep-th/0108114.

[82] L. Randall and M. D. Schwartz, "Unification and the hierarchy from AdS5," *Phys. Rev. Lett.* **88** (2002) 081801, arXiv:hep-th/0108115.

[83] S. Weinberg, *The Quantum Theory of Fields Vol. I* Cambridge University Press, June, 1995.

[84] S. Weinberg, *The Quantum Theory of Fields Vol. III* Cambridge University Press, May, 2000.

[85] T. Gherghetta, "Warped models and holography," `hep-ph/0601213`.

[86] T. Gherghetta, "TASI Lectures on a Holographic View of Beyond the Standard Model Physics," `arXiv:1008.2570 [hep-ph]`.

[87] K. Agashe, A. Delgado, and R. Sundrum, "Grand unification in RS1," *Ann. Phys.* **304** (2003) 145–164, `arXiv:hep-ph/0212028`.

[88] K. Agashe, A. E. Blechman, and F. Petriello, "Probing the Randall-Sundrum geometric origin of flavor with lepton flavor violation," *Phys. Rev.* **D74** (2006) 053011, `hep-ph/0606021`.

[89] K. Agashe, A. Delgado, M. J. May, and R. Sundrum, "RS1, custodial isospin and precision tests," *JHEP* **08** (2003) 050, `arXiv:hep-ph/0308036`.

[90] K. Agashe, G. Perez, and A. Soni, "Flavor structure of warped extra dimension models," *Phys. Rev.* **D71** (2005) 016002, `arXiv:hep-ph/0408134`.

[91] M. E. Albrecht, M. Blanke, A. J. Buras, B. Duling, and K. Gemmler, "Electroweak and Flavour Structure of a Warped Extra Dimension with Custodial Protection," `arXiv:0903.2415 [hep-ph]`.

[92] M.-C. Chen and H.-B. Yu, "Minimal Flavor Violation in the Lepton Sector of the Randall-Sundrum Model," *Phys. Lett.* **B672** (2009) 253–256, `arXiv:0804.2503 [hep-ph]`.

[93] S. Casagrande, F. Goertz, U. Haisch, M. Neubert, and T. Pfoh, "Flavor Physics in the Randall-Sundrum Model: I. Theoretical Setup and Electroweak Precision Tests," *JHEP* **10** (2008) 094, `arXiv:0807.4937 [hep-ph]`.

[94] S. J. Huber, "Flavor violation and warped geometry," *Nucl. Phys.* **B666** (2003) 269–288, `arXiv:hep-ph/0303183`.

[95] A. L. Fitzpatrick, G. Perez, and L. Randall, "Flavor from Minimal Flavor Violation & a Viable Randall- Sundrum Model," arXiv:0710.1869 [hep-ph].

[96] A. Falkowski and M. Perez-Victoria, "Holographic Unhiggs," *Phys. Rev.* **D79** (2009) 035005, arXiv:0810.4940 [hep-ph].

[97] O. Andreev, "1/q**2 corrections and gauge / string duality," *Phys. Rev.* **D73** (2006) 107901, arXiv:hep-th/0603170.

[98] H. Georgi, "Unparticle Physics," *Phys. Rev. Lett.* **98** (2007) 221601, arXiv:hep-ph/0703260.

[99] M. J. Strassler and K. M. Zurek, "Echoes of a hidden valley at hadron colliders," *Phys. Lett.* **B651** (2007) 374–379, arXiv:hep-ph/0604261.

[100] G. Cacciapaglia, G. Marandella, and J. Terning, "The AdS/CFT/Unparticle Correspondence," *JHEP* **02** (2009) 049, arXiv:0804.0424 [hep-ph].

[101] K. Skenderis and P. K. Townsend, "Gravitational stability and renormalization-group flow," *Phys. Lett.* **B468** (1999) 46–51, arXiv:hep-th/9909070.

[102] O. DeWolfe, D. Z. Freedman, S. S. Gubser, and A. Karch, "Modeling the fifth dimension with scalars and gravity," *Phys. Rev.* **D62** (2000) 046008, arXiv:hep-th/9909134.

[103] T. Gherghetta and N. Setzer, "On the stability of a soft-wall model," arXiv:1008.1632 [hep-ph].

[104] H. Davoudiasl, G. Perez, and A. Soni, "The Little Randall-Sundrum Model at the Large Hadron Collider," *Phys. Lett.* **B665** (2008) 67–71, arXiv:0802.0203 [hep-ph].

[105] C. Csaki, C. Grojean, H. Murayama, L. Pilo, and J. Terning, "Gauge theories on an interval: Unitarity without a Higgs," *Phys. Rev.* **D69** (2004) 055006, arXiv:hep-ph/0305237.

[106] C. Csaki, C. Grojean, L. Pilo, and J. Terning, "Towards a realistic model of Higgsless electroweak symmetry breaking," *Phys. Rev. Lett.* **92** (2004) 101802, arXiv:hep-ph/0308038.

[107] G. Cacciapaglia, C. Csaki, G. Marandella, and J. Terning, "The gaugephobic Higgs," *JHEP* **02** (2007) 036, arXiv:hep-ph/0611358.

[108] F. Coradeschi, S. De Curtis, D. Dominici, and J. R. Pelaez, "Modified spontaneous symmetry breaking pattern by brane- bulk interaction terms," *JHEP* **04** (2008) 048, arXiv:0712.0537 [hep-th].

[109] M. S. Carena, E. Ponton, J. Santiago, and C. E. M. Wagner, "Light Kaluza-Klein states in Randall-Sundrum models with custodial SU(2)," *Nucl. Phys.* **B759** (2006) 202–227, arXiv:hep-ph/0607106.

[110] **UTfit** Collaboration, M. Bona *et al.*, "Model-independent constraints on Δ F=2 operators and the scale of new physics," *JHEP* **03** (2008) 049, arXiv:0707.0636 [hep-ph].

[111] K. Agashe *et al.*, "LHC Signals for Warped Electroweak Neutral Gauge Bosons," *Phys. Rev.* **D76** (2007) 115015, arXiv:0709.0007 [hep-ph].

[112] C. Csaki, A. Falkowski, and A. Weiler, "The Flavor of the Composite Pseudo-Goldstone Higgs," *JHEP* **09** (2008) 008, arXiv:0804.1954 [hep-ph].

[113] K. Agashe, R. Contino, L. Da Rold, and A. Pomarol, "A custodial symmetry for Z b anti-b," *Phys. Lett.* **B641** (2006) 62–66, arXiv:hep-ph/0605341.

[114] R. Barbieri, A. Pomarol, and R. Rattazzi, "Weakly coupled Higgsless theories and precision electroweak tests," *Phys. Lett.* **B591** (2004) 141–149, arXiv:hep-ph/0310285.

[115] K. Agashe, C. Csaki, C. Grojean, and M. Reece, "The S-parameter in holographic technicolor models," *JHEP* **12** (2007) 003, arXiv:0704.1821 [hep-ph].

[116] Y. Grossman, R. Harnik, G. Perez, M. D. Schwartz, and Z. Surujon, "Twisted split fermions," *Phys. Rev.* **D71** (2005) 056007, arXiv:hep-ph/0407260.

[117] S. Mert Aybat and J. Santiago, "Bulk Fermions in Warped Models with a Soft Wall," *Phys. Rev.* **D80** (2009) 035005, arXiv:0905.3032 [hep-ph].

[118] M. Atkins and S. J. Huber, "Suppressing Lepton Flavour Violation in a Soft-Wall Extra Dimension," *Phys. Rev.* **D82** (2010) 056007, arXiv:1002.5044 [hep-ph].

[119] T. Hull and R. Julius, "Enclosed Quantum Mechanical Systems," *Can. J. Phys.* **34** (1956) 914–919.

[120] J. Gorecki and B. W. Brown, "Iterative boundary perturbation method for enclosed one-dimensional quantum systems," *Journal of Physics B: Atomic and Molecular Physics* **20** no. 22, (1987) 5953–5957 http://stacks.iop.org/0022-3700/20/5953.

[121] I. S. Gradshteyn and I. M. Ryzhik, *Tables of Integrals, Series, and Products* Academic Press, San Diego, Calif., 6 ed., 2000.

[122] A. Delgado, A. Pomarol, and M. Quiros, "Electroweak and flavor physics in extensions of the standard model with large extra dimensions," *JHEP* **01** (2000) 030, arXiv:hep-ph/9911252.

[123] H. B. Keller, *Numerical Solution of Two Point Boundary Value Problems* SIAM, Philadelphia, 1976.

[124] Y. Grossman and Y. Nir, "Lepton mass matrix models," *Nucl. Phys.* **B448** (1995) 30–50, arXiv:hep-ph/9502418.

[125] Y. Nir and N. Seiberg, "Should squarks be degenerate?," *Phys. Lett.* **B309** (1993) 337–343, arXiv:hep-ph/9304307.

[126] R. Fok and G. D. Kribs, "$\mu \to e$ in R-symmetric Supersymmetry," *Phys. Rev.* **D82** (2010) 035010, arXiv:1004.0556 [hep-ph].

[127] A. Falkowski, Z. Lalak, and S. Pokorski, "Five-dimensional gauged supergravities with universal hypermultiplet and warped brane worlds," *Phys. Lett.* **B509** (2001) 337–345, arXiv:hep-th/0009167.

[128] N. Alonso-Alberca, P. Meessen, and T. Ortin, "Supersymmetric brane-worlds," *Phys. Lett.* **B482** (2000) 400–408, arXiv:hep-th/0003248.

[129] M. J. Duff, J. T. Liu, and K. S. Stelle, "A supersymmetric type IIB Randall-Sundrum realization," *J. Math. Phys.* **42** (2001) 3027–3047, arXiv:hep-th/0007120.

[130] M. A. Luty and R. Sundrum, "Hierarchy Stabilization in Warped Supersymmetry," *Phys. Rev.* **D64** (2001) 065012, arXiv:hep-th/0012158.

[131] E. Shuster, "Killing spinors and supersymmetry on AdS," *Nucl. Phys.* **B554** (1999) 198–214, arXiv:hep-th/9902129.

[132] R. Altendorfer, J. Bagger, and D. Nemeschansky, "Supersymmetric Randall-Sundrum scenario," *Phys. Rev.* **D63** (2001) 125025, arXiv:hep-th/0003117.

[133] E. A. Mirabelli and M. E. Peskin, "Transmission of supersymmetry breaking from a 4- dimensional boundary," *Phys. Rev.* **D58** (1998) 065002, arXiv:hep-th/9712214.

[134] L. J. Hall, Y. Nomura, T. Okui, and S. J. Oliver, "Explicit supersymmetry breaking on boundaries of warped extra dimensions," *Nucl. Phys.* **B677** (2004) 87–114, arXiv:hep-th/0302192.

[135] I. Antoniadis, "A Possible new dimension at a few TeV," *Phys. Lett.* **B246** (1990) 377–384.

[136] R. Barbieri, L. J. Hall, and Y. Nomura, "A constrained standard model from a compact extra dimension," *Phys. Rev.* **D63** (2001) 105007, arXiv:hep-ph/0011311.

[137] A. Pomarol and M. Quiros, "The standard model from extra dimensions," *Phys. Lett.* **B438** (1998) 255–260, arXiv:hep-ph/9806263.

[138] I. Antoniadis, S. Dimopoulos, A. Pomarol, and M. Quiros, "Soft masses in theories with supersymmetry breaking by TeV-compactification," *Nucl. Phys.* **B544** (1999) 503–519, arXiv:hep-ph/9810410.

[139] A. Delgado, A. Pomarol, and M. Quiros, "Supersymmetry and electroweak breaking from extra dimensions at the TeV-scale," *Phys. Rev.* **D60** (1999) 095008, arXiv:hep-ph/9812489.

[140] N. Arkani-Hamed, M. A. Luty, and J. Terning, "Composite quarks and leptons from dynamical supersymmetry breaking without messengers," *Phys. Rev.* **D58** (1998) 015004, arXiv:hep-ph/9712389.

[141] M. A. Luty and J. Terning, "Improved single sector supersymmetry breaking," *Phys. Rev.* **D62** (2000) 075006, hep-ph/9812290.

[142] N. Arkani-Hamed and H. Murayama, "Can the supersymmetric flavor problem decouple?," *Phys. Rev.* **D56** (1997) 6733–6737, arXiv:hep-ph/9703259.

[143] K. Agashe and M. Graesser, "Supersymmetry breaking and the supersymmetric flavour problem: An analysis of decoupling the first two generation scalars," *Phys. Rev.* **D59** (1999) 015007, arXiv:hep-ph/9801446.

[144] C. Hamzaoui, M. Pospelov, and M. Toharia, "Higgs-mediated FCNC in supersymmetric models with large tan(beta)," *Phys. Rev.* **D59** (1999) 095005, arXiv:hep-ph/9807350.

[145] J. Hisano and D. Nomura, "Solar and atmospheric neutrino oscillations and lepton flavor violation in supersymmetric models with the right- handed neutrinos," *Phys. Rev.* **D59** (1999) 116005, hep-ph/9810479.

[146] A. J. Buras, A. Romanino, and L. Silvestrini, "K –¿ pi nu anti-nu: A model independent analysis and supersymmetry," *Nucl. Phys.* **B520** (1998) 3–30, arXiv:hep-ph/9712398.

[147] **Particle Data Group** Collaboration, W. M. Yao *et al.*, "Review of particle physics," *J. Phys.* **G33** (2006) 1–1232.

[148] M. Maltoni, T. Schwetz, M. A. Tortola, and J. W. F. Valle, "Status of global fits to neutrino oscillations," *New J. Phys.* **6** (2004) 122, hep-ph/0405172.